Regulatory Mechanisms of MarA, the Activator of Multiple Antibiotic Resistance

by

Rachel Andrea Kettles

A thesis submitted to the University of Birmingham for the degree of

DOCTOR OF PHILOSOPHY

November 2018

Institute of Microbiology and Infection
School of Biosciences
College of Life and Environmental Sciences
University of Birmingham

Abstract

The multiple antibiotic resistance (*mar*) operon in *Escherichia coli* is responsible for resistance to a broad range of antibacterial drugs. The *mar* operon is normally transcriptionally silent, but a faulty *mar* repressor (MarR) leads to constitutive expression of MarA (the *mar* activator). MarA transcriptionally regulates downstream targets leading to a *mar* phenotype of widespread resistance to antibiotics and other environmental stresses (e.g. oxidative stress, organic solvents and disinfectants). As the *mar* operon is conserved across a number of human pathogens, understanding the mechanisms through which it mediates antibiotic tolerance is essential.

A recent ChIP-seq analysis unveiled 33 targets of MarA, many of which were previously unknown. This work has characterised the regulation of one of these targets, *ycgZ-ymgABC*. The promoter upstream of *ycgZ-ymgABC* was found to be both σ^{70} and σ^{38}-dependent. However, MarA activates transcription from this promoter in a σ^{70}-dependent manner only, and was shown to act as a Class I activator. Furthermore, activation of *ycgZ-ymgABC* expression by MarA was shown to result in a reduction in biofilm formation, which may offer the cell alternative short-term survival strategies during antibiotic attack.

The requirements for activation of transcription at the regulatory region upstream of *mlaFEDCB* were investigated. Strict spacing and orientation requirements for MarA binding were observed; the MarA binding site (the marbox) only functions in the forward orientation, and cannot be moved more than 1 bp without loss of activation. Additionally, MarA was shown to require an UP element and contact with the C-terminal domain of RNAP for activation at this target.

Finally, the ChIP-seq targets, and a set of SoxS ChIP-exo targets from a separate study, were examined for binding by MarA and two related regulators, Rob and SoxS. These three proteins have an identical consensus site for DNA binding but bind non-consensus sites with hugely different affinities. It was noticed that SoxS requires a much closer match to the consensus site than MarA for optimal binding. We hypothesise here that this is due to a loss of amino acid side chains in SoxS that are key for hydrogen bonding interactions with the DNA backbone. To confirm this, we have shown here that MarA binds to the *ycgZ* promoter at a higher affinity than SoxS in high salt conditions only. At low salt conditions, hydrogen bonding is inhibited, significantly reducing MarA binding but not SoxS. This effect is dependent on residues E31 and Q58 of MarA, which make hydrogen bonding contacts with the DNA backbone; these contacts are lost in SoxS. Thus, this work predicts that intracellular salt conditions may influence the target preferences of these regulators.

Acknowledgments

To the many people who have helped over the last four years: thank you so, so much. First and foremost, my supervisor, Dave Grainger. Thanks so much for your guidance and support, your patience, and for giving me this opportunity. I couldn't ask for a cooler supervisor! I would also like to thank the wonderful members of the Grainger lab – I feel very lucky to work with such a great group of people! I'd particularly like to thank Dr. Prateek Sharma for his work on setting up the MarA project; Dr. James Haycocks, Dr. Lisa Lamberte, Dr. Jainaba Roussel and Dr. Shivani Singh for their help with techniques in the lab; and Dr. Gemma Warren, our lab fairy who makes sure everything keeps ticking along. To Emily, Alistair, Tom and Lucas: thanks for all the coffee, the laughter, and the many, many, many pub trips. You've been fantastic lab pals over the last few years - cheers for tolerating my terrible music taste, and not making fun of me *too* much when I break lab equipment/technology/myself!

My gratitude also goes to Kevin Lyons, a fantastic rotation student who worked with me on the biofilm experiments. You were a superstar! Thanks to my second supervisor Mark Webber, for his advice and contributions, and to the wider IMI for their help and generosity. Thanks also to the BBSRC for providing funding for my project through the MIBTP scheme.

Finally, I'd like to thank my family, particularly my parents, Grandma, and Tilly, for their never-ending support and confidence in me. I really couldn't have done any of this without you!

Table of Contents

List of Figures

List of Tables

List of Abbreviations

A	Adenine
Abs	Absorbance
Amp^R	Ampicillin resistance
APS	Ammonium persulfate
ATP	Adenosine triphosphate
bp	Base pair
BSA	Bovine serum albumin
C	Cytosine
cAMP	Cyclic AMP
Cam^R	Chloramphenicol resistance
CAT	Chloramphenicol acetyltransferase
ChIP-exo	Chromatin immunoprecipitation with exonuclease digestion
ChIP-seq	Chromatin immunoprecipitation with sequencing
Ci	Curie
CIP	Calf intestine alkaline phosphatase
CTD	C-terminal domain
CRP	cAMP receptor protein
°C	Degrees Celsius
dATP	Deoxyadeosine triphosphate
dCTP	Deoxycytidine triphosphate
ddH_2O	Deionised and distilled water
dGTP	Deoxyguanosine triphosphate

DNA	Deoxyribonucleic acid
dNTP	Deoxyribonucleoside triphosphate
dTTP	Deoxythymidine triphosphate
e^-	Electron
E. coli	*Escherichia coli*
EDTA	Diaminoethanetetra-acetic acid
EMSA	Electrophoretic mobility shift assay
ETEC	Enterotoxigenic *E. coli*
Fis	Factor for inversion stimulation protein
Fnr	Fumurate and nitrate reduction regulatory protein
G	Guanine
GDP	Gross domestic product
HEPES	4-(2-hydroxyethyl)-1-piperazineethanesulfonic acid
H-NS	Histone-like nucleoid structuring protein
HTH	Helix-turn-helix
IHF	Integration host factor
Kan^R	Kanamycin resistance
kb	Kilobase
LB	Lennox broth
mar	Multiplate antibiotic resistance
MarA	Activator of multiple antibiotic resistance
MarR	Repressor of multiple antibiotic resistance
MIC	Minimum inhibitory concentration
mRNA	Messenger RNA

Mg^{2+}	Magnesium ion
NAP	Nucleoid associated protein
NTD	N-terminal domain
NTP	Nucleoside triphosphate
NUS factors	N-utilisation factors
OD	Optical density
ONPG	Ortho-nitrrophenyl-β-galactosidase
PEG	Polyethylene glycol
PCR	Polymerase chain reaction
ppGpp	Guanosine tetraphosphate
RNA	Ribonucleic acid
RNAP	RNA polymerase
RNAP-σ^{38}	RNAP in complex with σ^{38}
RNAP-σ^{70}	RNAP in complex with σ^{70}
Rob	Right of origin binding protein
rRNA	Ribosomal RNA
SDS	Sodium dodecyl sulphate
SDS-PAGE	SDS-polyacrylamide gel electrophoresis
SoxS	Superoxide stress protein
T	Thymine
T4 PNK	T4 polynucleotide kinase
TBE	Tris-borate EDTA
TEMED	N, N, N', N'-tetramethylethylenediamine
TetR	Tetracycline resistance

Tm	Melting temperature
TNSC	Transcription buffer
Tris	Tris (hydroxymethyl) aminoethane
tRNA	Transfer RNA
TSS	Transcription start site
U	Uracil
UPEC	Uropathogenic *E. coli*
UTI	Urinary tract infection
UTP	Uridine triphosphate
UV	Ultraviolet
V	Volts
v/v	Volume/volume
W	Watts
w/v	Weight/volume

Chapter 1

Introduction

1.1 Bacterial transcription

1.1.1 The central dogma of molecular biology

The central dogma of molecular biology is the flow of information between the biopolymers DNA, RNA, and protein (Figure 1.1). The enzyme RNA polymerase (RNAP) copies information from the genes within DNA into mRNA via transcription. mRNA is then translated by ribosomes into proteins. This process allows for stable storage of information in DNA, with two levels of regulation (at the transcription and translation stage) before production of proteins. Thus, protein expression can be tightly controlled in response to environmental and genetic triggers.

1.1.2 The process of bacterial transcription

In *Escherichia coli* transcription is catalysed by a DNA-dependent RNA polymerase, which comprises a core enzyme in complex with a sigma factor to form the RNAP holoenzyme. Transcription comprises three stages: initiation, elongation and termination (Figure 1.2). During initiation, the RNAP holoenzyme recognises promoter DNA sequences upstream of the gene (Busby and Ebright 1994, deHaseth, Zupancic and Record 1998). Binding of RNAP to these sequences forms the 'closed complex'; unwinding of the DNA duplex at the region of the transcription start site then forms what is known as the 'open complex' (Tsujikawa, Tsodikov and deHaseth 2002, Hook-Barnard and Hinton 2009). NTPs are added to form an initiating complex, in which the downstream template DNA is 'scrunched' into the enzyme as an RNA molecule is synthesised (Kapanidis *et al.* 2006, Revyakin *et al.* 2006). At this stage, the RNAP complex is trapped at the promoter and may go through a number of abortive initiation cycles, in which small RNA transcripts are produced and released. This stressed

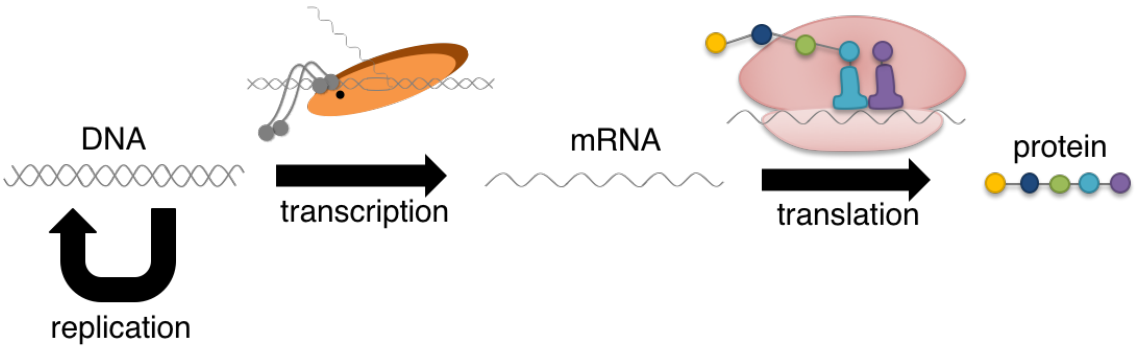

Figure 1.1 Flow of molecular information

The figure shows the flow of information between the biopolymers. Grey double helices show DNA. Wavy grey lines show mRNA. Coloured circles show amino acids, connected by straight grey lines (peptide bonds) to form a protein. Coloured T-shapes show tRNA. The orange oval shape shows RNAP, and pink ovals show the ribosome subunits.

intermediate results in free energy build-up, eventually allowing contacts with the promoter to be broken (Straney and Crothers 1987). This drives RNAP escape from the scrunched complex in order to enter elongation phase (Kapanidis *et al.* 2006, Henderson *et al.* 2017). At this point, polymerase dissociates from the sigma factor.

During elongation, NTPs (nucleoside triphosphates) are added to extend the RNA transcript. Firstly, a complementary NTP binds the active site. The cofactor Mg^{2+} then catalyses a chemical reaction forming a phosphodiester bond between the 3' OH of the nascent RNA and the α-PO_4 of the NTP, with the help of the Gre elongation factors (Laptenko *et al.* 2003). The 3' end of the nascent RNA is then translocated away from the active site to place the next template base in the centre. The elongation process is controlled by additional elongation factors, such as NusA and NusG, which control transcriptional pausing to allow the rate of elongation to be regulated (Schmidt and Chamberlin 1987, Burova *et al.* 1995)

Elongation continues until RNAP encounters a GC-rich hairpin in the transcript known as an intrinsic terminator, or until a termination factor such as Rho or Mfd binds the complex (Yarnell and Roberts 1999, Park, Marr and Roberts 2002, Ciampi 2006). The mRNA transcript is then released, and RNAP dissociates from the DNA in order to begin the cycle again. Termination is regulated by host and phage-generated antiterminators, which allow the complex to bypass termination signals and continue with elongation (Santangelo and Artsimovitch 2011).

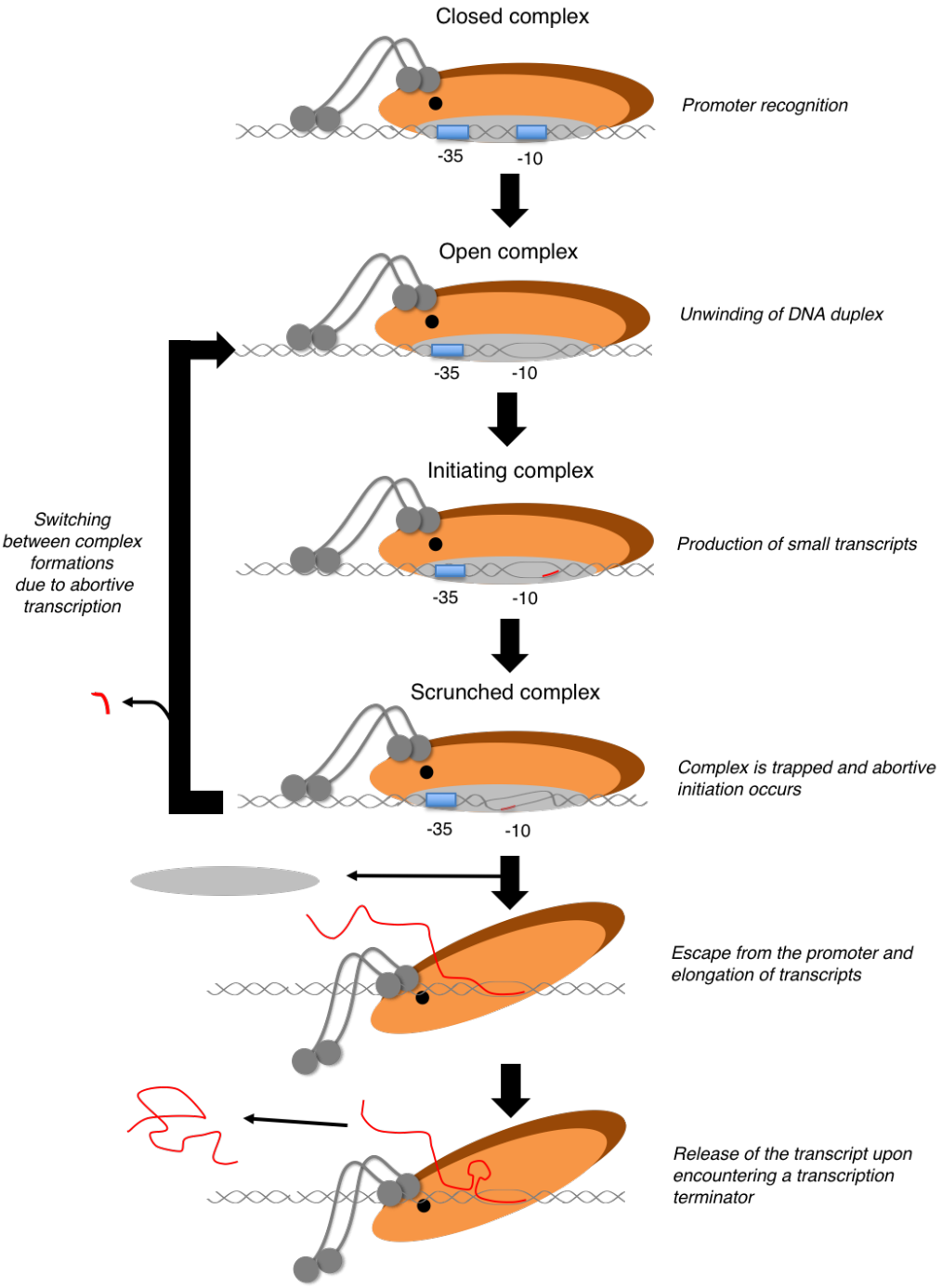

Figure 1.2 Transcription in *Escherichia coli*

Schematic showing initiation, elongation and termination of transcription. The subunits of RNAP are shown by orange ovals (β), dark orange ovals (β'), grey ovals (σ), black circles (ω) and dark grey circles (α). DNA is shown by a grey double helix. mRNA is shown as a red line. Binding to the -35 and -10 elements of the promoter is shown by blue rectangles.

1.1.3 RNA polymerase

The 400 kDA RNAP core enzyme is made up of five subunits: β, β', the small ω subunit, and two α subunits (Figure 1.3). The enzyme forms a 'crab-claw' structure, with two 'pincers' between which the template DNA is passed (Zhang *et al.* 1999, Murakami, Masuda and Darst 2002).

The β and β' subunits form the 'pincer', known as the β clamp, and bind the N-terminal domains of the α subunits to surround a cleft, on the back wall of which the active site is located (Zhang *et al.* 1999). The clamp can switch from an open conformation to a closed with the action of a hinge region located at the base of the clamp (Landick 2001, Darst *et al.* 2002, Chakraborty *et al.* 2012). This allows the clamp to open to allow DNA loading, with the clamp then able to close upon initiation of transcription. Within the active site, an essential Mg^{2+} co-factor is held in position by three Asp residues (Murakami and Darst 2003). The active site also contains the F bridge, the conformation of which is controlled by the G-trigger loop; the F-bridge and the substrate DNA act as 'ratchet' devices to drive elongation by RNAP (Bar-Nahum *et al.* 2005). These 'ratchets' move the four mobile modules of RNAP: the clamp, the β flap, and the β1 and β2 lobes, which all surround the active site channel (Murakami and Darst 2003).

Association of the β' subunit during polymerase assembly is aided by a chaperone, the 91 amino acid ω subunit, which contacts the N and C-terminal domains of β' (Zhang *et al.* 1999, Ghosh, Ishihama and Chatterji 2001). Additionally, the ω subunit is recognised by ppGpp, a nucleotide which accumulates during starvation and binds at the interface between the β' and the ω subunit to alter the transcriptional profile of the cell (Potrykus

and Cashel 2008, Mechold *et al.* 2013, Zuo, Wang and Steitz 2013). Further functions of the ω subunit are not fully understood and deletion studies have shown it to be a non-essential subunit (Gentry and Burgess 1989). However, loss of the ω subunit shows an increase in DNA relaxation, and has been shown to impact genome-wide expression in *E. coli* and cyanobacteria through increased binding of alternative sigma factors (Geertz *et al.* 2011, Gunnelius *et al.* 2014).

The α subunits are each 37 kDa and 329 amino acids long, and comprise two domains, the C-terminal domain (α-CTD, residues 249-329) and the N-terminal domain (α-NTD, residues 8-235), joined by a flexible linker 13 amino acids in length (Jeon *et al.* 1997). The α-NTD is key for polymerase assembly, with the α-NTDs of the two α subunits interacting to form a dimer; the other RNAP subunits can then assemble around them (Igarashi, Fujita and Ishihama 1991). Both the α-NTD and the α-CTD can interact with transcriptional regulators, with the α-CTD, which also dimerises, also able to recognise promoter UP elements by binding of residue R265 to the minor groove of the DNA (Ross *et al.* 1993, Blatter *et al.* 1994).

Although the α subunits are involved in promoter recognition, the core RNAP enzyme is only capable of synthesising RNA from DNA and cannot independently recognise promoters. Thus, the core enzyme cannot initiate transcription alone and requires association with a sigma factor in order to recognise bacterial promoters; this complex is known as the RNAP holoenzyme.

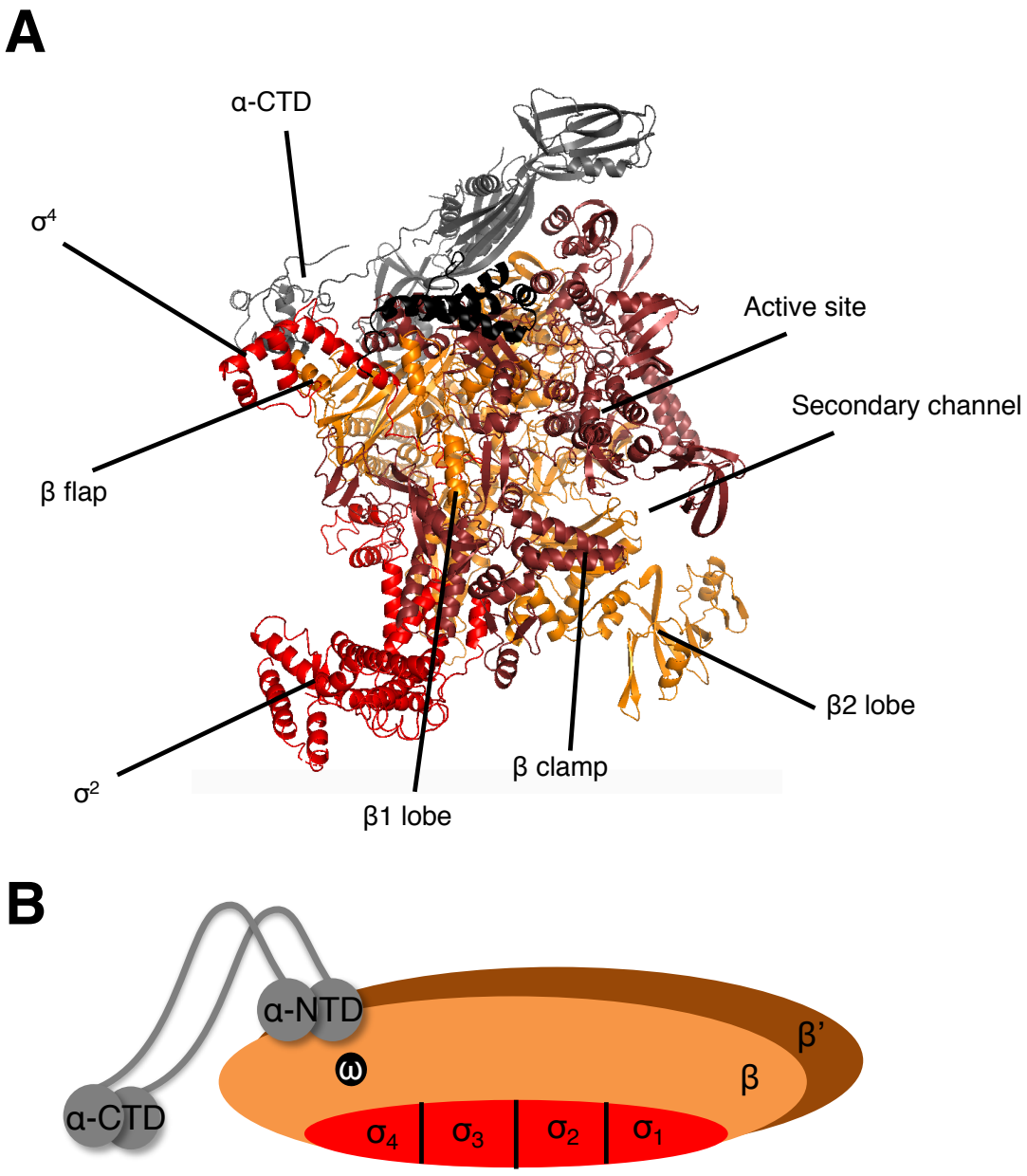

Figure 1.3 The subunits of *Escherichia coli* RNAP holoenzyme

Panel A shows a diagram of the crystal structure of RNAP in complex with σ^{70}. The diagram was constructed in PyMOL using the structural data from Murakami (2013). Panel B is a simple schematic showing the subunits of RNAP holoenzyme. The β and β' subunits of RNAP are shown in orange and brown, respectively. The σ^{70} subunit is shown in red, with the domains indicated. The α subunits are in dark grey. The ω subunit is shown in black.

1.1.4 Sigma factors

Bacteria possess a range of sigma factors to allow RNAP to be directed towards a specific set of promoters (Feklístov *et al.* 2014). The predominant sigma factor within a bacterium is known as the housekeeping sigma factor. This is responsible for the recognition of the majority of promoters within the genome.

RNAP can be redirected towards a different set of genes by alternative sigma factors (Gruber and Gross 2003, Feklístov *et al.* 2014). These sigma factors bind a smaller set of promoters than housekeeping sigma factors, due to greater stringency in their promoter sequence requirements, and their association with fewer transcription factors (Koo *et al.* 2009, Campagne *et al.* 2014). Thus, alternative sigmas are commonly used as a stress-response switch, modulating the promoter specificity of RNAP in response to environmental triggers (Rhodius *et al.* 2013). Most alternative sigma factors are related to the housekeeping sigma factor, with conservation of 2 or more of the domains.

1.1.5 The housekeeping sigma factor, σ70

In *Escherichia coli* the housekeeping sigma factor is σ^{70}, also known as RpoD. Its structure comprises four domains, connected by flexible linkers; when σ^{70} is bound to RNAP core enzyme, these subunits are optimally positioned for interaction of each domain with a specific promoter element, as shown in Figure 1.4 (Campbell *et al.* 2002). Domains 3 and 4 are involved in initial positioning of RNAP through interaction with the -10 and extended -35 promoter elements, respectively. Domains 1 and 2 interact with the discriminator region (domain 1) and the -10 promoter element (domain 2) and induce open complex formation (Mekler *et al.* 2002, Murakami 2013).

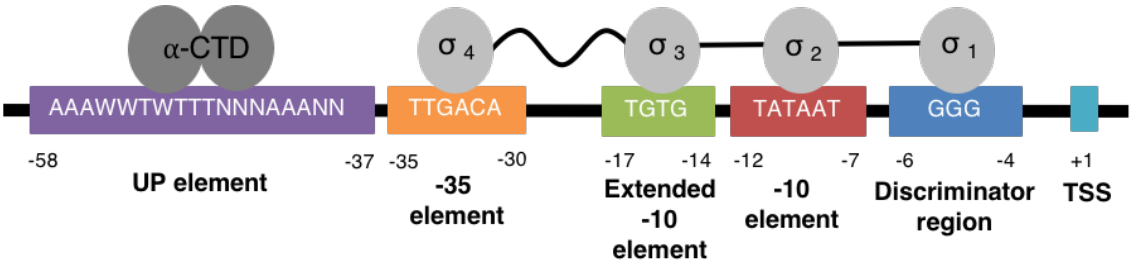

Figure 1.4 Bacterial promoter elements

The figure shows the consensus motifs of the bacterial promoter elements, as well as their locations relative to the transcription start site (TSS) at +1. The interactions of the promoter elements with RNAP are also shown. The two α C-terminal domains (CTD) of RNAP are shown in dark grey, interacting with the UP element. Domains of the σ RNAP subunit are shown in light grey, with domains 4, 3, 2 and 1 interacting with the -35 element, extended -10 element, -10 element and discriminator region respectively.

RNAP associates with σ^{70} via contacts with all four σ^{70} domains. A key feature of RNAP-σ^{70} binding is the contact formed by a hydrophobic pocket of σ_4 with the α-helix of the β flap (Campbell *et al.* 2002, Murakami and Darst 2003). As σ_4 is connected by a flexible linker, this provides flexibility to the promoter recognition region of the RNAP holoenzyme, allowing promoter bending during initiation of transcription (Murakami, Masuda and Darst 2002, Campbell, Westblade and Darst 2008). Additionally, σ_2 forms a well conserved interaction with the coiled-coil of the β subunit (Campbell *et al.* 2002). Domain 1 is also key in preventing DNA from accessing the active site of RNAP prior to polymerase-promoter binding; this domain induces a conformational change in the holoenzyme after promoter recognition which allows DNA to then enter the active site (Mekler *et al.* 2002).

1.1.6 The alternative sigma factors, σ^{38} and σ^{54}

There are two main families of alternative sigma factors in *Escherichia coli*: the σ^{70} family, which comprises sigma factors related to the housekeeping sigma factor, and the σ^{54} family which is uniquely unrelated to other sigma factors (Merrick 1993). The σ^{70} family is grouped phylogenetically and according to the domains they possess (Gruber and Gross 2003, Paget and Helmann 2003, Österberg, Peso-Santos and Shingler 2011). Group 1 comprises housekeeping sigma factors, whilst Groups 2 and 3 are highly related to Group 1 (possessing all four conserved domains: σ_2, σ_3, σ_4, and region 1.1 of σ_1). Group 2 includes stationary and stress response sigma factors such as σ^{38}, whilst Group 3 includes developmental and heat shock sigma factors. Group 4 sigma factors only possess two of the conserved domains (σ_2 and σ_4) and typically respond to extracytoplasmic

signals, such as metal transport, periplasmic stress, and infection of a host (Helmann 2002, Manganelli *et al.* 2004, Lane and Darst 2006).

There are two key alternative sigma factors present in *Escherichia coli*: σ^{38}, also known as RpoS, and σ^{54}, known as RpoN. σ^{38} responds to environmental stresses such as starvation, or entry into stationary phase growth (Lange and Hengge-Aronis 1994, Mandel and Silhavy 2005). Upon initiation of these triggers, σ^{38} increases in abundance due to interaction with Crl, whilst σ^{70} levels reduce due to the anti-sigma factor Rsd (Pratt and Silhavy 1998). Thus, environmental stress induces a pathway by which σ^{38} displaces σ^{70} and redirects RNAP towards key stress response genes (Battesti, Majdalani and Gottesman 2011). Microarray studies have estimated that over 10 % of the genome is regulated by σ^{38}; recent ChIP-seq and RNA-seq studies have increased this estimate to 23% (Patten *et al.* 2004, Weber *et al.* 2005, Wong *et al.* 2017).

The σ^{54} class of sigma factors recognise different promoter elements at the -12 and -24 positions (Wigneshweraraj *et al.* 2008). However, the σ^{54}-RNAP holoenzyme cannot form an open complex due to σ^{54} blocking the site of open complex formation (Yang *et al.* 2015). An additional ATP-dependent activator is thus required. As σ^{54} levels appear constant and unregulated, control at σ^{54}-dependent promoters is likely reliant on regulation of these activators, rather than on regulation of σ^{54} levels.

1.1.7 The bacterial promoter

RNAP holoenzyme recognises promoters upstream of transcription start sites (TSSs). Bacterial promoters contain a number of motifs for recognition by RNAP and its cognate

sigma factors, which allows RNAP to be directed to the adjacent TSS (Feklístov *et al.* 2014). The promoter elements are denoted relative to the TSS at the +1 position, and are shown in Figure 1.4 with their respective interactions with the various RNAP subunits.

RNAP in complex with σ^{70} recognises two core promoter elements, the -10 hexamer (5'-TATAAT-3') and the -35 hexamer (5'-TTGACA-3'). The core promoter elements are optimally spaced 17 bp (base pairs) apart, with the -10 hexamer optimally 7 bp from the transcription start site (Walker and Osuna 2002). The sequence of the spacer region between the -10 and the -35 hexamer is also important; spacer sequence influences sigma factor specificity due to contacts made by side chain R451 of σ^{70} with position -18 of the DNA, and a more AT-rich spacer region inhibits open complex formation (Typas and Hengge 2006, Hook-Barnard and Hinton 2009, Singh *et al.* 2011). Additionally, the β' zipper is proposed to make interactions with the spacer region, with promotion of either open or closed complex formation dependent on spacer sequence (Murakami, Masuda and Darst 2002, Nechaev and Geiduschek 2006, Yuzenkova *et al.* 2011).

Additional promoter elements may be recognised to enhance promoter strength, for example to compensate for a -35 or -10 element with a poor match to the consensus or with suboptimal spacing. The extended -10 element (5'-TG-3') immediately upstream of the -10 element can stabilise RNAP:DNA interactions (Barne *et al.* 1997). The UP element, meanwhile, is the only promoter element recognised by core RNAP, making contact with the α subunit C-terminal domain (α-CTD) to increase promoter activity 20-30 fold (Ross *et al.* 1993). The UP element consists of two subsites which independently interact with a copy of the α subunit (Murakami *et al.* 1997, Estrem *et al.* 1999). The α-

CTD is attached by a flexible linker, allowing recognition of additional nonspecific sequences up to 90 bp upstream of the transcription start site (Davis *et al.* 2005, Ross and Gourse 2005).

1.2 Regulation of transcription initiation

Transcription by RNAP can be regulated either directly through changes in RNAP holoenzyme formation or activity, or in a promoter-centric mechanism through modulation of promoter affinity or accessibility (Browning and Busby 2016). Direct regulation of holoenzyme activity occurs mostly at the elongation and termination stages of transcription, as seen with Nus factors which control N-utilisation (Washburn and Gottesman 2015). At the initiation stage, polymerase-centric systems vary across different bacterial species. For example, within the Enterobacteriaceae, DksA is a key regulator allowing for sigma factor independent switching of the transcriptome. DksA, along with ppGpp, inserts into the secondary channel of RNAP. This results in an interaction with the active site of RNAP which either stabilises or destabilises the complex in a promoter dependent manner (Doniselli *et al.* 2015). Thus, the transcriptome can be rapidly altered in response to ppGpp levels.

RNAP activity is altered predominantly via sigma factors, which direct the specificity of RNAP, as discussed earlier. Sigma factor regulation can be manipulated by additional regulators. For example, the global stress regulator 6S RNA mimics σ^{70} targets to bind σ^{70} and sequester away RNAP-σ^{70} holoenzyme, thus allowing the functional σ^{38} concentration to increase (Cavanagh and Wassarman 2014). Additionally, promoter preferences of RNAP can be adjusted by appropriators, which act similarly to sigma

factors by redirecting promoter specificity. For example, the T4-bacteriophage encoded AsiA binds and remodels σ^{70} to inhibit transcription from host promoters and redeploying *E. coli* RNAP towards T4 promoters (Colland *et al.* 1998, Baxter *et al.* 2006). Likewise, the *E. coli* oxidative stress regulator SoxS activates by prerecruitment: SoxS binds directly to RNAP to form a complex which recognises soxboxes instead of UP elements, allowing rapid activation of SoxS targets (Griffith *et al.* 2002, Zafar, Sanchez-Alberola and Wolf 2011).

RNAP activity is also responsive to levels of its substrates, nucleoside triphosphates (NTPs). Addition of the initiating nucleotide has the highest Michaelis constant, meaning this NTP is required in higher concentrations (Mangel and Chamberlin 1974). This can be seen for rRNA promoters in *E. coli*; the initiating nucleotide for these promoters is ATP, and thus ATP levels regulate rRNA synthesis (Schneider, Gaal and Gourse 2002, Murray, Schneider and Gourse 2003).

1.2.1 Transcription factors

Many regulators control transcription initiation through targeting of the promoter DNA, rather than RNAP itself. These proteins, known as transcription factors, bind a specific sequence within the promoter, known as the 'operator'. In *E. coli*, the operator is on average 24.5 bp in length, and may be repeated multiple times to improve specificity; as a result, many transcription factors bind as multimers (Robison, McGuire and Church 1998). Transcription factors provide an essential link between environmental conditions and transcriptional output; many contain a ligand-binding domain, or are bound and activated by other proteins, modifying the transcription factor to allow it to bind DNA

(Madan Babu and Teichmann 2003). Alternatively, transcription factors may be encoded from a transcription factor-regulated gene, or their levels may be controlled solely by protein turnover and sequestration. Thus, transcription factors can form complex regulatory networks, allowing fine-tuned activation of genes in response to environmental signals.

Transcription factors have been proposed to have evolved from nucleoid associated proteins (NAPs), which bind the DNA to organise and compact the bacterial chromosome (Visweswariah and Busby 2015). It is suggested that the acquisition of domains for RNAP and ligand binding, in conjunction with evolution of promoters, provided the first transcription factors and thus allowed for improved efficiency of transcription. Most transcription factors can be grouped into families based on phylogeny and function. Major families include:

LuxR/UhpA family: These regulators are part of the TetR protein superfamily, and possess a conserved HTH in the C-terminal of the DNA binding domain, and a conserved N-terminal signal-binding region (Zeng and Xie 2011). Most LuxR members are controlled by signal molecules called N-acyl-homoserine lactones, known as 'bacterial pheromones', synthesised by LuxI-type synthases (Tsai and Winans 2010). As such, many LuxR members are involved in quorum sensing.

OmpR family: Most family members are part of a two component signal transduction system, with phosphorylation of a conserved N-terminal regulatory domain controlling the activity of a conserved C-terminal DNA binding domain (Martínez-Hackert and Stock

1997). The best known family member is OmpR, which regulates the production of outer membrane porins.

LacI/GalR family: Characterised by the *lac* repressor, LacI. These regulators are bound by specific effector ligands which alter DNA binding affinity of the protein, which binds as a dimer to inverted repeat sequences of DNA (Swint-Kruse and Matthews 2009). Thus, LacI family proteins typically possess a HTH DNA binding domain linked to a regulatory domain with regions for effector binding.

LysR family: The LysR family regulators are the most abundant prokaryotic transcription factors. They possess a conserved N-terminal DNA binding HTH motif, and a C-terminal domain which binds a co-inducer (Maddocks and Oyston 2008). These co-inducers are usually the product of a pathway activated by that LysR member.

AraC/XylS family: Members of the AraC family are characterised by a conserved 100 amino acid DNA binding domain, and tend to be involved in carbon metabolism, stress response, and pathogenesis. In *E. coli* this family includes AraC, MelR, SoxS, Rob, and MarA. The DNA binding domain comprises two HTH motifs; for some family members, such as MarA, both HTH motifs have been shown to engage in DNA binding, which is unique amongst prokaryotic transcription factors (Gallegos *et al.* 1997, Rhee *et al.* 1998). These two HTH motifs have different amino acid sequences, and as such these regulators bind non-symmetrical sites. Most AraC family regulators also have a dimerisation domain at the N-terminal, for oligomerisation and binding of cofactors (Soisson *et al.* 1997, Kaldalu *et al.* 2000).

CRP family: The key member of the CRP family is CRP (cyclic-AMP receptor protein) itself, but the family also includes Fnr (fumurate and nitrate reductase regulator protein). Most family members respond to intracellular or extracellular stress signals (eg carbon monoxide, temperature, and oxidative stress) and respond with control of metabolic pathways, such as respiration and nitrogen fixation. Family members are characterised by their C-terminal HTH DNA-binding motif, and an N-terminal domain for binding effector molecules (Korner, Sofia and Zumft 2003).

1.2.2 Transcriptional activation

Transcriptional activators typically target promoters with a low basal level of activity. There are four key ways in which transcriptional activators function to increase RNAP binding, shown in Figure 1.5. These are Class I and Class II activation, remodelling of the promoter DNA, and action as anti-repressors, which interact with transcriptional repressors to lift repression (Browning and Busby 2016).

Class I activation targets operators located upstream of the -35 element. A surface-exposed patch of the activator makes contact with the α-CTD of RNAP; as a result, for some transcriptional activators, such as CRP, it has been shown that activation is optimal when the activator is bound on the same face of the DNA as polymerase (Kolb 1995, Benoff *et al.* 2002, Zhou *et al.* 2014).

Class II activation meanwhile targets operators overlapping the -35 element. This prevents the α-CTD of RNAP from binding in its usual location, and thus results in

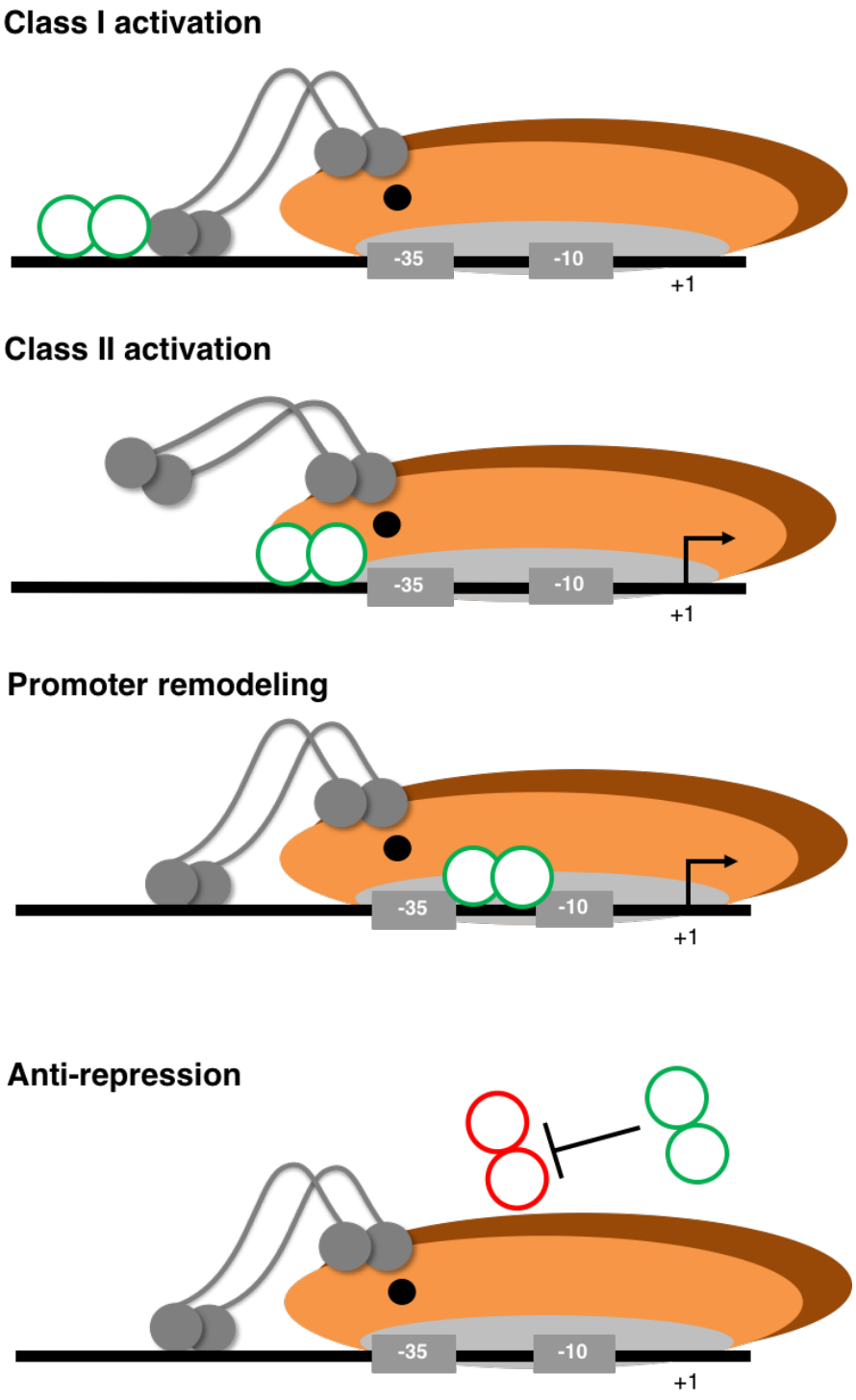

Figure 1.5 Mechanisms for the regulation of transcription by transcriptional activators

Activator proteins are shown by green circles, with repressor proteins shown in red. The thick black line indicates the DNA, with the -35 and -10 elements indicated by grey boxes. Black T-shapes indicate inhibition.

binding of α-CTD further upstream (Lee, Minchin and Busby 2012). The key contacts formed with RNAP during Class II activation are typically with either σ_4 or the α-NTD.

Finally, as discussed previously, non-optimal spacing between the -35 and -10 element can lead to inefficient transcription. Some transcription factors can bind between these two elements and remodel the DNA to recruit RNAP from a more favourable position. This can be seen with the MerR regulator family (Brown *et al.* 2003).

1.2.3 Transcriptional repression

The mechanisms of transcriptional repression are shown in Figure 1.6. Transcriptional repression occurs predominantly by steric hindrance, in which the repressor binds over the -10 or -35 elements to block access by RNAP, as seen by the LacI repressor (Lewis 1996). Multiple operators located next to each other increases the strength of repression. Likewise, a repressor may bind two operators at distal sites, causing a loop in the DNA to prevent access for RNAP, or use a combination of both steric hindrance and DNA looping to further increase repression (Swint-Kruse and Matthews 2009). Access of RNAP to genes may also be inhibited by large-scale compaction of the chromosome. For example, nucleoid associated proteins (NAPs) can bend, wrap, or loop the DNA, often in a promiscuous manner (Luijsterburg *et al.* 2006, Dillon and Dorman 2010). Some NAPs, however, such as Fis and IHF, show specificity in the sequences they bind, with IHF displaying 1000-fold greater selectivity for certain sites over random DNA, despite its known sites showing poor sequence conservation (Wang *et al.* 1995, Browning, Grainger and Busby 2010).

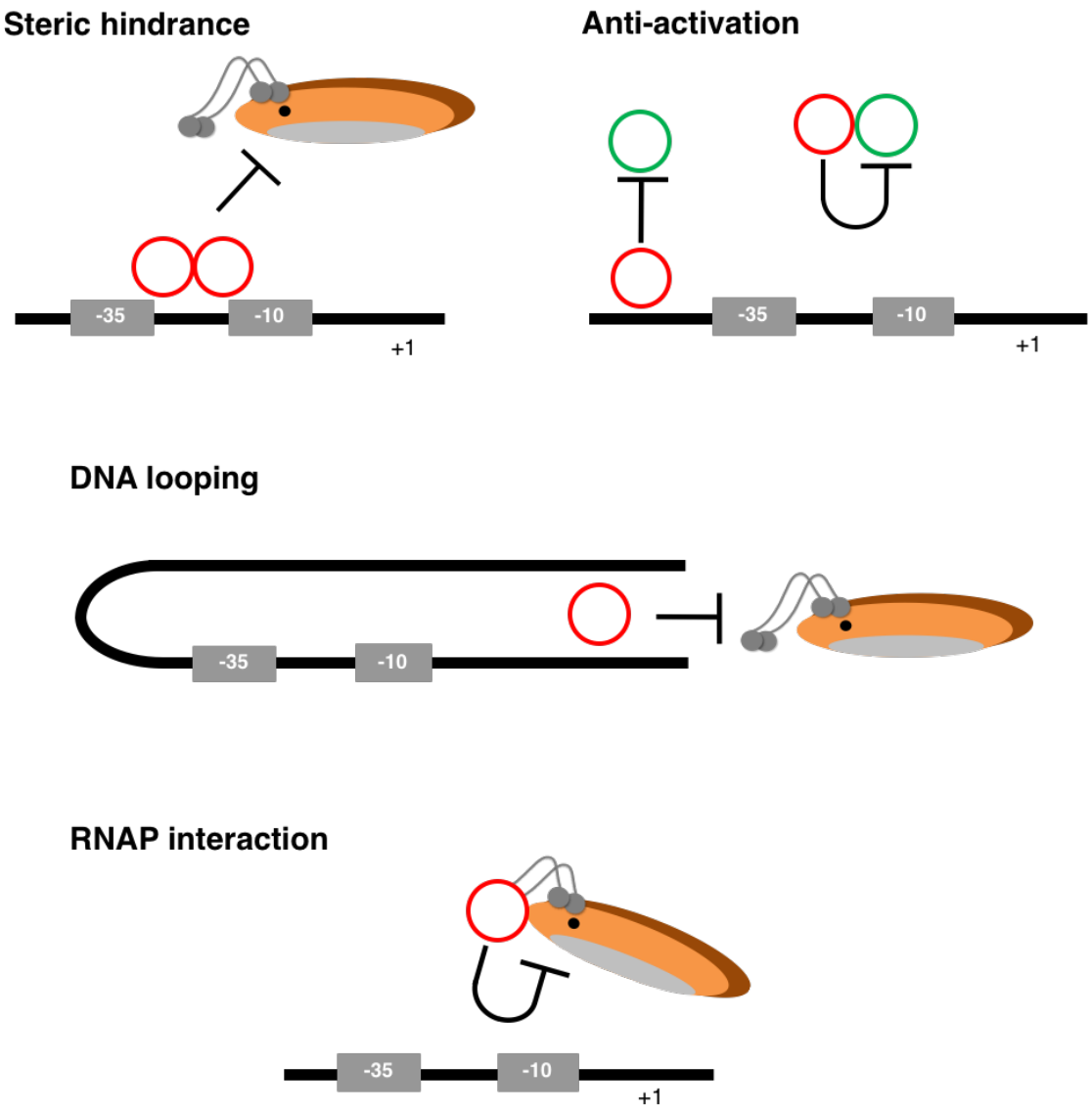

Figure 1.6 Mechanisms for repression of transcription by transcriptional repressors

Activator proteins are shown by green circles, with repressor proteins shown in red. The thick black line indicates the DNA, with the -35 and -10 elements indicated by grey boxes. Black T-shapes indicate inhibition.

Alternatively, a repressor may bind other components of transcription. Direct interaction with RNAP can prevent transcription, for example by preventing promoter clearance (Valentin-Hansen, Sogaard-Andersen and Pedersen 1996). For example, protein p4 of phage φ29 binds the α subunit of RNAP, and the DNA at position -71 (Monsalve *et al.* 1996, Monsalve *et al.* 1998). This excessively stabilises the initiating complex and traps RNAP, which is now unable to escape abortive transcription (Monsalve *et al.* 1996). This prevents transcription from an early-stage viral promoter, A2c; p4 simultaneously activates transcription from a late-stage viral promoter, A3, allowing a switch from early to late transcription in the virus' life cycle (Monsalve *et al.* 1996).

Transcriptional repressors show surprising versatility with the mechanisms of repression; for example, movement of the LacI operator to 3' of the transcription start site can switch repression from steric hindrance to inhibition of promoter escape (Lopez *et al.* 1998). Finally, repressors may inhibit transcription through anti-activation by binding a transcriptional activator. At transcription factor-dependent promoters, this may be enough to repress transcription; at others, additional mechanisms may be required (Valentin-Hansen, Sogaard-Andersen and Pedersen 1996).

1.3 Regulation of antibiotic resistance in *E. coli*

1.3.1 Challenges and development of antibiotic resistance

Overuse of antibiotics in agriculture and healthcare, and a slowdown in novel antimicrobial development, has lead to increasing rates of antimicrobial resistance (Goossens *et al.* 2005). This has created a worldwide health crisis, causing unnecessary

deaths, increased risks during routine medical procedures, and an economic burden on healthcare systems. By 2050, 10 million deaths per year will be attributable to antimicrobial resistance, along with a reduction in GDP of up to 3.5 % (O'Neill 2014). Multidrug resistance presents particular challenges, with strains of hospital 'superdrugs' arising which are resistant to all lines of treatment (Hampton 2013). Due to selective pressure, resistance is inevitable, however understanding the mechanisms of how bacteria acquire resistance can help inform prescribing practices and future drug development.

Antibiotic resistance occurs through three main mechanisms (Blair *et al.* 2015, Munita and Arias 2016). Firstly, the antibiotic's cellular target may be modified or protected. For example, Tet(M) in *Streptococcus* species provides protection for the cell against tetracycline toxicity, by interacting directly with the ribosome to remove tetracycline from its target site (Donhofer *et al.* 2012). The conformation of the ribosome is then altered by Tet(M) to prevent further binding of tetracycline.

Secondly, the antibiotic itself can be inactivated. Bacteria can produce enzymes which either destroy the drug itself or alter its structure to prevent interaction with the cellular target. This can be seen with chloramphenicol resistance; chloramphenicol acetyltransferases (CATs) provide the key resistance mechanism, inactivating the drug by acetylation (Schwarz *et al.* 2006). In other examples, inactivation may occur through phosphorylation, adenylation, dehalogenation, or glucuronidation of the compound.

Finally, reduced penetration or increased efflux of the antibiotic can result in reduced intracellular antibiotic concentrations. This mechanism would, of course, only be

appropriate for antibiotics with intracellular targets. Gram-negative bacteria have an additional advantage here; the increased selectivity of the outer membrane prevents antibiotics such as vancomycin from entering the cell. *E. coli* produces a number of porins which regulate entry into the cell, the main porins being OmpF, OmpC and PhoE. Porins form water-filled pores in cell membranes, through which small hydrophilic molecules can diffuse but large and lipophilic molecules cannot (Nikaido 1994). Thus, they can be a route of entry for some antibiotics and therefore also a route for resistance; loss of OmpF porin, for example, results in resistance to β-lactam antibiotics (Harder, Nikaido and Matsuhashi 1981).

Likewise, efflux pumps can pump compounds out of the cell via active transport to reduce intracellular antibiotic concentrations. These pumps may be associated with the efflux of just one compound, or have broad specificity (Webber and Piddock 2003). There are five major families of efflux pumps allowing for efflux of a range of compounds from the cell: ATP binding cassette (ATP), major facilitator (MF), multidrug and toxic efflux (MATE), resistance-nodulation-division (RND) and small multidrug resistance (SMR). Efflux pumps provide a certain amount of intrinsic resistance for the cell, with mutation resulting in overexpression of pumps allowing reduced susceptibility. Efflux pumps alone may not result in a clinical level of resistance; however, they may reduce susceptibility enough to allow for acquisition of additional mutations in a 'stepwise' manner (Kern *et al.* 2000, May, Ito and Okabe 2009). A key example of this is at the *mar* (multiple antibiotic resistance) locus found in *Escherichia coli*, which is a regulator of efflux. Mutation or overexpression of the *mar* operon can provide sufficient changes in tolerance and survivability to allow the cell to acquire further mutations leading to clinical resistance

(Cohen *et al.* 1989, Randall and Woodward 2002, Marcusson, Frimodt-Moller and Hughes 2009, Tavio *et al.* 2010). Likewise, the *mar* operon can be mutated subsequent to mutation of other genes implicated in antibiotic susceptibility, such as *gyrA* topoisomerase (Huseby *et al.* 2017).

1.3.2 Emerging antibiotic resistance challenges in *Escherichia coli*

Pathogenic *E. coli* strains are a major causative agent of gastroenteritis, urinary tract infections (UTIs), septicaemia, and meningitis. Antibiotic resistance is an current challenge within pathogenic *E.coli* strains; in 2015, the level of ciprofloxacin resistance in bloodborne *E. coli* infections was reported to be 18.8 %, with > 10 % resistance also seen to piperacillin, cefotaxime, ceftazidime, and gentamicin (Guy *et al.* 2016, Ukah *et al.* 2018). Resistance is also a major concern in UTIs, with Extended-Spectrum-Beta-Lactamase (ESBL)-producing *E. coli* on the increase, causing a rise of both resistant infections and complications such as sepsis (Briongos-Figuero *et al.* 2012, Picozzi *et al.* 2014, Ukah *et al.* 2018).

Worldwide, challenges can be seen with enterotoxigenic *Escherichia coli* (ETEC), which the primary cause of infant and traveller's diarrhoea in developing countries, resulting in over 700,000 deaths in children under the age of 5 every year (Gupta *et al.* 2008, Gonzales-Siles and Sjöling 2016). It is also a major pathogen of pigs, calves and small ruminants, causing farming losses of $100 million annually (Harvey *et al.* 2005). However, although childhood diarrhoea has a number of bacterial and viral aetiological agents, antibiotics are often dispensed without a prescription in countries where ETEC is endemic (Chuc and Tomson 1999). As a result, resistance to multiple antibiotics is

common; one study in Vietnam found multiple antibiotic resistance in 78.6 % of clinical ETEC samples (Nguyen *et al.* 2005). This is concerning, as antibiotic resistant ETEC is a threat not only to local populations, but also globally due to the advent of international travel.

1.3.3 *Mar* mediated multiple antibiotic resistance

Escherichia coli may possess mutations in the *mar* locus which cause constitutive activation. This has been reported in association with fluoroquinolone resistance in a number of human and animal clinical *E. coli* and *Salmonella* clinical isolates, including enterotoxigenic *E. coli* (ETEC) strain H10407 (Maneewannakul and Levy 1996, Oethinger *et al.* 1998, Webber and Piddock 2001, Crossman *et al.* 2010, Praski Alzrigat *et al.* 2017). Strains showing clinical fluoroquinolone resistance often display a phenotype consistent with *mar* overexpression; in one study, 21/57 clinical isolates showing high-level fluoroquinolone resistance also displayed cyclohexane tolerance, a phenotype highly associated with the *mar* genes, with 6 of these strains found to possess *mar* mutations resulting in constitutive expression (Oethinger *et al.* 1998). Additionally, 90 % of high-level fluoroquinolone-resistant isolates show AcrA overexpression, a key gene regulated by the *mar* sysyem (Mazzariol *et al.* 2000). As resistance to fluoroquinolones, a first-line antibiotic for treatment of *E. coli* infection, have risen from 1-3 % in 2008 to over 50 % in certain countries in recent years, *mar* mutations may therefore be presenting a very real clinical challenge (Spellberg and Doi 2015).

Strains containing *mar* mutations alone generally do not cross the threshold for clinical resistance for any antibiotics bar tetracycline, nalidixic acid and rifampicin (Alekshun

and Levy 1997, Randall and Woodward 2002). However, *mar* mutants show reduced sensitivity to a large number of unrelated antibiotics and can act both as a stepping stone to the development of further changes in antibiotic tolerance or as an add-on to existing susceptibility mutations (Cohen *et al.* 1989, Randall and Woodward 2002, Marcusson, Frimodt-Moller and Hughes 2009, Tavio *et al.* 2010). For example, *mar* mutants have been shown to develop high-level fluoroquinolone resistance at a higher rate than wildtype strains, and cross-resistance to fluoroquinolones can develop during selection with tetracycline and chloramphenicol (Cohen *et al.* 1989). The *mar* locus is therefore considered to play a much larger role in the development of clinical antibiotic resistance than previously thought (Randall and Woodward 2002).

Activation of the locus induces drug efflux via membrane transporters, as well as decreased uptake of antibiotic by porins (Cohen, McMurry and Levy 1988, Cohen *et al.* 1989, George 1996). This non-specific mechanism results in reduced susceptibility not only to a large number of unrelated antibiotics but also to other stress agents including oxygen radicals, weak acids, disinfectants and organic solvents (George and Levy 1983, Ariza *et al.* 1994, Rosner and Slonczewski 1994, White *et al.* 1997, McMurry, Oethinger and Levy 1998). This is known as the *mar* phenotype, a general stress response phenotype of both multiple antibiotic resistance and adaptational responses (Alekshun and Levy 1999).

The *mar* locus is usually transcriptionally silent due to inhibition by the *mar* repressor, MarR. However, the wildtype *mar* locus can be upregulated in response to stress and other environmental triggers, with a number of compounds including salicylate, 2,4-

dinitrophenol, paracetamol, chloramphenicol, tetracycline, and sodium benzoate shown to be inducers of *mar* (Hachler, Cohen and Levy 1991, Cohen, Hachler and Levy 1993, Seoane and Levy 1995*)*. Interestingly, upregulation of the *mar* system has also been shown during adherence of ETEC to epithelial cells (Kansal *et al.* 2013). Induction of the wildtype *mar* genes therefore raises questions on the clinical role of the *mar* system as challenging the view of the *mar* locus as one which is only clinically relevant when mutated. It is therefore vital to understand not only *mar* mutants, but also how the wildtype *mar* response may contribute to changes in antibiotic tolerance.

1.4 The *marRAB* operon

The *mar* locus comprises two divergent transcriptional units, *marRAB* and *marC* (Figure 1.7) (Alekshun and Levy 1997). Between the two is a central operator, *marO*, which controls operon expression via the promoters $Pmar_I$ and $Pmar_{II}$ (Cohen, Hachler and Levy 1993). Regulation of the operon is mediated at this operator region, by binding of the transcription factors MarR and MarA, the first two proteins encoded by *marRAB*, with the former inducing repression and the latter activation (Seoane and Levy 1995, Martin *et al.* 1996).

MarR binds as a dimer to two 21 bp palindromic sites in *marO*, shown in Figure 1.7, Panel A. Site I overlaps the -35 and -10 elements, whilst Site II is immediately upstream of *marR* (Martin, Nyantakyi and Rosner 1995). This binding is relieved in the presence of phenolic compounds such as salicylate, benzoate, and redox-cycling agents, which bind directly to MarR and inactivate it (Seoane and Levy 1995, Alekshun and Levy 1999). MarA binds upstream of *marO* to its binding site, the marbox, and thus activates

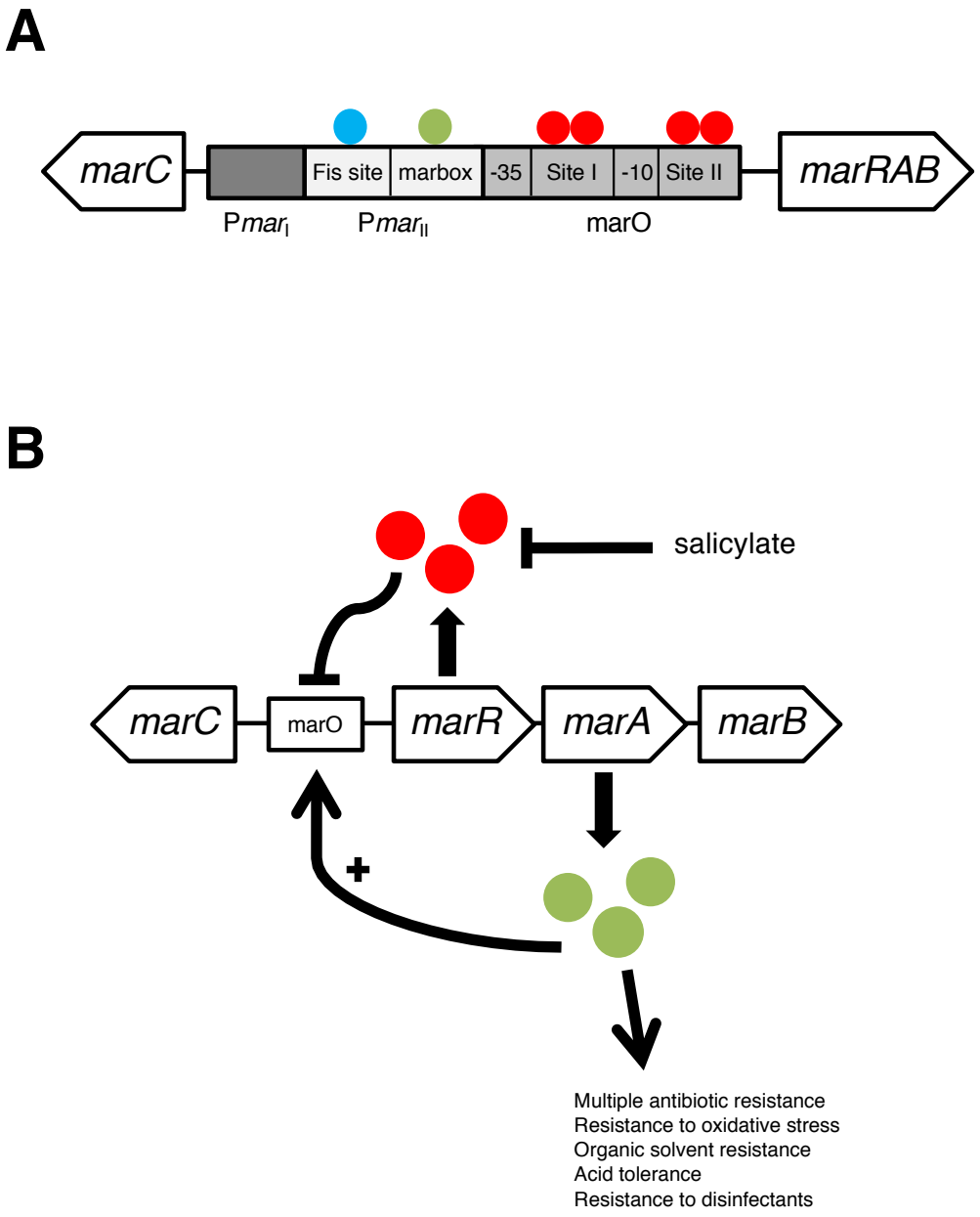

Figure 1.7 The *mar* locus.

White block arrows indicate genes; rectangles indicate marO. Coloured circles indicate the proteins MarR (red), MarA (green) and Fis (blue). Two divergent transcriptional units, *marRAB* and *marC*, are both controlled from a central operator region marO. MarR, encoded by *marR*, autorepresses *marRAB* at the central operator region marO. Mutations in either *marR* or marO lift this repression to allow MarA, encoded by *marA*, to bind to marO and induce transcription of *marRAB*. Efficient expression of MarA can then occur, allowing it to bind to downstream targets to induce the mar phenotype.

transcription from *marRAB*. Fis (factor for inversion stimulation protein) acts as an accessory transcription factor upstream of the marbox, bending the DNA to increase *marRAB* transcription twofold (Martin and Rosner 1997). Further regulation of MarA occurs post-translationally. Lon protease degrades MarA rapidly, resulting in a MarA half-life of 3 minutes; this ensures that the *mar* phenotype ends rapidly after stress signals are removed. As a result, MarA levels within the cell are very low (Griffith, Shah and Wolf 2004).

Mutation in either *marR* or *marO* leads to a loss of repression by MarR, allowing the *mar* genes to be constitutively expressed (Cohen, Hachler and Levy 1993, Ariza *et al.* 1994). The *mar* activator, MarA, can then bind downstream targets to mediate the *mar* stress phenotype. Mutations in MarR homologs in other bacteria result in a similar phenotype, such as Ms6508 in mycobacterium and MexR in *Pseudomonas aeruginosa* (Srikumar, Paul and Poole 2000, Zhang *et al.* 2014).

MarB, the third protein encoded by *marRAB*, is a small periplasmic protein but has no known function (Martin, Nyantakyi and Rosner 1995, Vinué, McMurry and Levy 2013). However it appears to indirectly repress *marRAB*; gene knockout results in increased antibiotic and stress resistance similar to that seen in Δ*marR* strains (Nichols et al. 2011, Vinué, McMurry and Levy 2013). MarC, which is encoded by *marC* divergent to *marRAB*, is putative inner membrane protein of unknown function which is not required for the *mar* phenotype (McDermott *et al.* 2008).

1.4.1 MarA, the activator of multiple antibiotic resistance

MarA is an AraC type transcriptional regulator (Rhee *et al.* 1998). They possess a conserved 100 amino acid C-terminal region which is predicted to form two helix-turn-helix DNA binding motifs (Gallegos *et al.* 1997). The two motifs have different amino acid sequences and therefore different binding specificities, meaning MarA binding is non-symmetrical and orientation specific.

The X-ray structure of MarA and its binding site (the marbox) is shown in Figure 1.8 (Rhee *et al.* 1998). MarA binds as a monomer, with the two helix-turn-helix DNA binding motifs inserting into two adjacent sections of the major groove of the DNA, bending the DNA by 35 degrees and making 15 contacts with the marbox (Gillette, Martin and Rosner 2000). Unlike other AraC members, MarA does not have a characteristic N-terminal dimerisation domain (Rhee *et al.* 1998); instead, the N-terminus (around helix 1) is key in DNA-binding. Two arginine residues (residue 5/6) in this region form crucial hydrogen bonds and potentially allow different conformations of MarA through their electrostatic contacts with the DNA backbone, facilitating MarA's ability to bind to divergent sequences (Dangi *et al.* 2001).

1.4.2 The marbox

MarA binds to its 20 bp marbox upstream of the RNAP binding site to activate transcription. The marbox can also be bound by two highly related proteins, SoxS and Rob (Martin *et al.* 1999). The marbox is non-palindromic; inversion of the marbox results in complete loss of regulation (Jair *et al.* 1995). Additionally, the marbox is highly degenerate, and as such defining the marbox presents a challenge; Figure 1.9 shows the

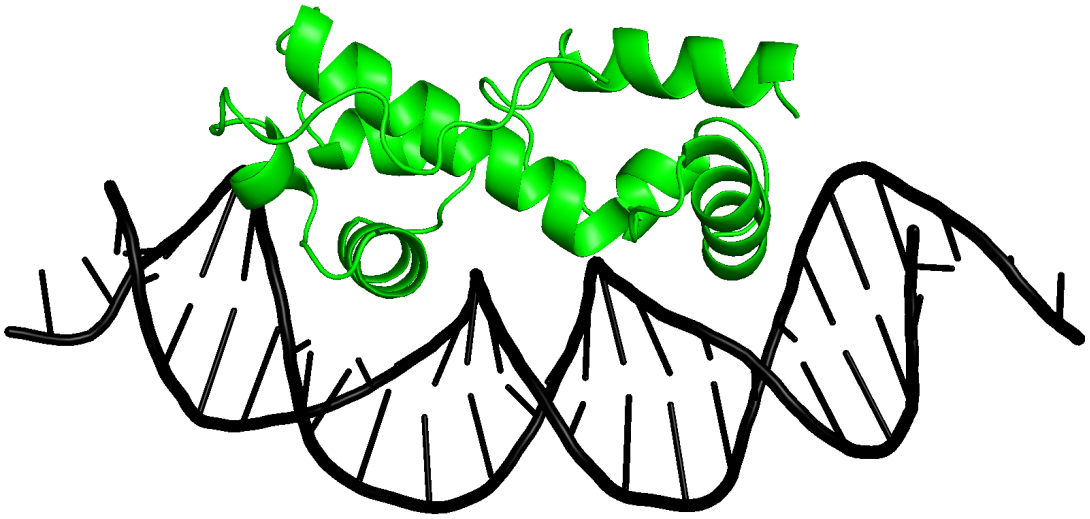

Figure 1.8 Crystal structure of MarA in complex with the marbox

Diagram of the structure of MarA in complex with the marbox, made using PyMOL from crystal structure data (Rhee *et al.* 1998). The DNA double helix is shown in black; MarA is shown in green. Helix 2 and 3 form the N-terminal helix-turn-helix motif, whilst helix 5 and helix 6 form the C-terminal motif; helix 4 connects them. Helix 3 and helix 6 are the major DNA binding elements, and can be seen binding two adjacent major grooves to cause bending of the DNA.

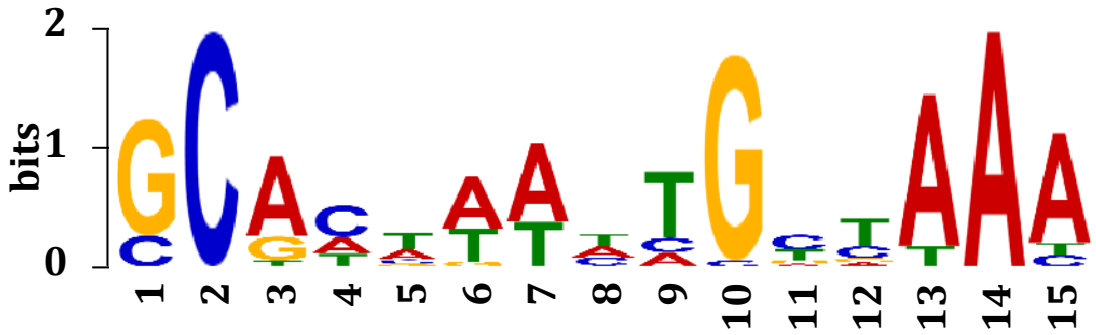

Figure 1.9 The marbox consensus sequence

The marbox consensus generated by a recent ChIP-seq experiment (Sharma *et al.* 2017). Numbering of the bases is shown; base positions referred to throughout will be in reference to the positions shown here.

published consensus from a MarA ChIP-seq (chromatin immunoprecipitation with sequencing) experiment by Sharma *et al.* (2017). The marbox is characterised by a conserved 5' GCA motif and 3' AAA motif; much of the sequence between is highly degenerate.

Location of the marbox is variable in relation to the -10 and -35 elements, but generally the marbox is found in one of three specific configurations (Martin *et al.* 1999):

Class I promoters - The activator binding site starts 38-40 or 50bp upstream of the -10 promoter element, in the backward orientation. The N-terminal helix-turn-helix therefore binds the downstream half of the target. Interaction with the α-CTD of RNAP is required (Jair *et al.* 1996, Jair *et al.* 1996).

Class I* promoters - The activator binding site is located 30bp upstream of the -10 promoter element, in the forward orientation, with the N-terminal helix-turn-helix therefore bound to the upstream half of the DNA target. This is seen only for *zwf*.

Class II promoters - The activator binding site overlaps the -35 promoter element, and is separated from the -10 promoter element by 18-19 bp. The binding site is orientated in forward direction, with the N-terminal helix-turn-helix motif bound to the upstream half of the target. In this location, activation involves interaction with region 4 of the σ^{70} subunit of RNAP (Zafar, Sanchez-Alberola and Wolf 2011).

1.4.3 Regulation of antibiotic resistance by MarA

As well as binding to *marO* to initiate expression of *marRAB*, MarA binds the marbox upstream of its target genes to induce the *mar* phenotype. This is characterised by increased tolerance to multiple antibiotics as well as to a range of environmental stresses including oxidative stress (Ariza *et al.* 1994), weak acids (Rosner and Slonczewski 1994), organic solvents (White *et al.* 1997, Aono 1998) and disinfectants (McMurry, Oethinger and Levy 1998).

The broad specificity of the *mar* phenotype is largely due to upregulation of membrane transporters, enabling non-specific drug efflux (George 1996). MarA binds upstream of *acrAB*, which encodes the AcrAB, which makes up part of the AcrAB-TolC efflux pump (Okusu, Ma and Nikaido 1996). AcrB is a channel protein connecting the cytoplasm and periplasm. AcrA is its adaptor protein, allowing AcrB to interact with TolC, which further continues the channel into the extracellular space. MarA also targets *tolC*, as well as *acrZ,* which controls the specificity of the pump (Hobbs *et al.* 2012). The AcrAB-TolC efflux pump plays a crucial role in antibiotic resistance and also in the efflux of lipophilic compounds (Nikaido and Takatsuka 2009).

An alternative mechanism for reduced antibiotic susceptibility in *mar* mutants is by decreased antibiotic uptake (Cohen *et al.* 1989). The MarA target *micF* is responsible for downregulation of the outer membrane general diffusion porin OmpF, reducing antibiotic accumulation in the cell (Cohen, McMurry and Levy 1988, Ziervogel and Roux 2013).

Additional experimentally confirmed MarA targets include *ybjC, zwf, fpr*, *fumC*, *sodA* and *inaA* ((Rosner and Slonczewski 1994, Jair *et al.* 1995, Martin *et al.* 2002). The total number of genes in the MarA regulon is unclear; differential expression studies indicate that MarA regulates up to 100 genes, but roughly 13,000 sequences matching the marbox can be found in the *E. coli* genome (Barbosa and Levy 2000, Griffith *et al.* 2002). A recent ChIP-seq experiment identified 33 targets, of which many were previously uncharacterised (Sharma *et al.* 2017).

1.4.4 Prerecruitment of RNAP by MarA

It is usually agreed that assembly of the activator-DNA-RNAP tertiary complex occurs first by formation of an activator-DNA complex, which then recruits RNAP (reviewed by Browning and Busby (2004)). However, activation of transcription by MarA occurs via pre-recruitment (Martin *et al.* 2002). This has also been described for the MarA homolog SoxS (Griffith *et al.* 2002). The activator-RNAP complex forms independently, then scans the DNA to specifically recognise activator binding sites. This activator-RNAP complex will only bind to genuine sites which are in the correct orientation and position for transcriptional activation. This complex is therefore able to scan and bind promoters more efficiently than the individual constituents as it has three 'reading heads' (one for the marbox, one for the -35, and one for the -10). This allows MarA and SoxS to respond rapidly under stress conditions (Griffith *et al.* 2002).

Pre-recruitment is thought to be necessary as there is a large abundance of marboxes per cell relative to the number of MarA molecules; approximately 65,000 possible binding sites would be present in rapidly dividing cells, of which only a small number are in the

correct position and orientation to be genuine targets (Griffith *et al.* 2002). A comparative number of MarA molecules would therefore be needed to activate transcription by classical recruitment of RNAP, which would be unfeasible. The pre-recruitment model allows for rapid activation of the *mar* phenotype without high concentrations of MarA in the cell.

1.4.5 Repression of transcription by MarA

Whilst MarA is an activator at the majority of its targets, it has been shown to act as a repressor at the *hdeA*, *purA* and *rob* promoters (Schneiders *et al.* 2004, Schneiders and Levy 2006). At the *hdeA* and *purA* promoters, MarA binds in the backward orientation overlapping the -35 element, in contrast to Class II activation in which MarA binds over the -35 in the forward orientation (Schneiders *et al.* 2004). This likely results in either differences in DNA bending, or different interactions being formed with RNAP which prevent the initiation of transcription, although no MarA-RNAP contacts have been identified which are specifically involved in repression (Schneiders and Levy 2006, McMurry and Levy 2010).

At the *rob* promoter however MarA binds in the backward orientation partly overlapping both the -10 and the -35 elements (Schneiders *et al.* 2004, Schneiders and Levy 2006). Here, MarA is thought to repress transcription by steric hindrance, binding the DNA prior to open complex formation to prevent access to the promoter elements by RNAP (Schneiders and Levy 2006, McMurry and Levy 2010). This mechanism however would not work with the prerecruitment theory, and raises questions on how MarA is able to effectively locate repressor sites within the cell, although it has been suggested that

disassociation of the MarA-RNAP complex could occur immediately prior to promoter binding in the case of repression (Schneiders and Levy 2006).

1.5 Rob and SoxS

1.5.1 SoxS, the regulator of oxidative stress

Two MarA homologs are present in *Escherichia coli*: Rob and SoxS. These co-regulators share MarA's degenerate binding site, allowing for overlapping control of the MarA/Rob/SoxS regulons. However, the three regulators respond to different stimuli and activate their targets to varying extents. This allows a highly adaptive response to cellular stresses, with small adjustments in the transcriptome possible.

SoxS promotes superoxide resistance within the cell, in response to oxidative stress agents such as paraquat. In the absence of oxidative stress SoxS exists at low basal levels in the cell due to repression by SoxR, a MerR family protein encoded divergently to SoxS, which binds as a homodimer to the *soxS* promoter (Wu and Weiss 1991). However, when the cell is under oxidative stress, SoxR is oxidised by redox cycling drugs; this converts SoxR into an activator of SoxS transcription (Figure 1.10) (Wu and Weiss 1992). Structurally, SoxS has 41 % identity and 67 % similarity with MarA, binding as a monomer via two helix-turn-helix motifs into two adjacent major grooves of the DNA (Li and Demple 1994). 25 SoxS targets have been identified by ChIP-exo (Seo *et al.* 2015). These include *zwf*, which encodes glucose-6-phosphate-dehydrogenase, *fpr*, which encodes ferredoxin NADP+ reductase, and *fumC*, which encodes fumarase C (Liochev and Fridovich 1992, Giro, Carrillo and Krapp 2006). Of these 25 targets, 7 were also

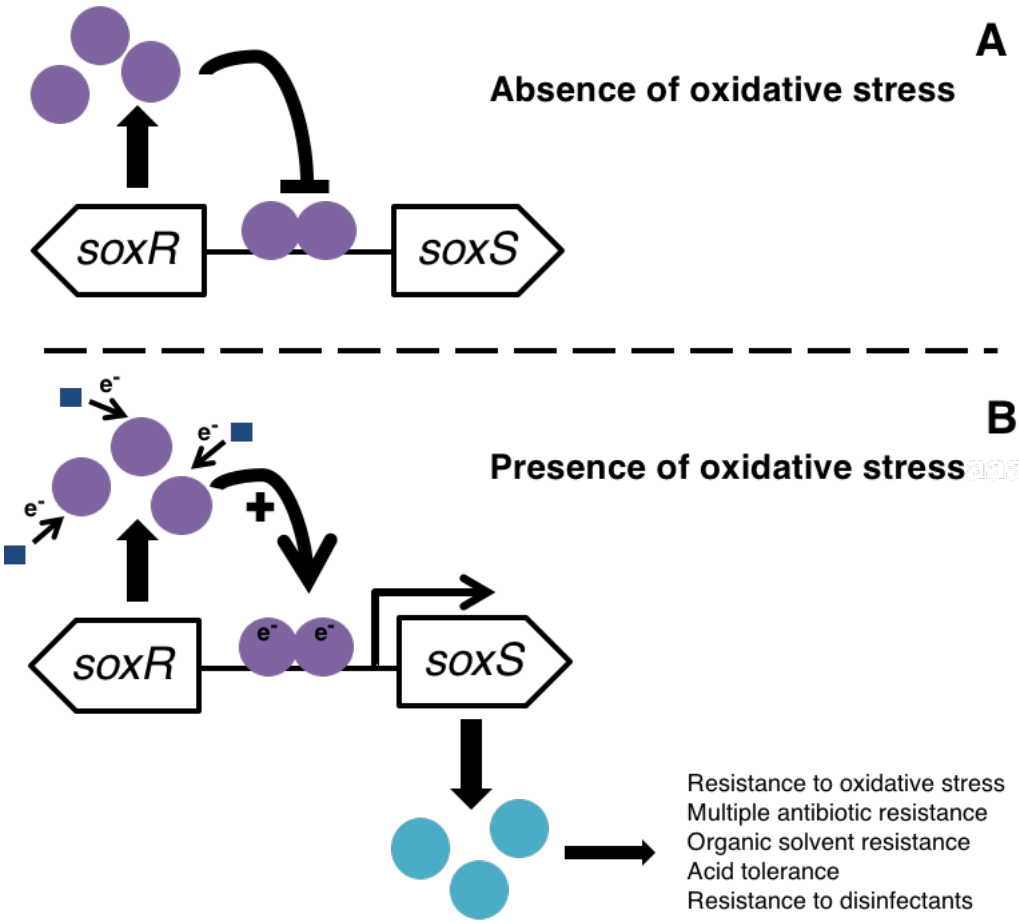

Figure 1.10 Activation of SoxS in response to oxidative stress

Adapted from Duval and Lister (2013). White arrows indicate genes. Coloured circles indicate proteins (purple = SoxR, blue = SoxS). Navy squares represent redox-cycling drugs.

A – In the absence of oxidative stress, SoxR binds as a homodimer to the *soxS* promoter to repress SoxS. Protease degradation ensures that SoxS levels remain low.

B – Under oxidative stress, the [2Fe-2S] cluster of SoxR is oxidised by redox-cycling drugs. SoxR repression is lifted; SoxR instead binds the same site to activate the *soxS* promoter (Hidalgo *et al.*, 1998). SoxS then acts back upon the P*soxS* mar/soxbox to repress its own transcription.

found to be regulated by MarA in our recent ChIP-seq study, highlighting the overlap between these two regulons (Sharma *et al.* 2017).

1.5.3 Rob

Rob shares 51 % identity and 71 % similarity with MarA. As with MarA and SoxS, Rob possesses two HTH motifs, however it is debated whether one or both motifs interact with the major groove of the DNA; the second is reported to interact with the DNA backbone instead and thus provide greater degeneracy in Rob's DNA binding properties (Kwon *et al.* 2000, Taliaferro *et al.* 2012). Rob also possesses the C-terminal domain lacking in MarA and SoxS (Kwon *et al.* 2000). This domain is responsible for sequestration of Rob in intracellular foci, as well as protection from Lon protease degradation (Griffith *et al.* 2009). Thus, Rob is constitutively expressed and abundant within the cell. However, due to sequestration, it mostly exists in an inactive state within the cell (Jair *et al.* 1996). Compounds such as dipyridyl, bile salts and fatty acids interact with the C-terminal to relieve Rob aggregation, freeing it from its intracellular clusters and allowing it to access the transcriptional machinery so that it may act upon downstream targets (Rosner *et al.* 2002, Griffith *et al.* 2009). Thus, activation of Rob occurs post-transcriptionally via a proposed 'sequestration-dispersal' mechanism. It is unclear, however, whether Rob is then re-sequestered after the inducing stress has been alleviated (Griffith *et al.* 2009).

1.5.4 Co-regulation by MarA, Rob and SoxS

Due to their shared binding site the MarA, Rob and SoxS regulons, and thus their resultant phenotypes, overlap. MarA and SoxS are equally effective at enhancing antibiotic resistance; SoxS has been shown to activate all known MarA targets to varying extents,

botb *in vivo* and *in vitro* (Greenberg *et al.* 1990, Martin, Gillette and Rosner 2000). MarA meanwhile is half as effective as SoxS at enhancing superoxide resistance (Martin *et al.*, 2000).

Many known MarA targets are shared with SoxS, such as *inaA, micF, fpr* and *fumC,* although the extent of binding and activation differs (Rosner and Slonczewski 1994, Martin, Gillette and Rosner 2000). Rob, however, shows less involvement in the MarA and SoxS co-regulons; although it is capable of binding to known MarA targets, at basal levels, it has been shown to activate only *mar* and *micF* (Martin, Gillette and Rosner 2000). However, overexpression of Rob results in a superoxide and antibiotic resistance phenotype similar to that seen for SoxS and MarA (Ariza *et al.* 1995). Intracellular concentration (or availability in the case of Rob) may therefore be key in allowing varied responses for these transcription factors.

As well sharing their targets, MarA, Rob and SoxS are also capable of regulating each other. Rob and SoxS are both transcriptionally repressed by all three transcription factors, whilst MarA is activated by all three (Martin and Rosner 1997, Michán, Manchado and Pueyo 2002, Schneiders and Levy 2006, Chubiz, Glekas and Rao 2012). Interestingly, autoregulation is only important at P*marRAB*; at P*soxS* and P*rob,* repression by their co-regulators is predominant over autoregulation (Chubiz, Glekas and Rao 2012). Transcriptional crosstalk between the regulons thus makes it impossible to consider these regulons in isolation.

1.6 Objectives of this project

Until recently, the full MarA regulon has remained a mystery, due to the challenges presented by MarA's uniquely degenerate binding site and the overlap with Rob and SoxS. Recent ChIP-seq analysis has unveiled novel targets which have previously remained uncharacterised (Sharma *et al.* 2017). Thus, this work aims to characterise the role of MarA regulation at some of these targets to elucidate novel mechanisms by which MarA can respond to cellular stress.

Secondly, the ChIP-seq targets may also be regulated by Rob and SoxS, due to a shared binding site. Above, we have discussed the importance of the regulatory overlap between these systems. Thus, in this work we have aimed to verify not only the presence of the MarA targets within the Rob and SoxS regulons, but also the nature by which these regulators discriminate between their targets.

Chapter 2
Materials and Methods

2.1 Materials

2.1.1 General buffers, reagents and solutions

Unless otherwise stated, all solutions were made with deionised and distilled water (ddH_2O) and autoclaved for 20 minutes at 121 °C prior to use. Where a pH is stated, solutions were pH adjusted at room temperature prior to autoclaving.

Polymerase chain reaction:

- 100 mM dNTP mix (Bioline): 25mM each of dATP, dGTP, dCTP and dTTP. This mix was diluted 1 in 10 with ddH_2O.
- Phusion DNA polymerase (New England Biolabs)
- Velocity DNA polymerase (Bioline)
- 5 x Phusion HF Buffer (New England Biolabs): PCR reaction buffer for use with Phusion DNA polymerase.
- 5 x Hi-Fi Buffer (Bioline): contains 10 mM Mg^{2+}. PCR reaction buffer for use with Velocity DNA polymerase.

Agarose gel electrophoresis:

- Agarose, powdered (Bioline)
- 6 x gel loading dye (New England Biolabs): 10 mM EDTA (diaminoethanetetra-acetic acid), 3.3 mM Tris-HCl, 0.02 % pink/red dye, 0.001 % blue dye, 2.5 % Ficoll®-400, pH 8
- 1 x TBE: diluted in ddH_2O from a 5 X stock from Fisher Scientific (0.445 M Tris borate pH 8.3, 10 mM Na_2EDTA)

Restriction digests

- 10 x CutSmart® buffer (New England Biolabs): 50 mM potassium acetate, 20 mM Tris-acetate, 10 mM magnesium acetate, 100 µg/ml BSA, pH 7.9

Phenol-chloroform extraction and ethanol precipitation

- Phenol/chloroform/isoamyl alcohol, pH 8.0 (25:25:1)
- 3 M sodium acetate (CH_3COONa), pH 5.2
- 100 % (*v/v*) ethanol
- 70 % (*v/v*) ethanol

Ligation of DNA fragments

- 10 x T4 DNA ligase buffer (New England Biolabs): 50 mM Tris-HCl, 10 mM $MgCl_2$, 1 mM ATP, 10 mM DTT, pH 7.5
- T4 DNA ligase (New England Biolabs)

Gene doctoring

- 20 % (*w/v)* arabinose solution: 1 g L(+) arabinose powder in 5 ml ddH_2O. The solution was sterilised using a 0.22 µM filter before use.

Preparation of chemically competent cells

- 100 mM calcium chloride
- 50 % (*v/v*) glycerol

End-labelling of fragments

- G-50 sephadex beads: these were resuspended with Tris-EDTA (TE) and washed three times before resuspension in TE to form a 12 % (*w/v*) slurry.
- Tris-EDTA: 10 mM Tris-HCl, 1 mM EDTA, pH 8.0
- T4 polynucleotide kinase (New England Biolabs)
- 10 x T4 polynucleotide kinase buffer (New England Biolabs): 70 mM Tris-HCl, 10mM $MgCl_2$, 5 mM DTT, pH 7.6
- [γ-^{32}P]-ATP (Perkin Elmer): 10 µCi/µl

Electrophoretic mobility shift assay (EMSA)

- 10 x TNSC buffer: 400 mM Tris acetate (pH 7.9), 10 mM $MgCl_2$, 1 M KCl, 10 mM DTT

In vitro *transcription*

- STOP solution: 97.5 % (*w/v*) deionised formamide, 10 mM EDTA, 0.3 % (*w/v*) bromophenol blue, 0.3 % (*w/v*) xylene cyanol
- NTP mix: 1 mM ATP/GTP/CTP, 50 µM UTP. Final concentrations in assay 200 µM ATP/GTP/CTP and 10 µM UTP
- 1 mg/ml bovine serum albumin (BSA). Final concentration in assay 100 µg/ml
- [α-^{32}P]-UTP (Perkin Elmer): 10 µCi/µl
- *E. coli* RNA polymerase core enzyme (New England Biolabs)

6 % denaturing sequencing gel and 7.5 % acrylamide gel electrophoresis

- UreaGel Concentrate (National Diagnostics): per 1 litre, contains 237.5 g acrylamide, 12.5 g methylene bisacrylamide, and 7.5 M urea.
- UreaGel Diluent (National Diagnostics): 7.5 M urea
- UreaGel Buffer (National Diagnostics): 0.89M Tris-Borate – 20 mM EDTA pH 8.3, 7.5 M urea
- 10 % (*w/v*) ammonium persulfate (APS) solution: 100 mg APS (Sigma-Aldrich) in 1 ml ddH_2O. Made fresh for use without autoclaving.
- TEMED (N, N, N', N'-tetramethylethylenediamine;)
- ProtoGel (National Diagnostics): 37.5:1 acrylamide:bisacrylamide

Beta galactosidase assays

- 1 % (*w/v*) sodium deoxycholate ($C_{24}H_{39}O_4Na$)
- 100 % (*v/v*) toluene (C_7H_8)
- Z-buffer: 8.53 g Na_2HPO_4, 4.87 g $NaH_2PO_4.2H_2O$, 0.75 g KCl, 0.25 g $MgSO_4$, made to 1 litre with ddH_2O.
- ONPG solution: 100 mg 2-nitrophenyl β-D-galactopyranoside (ONPG, $C_{12}H_{14}NO_8$; Sigma-Aldrich) and 677 µl β-mercaptoethanol (C_2H_6OS) dissolved in 250 ml Z-buffer, to make a final ONPG concentration of 13 mM. This was made fresh on the day without autoclaving.
- 1 M sodium carbonate (Na_2CO_3)

Crystal violet assay

- 0.1 % (*w/v*) crystal violet ($C_{25}H_{30}N_3Cl$) solution; 50 mg crystal violet powder dissolved in 50 ml ddH_2O.

Bradford assay

- Bradford reagent (Bio-Rad)

SDS-PAGE

- Protein ladder
- 5 x SDS loading dye: 10 mM Tris-HCl pH 7.5, 1 mM EDTA, 20 % glycerol, 0.025 % bromophenol blue, 0.025 % xylene cyanol
- NuPAGE™ 4-12 % Bis-Tris protein gel (Invitrogen)
- 10X NuPAGE™ MES SDS Running Buffer (Invitrogen): 500 mM MES, 500 mM Tris base, 10 % SDS, 10 mM EDTA, pH 7.3. Diluted to 1 x in ddH_2O.
- Staining solution: 50 % (*v/v*) methanol, 10 % (*v/v*) acetic acid, 2 g Brilliant Blue R, made to 1 litre with ddH_2O.
- Fast Destain solution: 40 % (*v/v*) methanol + 10 % (*v/v*) acetic acid, made to 1 litre with ddH_2O.

Purification of MarA and SoxS

- 1 M IPTG solution
- Lysis buffer: 50 mM Tris-HCl (pH 7.5)-1 mM EDTA-1 M NaCl
- Wash buffer: 4 M urea-50 mM Tris-HCl (pH 8.5)
- Denaturing buffer: 50 mM Tris-HCl (pH 8.5)-6 M guanidinium-HCl
- Buffer A: 1 M NaCl-50 mM Tris-HCl (pH 8.5)
- Buffer B: Buffer A + 1 M imidazole
- Buffer X: 1 M NaCl - 50 mM HEPES [N-2-hydroxyethylpiperazine-N'-2-ethanesulfonic acid, pH 8.0] - 1 mM dithiothreitol - 5 mM EDTA - 0.1 mM Triton X-100
- Thrombin sepharose beads (BioVision): 6 % cross linked sepharose beads in a 50 % slurry with glycerol.

2.1.2 Bacterial strains and plasmid vectors

All bacterial strains used in this study are shown in Table 2.1. All plasmid vectors used in this study are shown in Table 2.2.

2.1.3 Oligonucleotides

Oligonucleotides were obtained from Life Technologies. All oligonucleotides used in this study are shown in Table 2.3.

Table 2.1 *Escherichia coli* strains used in this study

Strain	Description	Source
JCB387	Δ*nirB Δlac*	Typas and Hengge (2006)
JCB387 *ΔycgZ-ymgA-ariR-ymgC*	Δ*nirB Δlac ΔycgZ-ymgA-ariR-ymgC*	This work
NCTC 10418	Reference strain for antimicrobial susceptibility testing	London, 1965
ATCC 25922	Reference strain for antimicrobial susceptibility testing	Human clinical sample, Seattle, 1946 (Minogue *et al.* 2014)
T7 Express	*fhuA2 lacZ::T7 gene1 [lon] ompT gal sulA11 R(mcr73::miniTn10--Tet^S)2 [dcm] R(zgb-210::Tn10--Tet^S) endA1 Δ(mcrCmrr)114::IS10*	New England Biolabs

Table 2.2 Plasmids vectors used in this study

Plasmid	Size	Description	Source
pRW50	16 kb	Encodes Tet^R. Features a cloning site upstream of a *lacZ* fusion. Used for β-galactosidase assays.	Lodge *et al.* (1992)
pSR	4 kb	Encodes Amp^R, derived from pBR322. Features a cloning site upstream of a λ*oop* terminator site. Used for *in vitro* transcription.	Kolb (1995)
pDOC-C	5.8 kb	Encodes Amp^R, derived from pEX100T. Used as a cloning vector for gene doctoring. Features a cloning region flanked by two I-SceI recognition sites.	Lee *et al.* (2009)
pDOC-K	7.2 kb	Encodes Amp^R, derived from pEX100T. Template for gene doctoring; features a kanamycin resistance cassette between two Flp recombinase recognition sites.	Lee *et al.* (2009)
pACBSR	7.3 kb	Encodes Cam^R. Recombination plasmid for gene doctoring; carries arabinose inducible λ-Red and I-SceI endonuclease genes.	Herring *et al.* (2003)
pCP20	9.4 kb	Encodes Cam^R and Amp^R. Encodes yeast FLP recombinase gene. Used to remove the kanamycin cassette in gene doctoring.	Cherepanov and Wackernagel (1995)
pBR322	4.4 kb	Encodes Tet^R and Amp^R.	Bolivar *et al.* (1977)
pBR322 *Δbla*	3.6 kb	Encodes Tet^R. Cloning vector used for complementation of *ycgZ-ymgA-ariR-ymgC*; the beta lactamase gene has been excised.	This study
pET28a	5.4 kb	Encodes Kan^R. Protein overexpression vector using the T7*lac* promoter; features both C-terminal and N-terminal His tags, an internal T7 tag, and a thrombin cleavage site.	Novagen

Table 2.3 Oligonucleotides used in this study

Name (F – forward; R – reverse)	Sequence (5' → 3') Restriction sites are underlined
Oligonucleotides for amplification of *ycgZ* regulatory region derivatives	
ycgZ.1-F, ycgZ.2-F, and ycgZ.1^{M}-F were used with ycgZ-R to generate derivatives of the regulatory region upstream of ycgZ, and with ycgZ-ymgABC-R to amplify the ycgZ-ymgABC operon under the control of the regulatory region derivatives.	
ycgZ.1-F	GCTGCTGAATTCATATGCATTAGCACTAATTGCA
ycgZ.2-F	GGTGTCGAATTCAATTTATCATTCTGTACACATATTTCG
ycgZ.1^{M}-F	GCTGCTGAATTCATATGCATTACGTCTAATTCGAAAAAATTAATT TATCATTCTGTACACATATTTCG
ycgZ-R	AGTAGTAAGCTTCATGCTACGCCTCTGTTA
ycgZ-ymgABC-R	GCATTGGACGTCCTAAGAGAGCACGGATTC
Oligonucleotides for creation of the pBR322Δ*bla* linker	
Δ*bla*-F	GCATCTATTAATCCAGCACTAACTACGATGCGCAGCGATAAGCA GGTAGGTCAACGTGCGATGCGTCATTCGGATTGCGATTTAGC
Δ*bla*-R	GCATGAGACGTCAAGTAACGATGCTCTGACTCGAAGATAGACTT GTGTTCTCTAAGCTAAATCGCAATCCGAATGACGCATCGCAC
Oligonucleotides for deletion of the *ycgZ-ymgABC* operon by gene doctoring	
ycgZ-ymgABC.GD-F	GCTGCTGAATTCTTCACTTAACATTGATTAACATTTTTAACAGAG GCGTAGCGACCGGTCAATTGGCTGGAG
ycgZ-ymgABC.GD-R	AGTAGTAAGCTTGTGATACAGCTGATGTTTATTCTAAAACCTTAC TCAAGTTAATATCCTCCTTAGTTCC
Oligonucleotides for amplification of the *mlaF* regulatory region derivatives	
All oligonucleotides were used with mlaF-R to generate derivatives of the mlaF.1 fragment	
mlaF.1-F	GGCTGCGAATTCTTTATGCGGCTAAAAAGTAAAAC
mlaF.1.inv-F	GGCTGCGAATTCTTTATGCGGCTAAAAAGTAAAACAAATGCAAT CGCTTTCGACCCACGGCGGGTAATATTCTG

mlaF.upE-F	GGCTGCGAATTCGCCAGCTTTCGCTAACCACG
mlaF.1.P1-F	GGCTGCGAATTCTTTATGCGGCTAAAAAGTAAAACAAATGCCAG CTTTCGCTAACCACGGCGGGTAAGGTTCTGTAAATATGTTGG
mlaF.1.U1-F	GGCTGCGAATTCTTTATGCGGCTAAAAAGTAAAACAAATGCCAG CTTTCGCTAACGCACGGCGGGTAATATTCT
mlaF.1.U2-F	GGCTGCGAATTCTTTATGCGGCTAAAAAGTAAAACAAATGCCAG CTTTCGCTAACCGCACGGCGGGTAATATTCT
mlaF.1.U3-F	GGCTGCGAATTCTTTATGCGGCTAAAAAGTAAAACAAATGCCAG CTTTCGCTAACACGCACGGCGGGTAATATTCT
mlaF.1.U4-F	GGCTGCGAATTCTTTATGCGGCTAAAAAGTAAAACAAATGCCAG CTTTCGCTAACGACGCACGGCGGGTAATATTCT
mlaF.1.U5-F	GGCTGCGAATTCTTTATGCGGCTAAAAAGTAAAACAAATGCCAG CTTTCGCTAACTGACGCACGGCGGGTAATATTCT
mlaF.1.U6-F	GGCTGCGAATTCTTTATGCGGCTAAAAAGTAAAACAAATGCCAG CTTTCGCTAACCTGACGCACGGCGGGTAATATTCT
mlaF.1.U7-F	GGCTGCGAATTCTTTATGCGGCTAAAAAGTAAAACAAATGCCAG CTTTCGCTAACACTGACGCACGGCGGGTAATATTCT
mlaF.1.U8-F	GGCTGCGAATTCTTTATGCGGCTAAAAAGTAAAACAAATGCCAG CTTTCGCTAACGACTGACGCACGGCGGGTAATATTCT
mlaF.1.U9-F	GGCTGCGAATTCTTTATGCGGCTAAAAAGTAAAACAAATGCCAG CTTTCGCTAACTGACTGACGCACGGCGGGTAATATTCT
mlaF.1.U10-F	GGCTGCGAATTCTTTATGCGGCTAAAAAGTAAAACAAATGCCAG CTTTCGCTAACCTGACTGACGCACGGCGGGTAATATTCT
mlaF.1.D1-F	GGCTGCGAATTCTTTATGCGGCTAAAAAGTAAAACAAATGCCAG CTTTCGCTAACACGGCGGGTAATATTCTG
mlaF.1.D2-F	GGCTGCGAATTCTTTATGCGGCTAAAAAGTAAAACAAATGCCAG CTTTCGCTAACCGGCGGGTAATATTCTG
mlaF-R	GCCCGAAGCTTCATAATTCACCCTTCGTCTTGC

Oligonucleotides for amplification of the MarA ChIP-seq targets for EMSAs

thrL-F	GGCTGCGAATTCGCTTTTCATTCTGACTGCAATG
thrL-R	CGCCCGAAGCTTCATGGATGTTGTGTACTCTG
leuL<>leuO-F	GGCTGCGAATTCGAAAAGCGTCGGTAGTTAAGCAG
leuL<>*leuO*-R	CGCCCGAAGCTTCATTAAATCAGCTCCAGATG

degP-F	GGCTGCGAATTCCTATAAAACGAATCTGAAGAACAC
degP-R	GCCCGAAGCTTCAGAGAGCGGAGATAACGCCAAAC
lacZ-F	GGCTGCGAATTCGGAAAGCGGGCAGTGAGCG
lacZ-R	CGCCCGAAGCTTCATAGCTGTTTCCTGTGTGAAATTG
ybaO-F	GGCTGCGAATTCTAACGAGATCCCTTCCAGCACCG
ybaO-R	CGCCCGAAGCTTCATAGCCCTTCCACAGAGAATTTTTTTCTC
pheP-F	GGCTGCGAATTCGGCGTATAAGCTGATGTGGCTG
pheP-R	CGCCCGAAGCTTCACGCCTTTCCCCTGTGTGTCTTTTTTGTTGAG
modE<>acrZ-F	GGCTGCGAATTCGTCTTATTGTGACGGAAAACGAACG
modE<>acrZ-R	GCCCGAAGCTTAATAACTCTAACATGGTCAACTCC
ybiV-F	GGCTGCGAATTCCGTCGTTAAGAAAAGTACCGTCCAT
ybiV-R	CGCCCGAAGCTTATTCGAAATATAATTTGTGCTCTGC
grxA<>ybjC-F	GGCTGCGAATTCGCGCGCATACGCTTCCCTCTG
grxA<>ybjC-R	CGCCCGAAGCTTCATTATTTCTCTCCTCATAG
ycgZ<>bluF-F	GGCTGCGAATTCTTGAACACTAGTTGGCGAAAAATCTTG
ycgZ<>bluF-R	CGCCCGAAGCTTCATGCTACGCCTCTGTTAAAAATG
fnr-F	GGCTGCGAATTCAGGTTATCTTTTGCTGTAAACATTAAACAATTTGTG
fnr-R	CGCCCGAAGCTTCATAGGTCTGCTCAAGCCGTAATTG
yneO-F	GGCTGCGAATTCGAAAACTGTTTCTTTCAATAGGA
yneO-R	GCCCGAAGCTTGCATTAAGCACAACCCTTATTTTATA
marC<>marR-R	GGCTGCGAATTCTTCCGCTTCGGGGTGAAATAGTAG
marC<>marR-R	CGCCCGAAGCTTCATTAGTTGCCCTGGCAAGTAATTAG
yeeF-F	GGCTGCGAATTCCATAATAATTTTTCTTTAAATGGC
yeeF-R	GCCCGAAGCTTGGACTTGCCAGTGGCTGGTGGCGG
ompC<>micF-F	GGCTGCGAATTCGGTTAAAATCAATAACTTATTCT
ompC<>micF-R	GCCCGAAGCTTATTCAGAAATGAATGACGGTAATA

ypeC-F	GGCTGCGAATTCATCGTCCGAAGCAACAGCCCC
ypeC-R	CGCCCGAAGCTTCATTGTTATTCTCCTTCACGATCG
yfeS><cysM-F	GGCTGCGAATTCCGGCGTTTCCTCACGAAAATTAA
yfeS><cysM-R	GCCCGAAGCTTTGCAATATATTGAATTAGCACGAT
guaB<>xseA-F	GGCTGCGAATTCGTAACCGATTGCATCTACCCCTTTTTGC
guaB<>xseA-R	GCCCGAAGCTTCATGTGAGCGAGATCAAATTCTAAATCAG
ETEC_3200-F	GGCTGCGAATTCGCCGCCAGACAACAACCCATACTTT
ETEC_3200-R	CGCCCGAAGCTTTGACTATCTCGCGAAAGAGTACACCA
nudF<>tolC-F	GGCTGCGAATTCGACTGCCGTTTGAGCAGTCATGTG
nudF<>tolC-R	GCCCGAAGCTTTTCTAGCAGAAGCCGCTACCGCAA
yhbV-F	GGCTGCGAATTCCTGGCTGGAGATGGCAAAATCGCT
yhbV-R	GCCCGAAGCTTTCAATCAGAAACTCACCGTTCTC
mlaF<>yrbG-F	GGCTGCGAATTCTTTATGCGGCTAAAAAGTAAAAC
mlaF<>yrbG-R	GCCCGAAGCTTCATAATTCACCCTTCGTCTTGCG
ibpA<>yidQ-F	GGCTGCGAATTCCCCTCAGTCTATGCAATAGACCATAAACTG
ibpA<>yidQ-R	CGCCCGAAGCTTCATAATCAATAGCTCCTGAAATCAG
yihT-F	GGCTGCGAATTCGATATGGTCATTCAGACGTTGTGA
yihT-R	GCCCGAAGCTTAAATTCGATCGCGAACAAGCGATC
ETEC4304-F	GGCTGCGAATTCGTAAGCCTATAGACCTGAAAGAA
ETEC4304-R	GCCCGAAGCTTGTTCCTTTCCTGTATGGCTGATA
ETEC4307-F	GGCTGCGAATTCATGGTGGGAATATATACCATAGC
ETEC4307-R	GCCCGAAGCTTAATAGCTTTCTGGCAAAAACACC
ETEC4702-F	GGCTGCGAATTCGACAGATGATAATTATTTCATGA
ETEC4702-R	GCCCGAAGCTTGACCGCTAATGCTGTTGTCAGCC
deoB-F	GGCTGCGAATTCCGAAAGACGAAAACAGCTGGCA
deoB-R	GCCCGAAGCTTCAGTATACCGTTATTCACTGATA
ETEC p9480770-F	GGCTGCGAATTCGCAGATTCGAGATTAATTTTGGGTC

ETEC p9480770-R	GCCCGAAGCTTTAAAGGATTAGGCAAAAATAGCG
estA-F	GGCTGCGAATTCTAACATGATGCAACTCACAAAAAAAAT AAAAAAATTGCAAAATCCGTTTAACTAATCT
estA-R	GCCCGAAGCTTCATGTTACCTCCCGTCATGTTGTTTCACGGATA TTTGAGATTAGTTAAACGGATTTTG

Oligonucleotides for amplification of the SoxS ChIP-exo targets for EMSAs

lpxC-F	TCTACTGAATTCGCATTCCTGCGTAAGCAAGC
lpxC-R	TCTACTAAGCTTTGTAAACCGACACCCGTCGC
acrAB-F	TCTACTGAATTCAGCTGCTTTTGCAATCTCGC
acrAB-R	TCGACGAAGCTTGTTAATAAACCCATTGCTGC
uof-fur-F	TCTACTGAATTCACAGATTTCTGAAGAGTTGC
uof-fur-R	TCTACTAAGCTTTTACATTTACAACGGCAAGG
acnA-F	TCTACTGAATTCCTCTGTCGATGCTCTTCTGG
acnA-R	TCGACGAAGCTTCATAGCTCCTCCTTAATGAC
ribA-F	TCTACTGAATTCGTACGTCTGGCAATCGAACG
ribA-R	TCGACGAAGCTTCATGAAATTCTCCAGATAATGC
ydbK-F	TCTACTGAATTCAATAATAGGCAGCACAGAGG
ydbK-R	TCTACTAAGCTTCATATGACACCCTTACATTGC
nhoA-F	TCGACGGAATTCAACGAAATTAACGGGATTGG
nhoA-R	TCTACTAAGCTTTGTTTCAGGTGCAATGCACG
fumC-F	TCTACGGAATTCAGGAAATGACTTCTTCCAGCAG
fumC-R	TCTACTAAGCTTCATGACCTGCTCCTCACCTG
zwf-F	TCGACTGAATTCCATAACATGATCAGTGTCAG
zwf-R	TCTACTAAGCTTAACTAACCCGGTACTTAAGC
nfo-F	TCTACTGAATTCGGCGAAACCTCTGCTGATGG
nfo-R	TCTACTAAGCTTCATGCGAGGACTCCTGTTAAACC
aroF-tyrA-F	TCTACTGAATTCCAGAGGTAAGGGTTGAAAGC

aroF-tyrA-R	TCGACTAAGCTTGAGTCATTAAAACCTGTTCG
yrbL-F	TCTACTGAATTCGTCATTTGTACATTTTGTGC
yrbL-R	TCTACTAAGCTTGTAGACAATCTTGATACAGC
nepI-F	TCTACTGAATTCCTTTGCCCTGTTCCGTTTCG
nepI-R	TCGACTAAGCTTAAAACGCCACCGAGAAAACG
sodA-F	TCTACTGAATTCTCGATTTACTGGCAATCACG
sodA-R	TCGACTAAGCTTCATATTCATCTCCAGTATTGTCG
fpr-F	TCTACTGAATTCGGCAAGTCACGCACCATTCG
fpr-R	TCGACGAAGCTTTTGCCTGTTACCCAATCAGC
soxS-F	TCTACTGAATTCGGTTAGCAGCGCTTTAATGC
soxS-R	TCGACGAAGCTTCGACTACATCAATGTTAAGC

Oligonucleotides for generation of constructs for MarA and SoxS overexpression

MarA.OE-F/R generate the WT MarA fragment. E31D-R and MarA.Q58D-R primers were used with MarA.OE-F to create a megaprimer for a second round of PCR with MarA-OE.R, to generate the E31D and Q58D mutants. SoxS.OE-F/R generate the WT SoxS fragment.

MarA.OE-F	CCCAATTCCATATGTCCAGACGCAATACTGACGC
MarA.E31D-R	CACTTTGTCCAGTGACAGTGGCGATTCCAGG
MarA.Q58D-R	GCGGATGTAATCGCCTAATGAATGACCGGTTTC
MarA.OE-R	GGCGGATCCCTACGACTTATCACTGCCAGTACC
SoxS.OE-F	CGCAGGTGCATATGTCCCATCAGAAAATTATTCAGG
SoxS.OE-R	AATAATGGATCCTTACAGGCGGTGGCGATAATCG

Oligonucleotides for sequencing of candidate plasmid constructs

pRW50-F	GTTCTCGCAAGGACGAGAATTTC
pRW50-R	AATCTTCACGCTTGAGATAC
pSR-F	CCATATATCAGGGTTATTGTCTC
pSR-R	CATCACCGAAACGCGCGAGG
pBR322-F	GGCTGCGTGCCACCTGACGTCTAAGAAACC

pBR322-R	GCCCGCAGCATCCAGGGTGACGGTGCCGAG
pET-F	GATTATGCGGCCGTGTAC
pET-R	ATGCGTCCGGCGTAG

2.1.4 Media for bacterial growth

The following media were used for bacterial growth:

- LB broth (Sigma-Aldrich): 10 g/L tryptone, 5 g/L yeast extract, 5 g/L NaCl
- LB agar (Sigma-Aldrich): 10 g/L tryptone, 5 g/L yeast extract, 5 g/L NaCl, 15 g/L agar
- MacConkey agar (Oxoid): 20 g/L peptone, 10 g/L lactose, 5 g/L bile salts, 5 g/L sodium chloride, 0.075 g/L neutral red, 12 g/L agar, pH 7.4

All media were dissolved in ddH_2O and autoclaved at 121 °C for 20 minutes to sterilise. Agar plates were dried for 20 minutes in a flow hood prior to use.

2.1.5 Antibiotics

Antibiotics were added to media as appropriate for the plasmid and strain to be selected (Table 2.1 and Table 2.2), at the following concentrations:

Ampicillin: 100 μg/ml (stock 100 mg/ml, dissolved in ddH_2O)

Chloramphenicol: 35 μg/ml (stock 35 mg/ml, dissolved in ethanol)

Kanamycin: 50 μg/ml (stock 50 mg/ml, dissolved in ddH_2O)

Tetracycline: 35 μg/ml (stock 35 mg/ml, dissolved in methanol)

All antibiotic stocks were stored at -20 °C.

2.2 Methods

2.2.1 Polymerase chain reaction

PCR reactions were done in a 50 µl volume containing 0.5 mM deoxynucleotide triphosphates (dNTPs), 1 µl of Phusion (Bioline) or Velocity (New England Biolabs) DNA polymerase, and 10 µl of corresponding reaction buffer. 20 pmol of each oligonucleotide primer (Table 2.3) and 1 µl of template DNA (derived from either a plasmid miniprep or from a bacterial boilprep) was used per reaction. Typical cycling parameters are shown in Table 2.4. Annealing temperatures varied and were calculated as 5 °C below the T_m of the primers. For generation of DNA fragments larger than 1 kb, an elongation time of 45 seconds was used.

2.2.2 Megaprimer polymerase chain reaction

Megaprimer PCR was used to generate mutations in DNA fragments lacking an appropriately position restriction site. The method is outlined in Figure 2.1. An initial round of PCR was used to generate the megaprimer containing the mutation. This megaprimer was purified by gel extraction, then used as a primer for a second round of PCR to generate the full-length mutated product.

2.2.3 Agarose gel electrophoresis

Gel electrophoresis was used to check DNA fragment sizes and for purification of specific DNA bands. 1 % (*w/v*) agarose gels were made by the addition of 1 g agarose per 100 ml of 1 X TBE. The solution was microwaved at full power for one minute until agarose was dissolved, and 10 µl (1 % *v/v*) of ethidium bromide or SYBR® Safe was then added before the gel was left to set. After loading of DNA samples in 1 x

Table 2.4 Typical PCR cycling conditions used

Stage	Description	Number of cycles	Temperature	Time
1	Initial denaturation	1	95 °C	5 min
2	Denaturation	35	95 °C	30 sec
	Annealing		50 °C – 65 °C	30 sec
	Elongation		72 °C	30 sec
3	Final elongation	1	72 °C	10 min

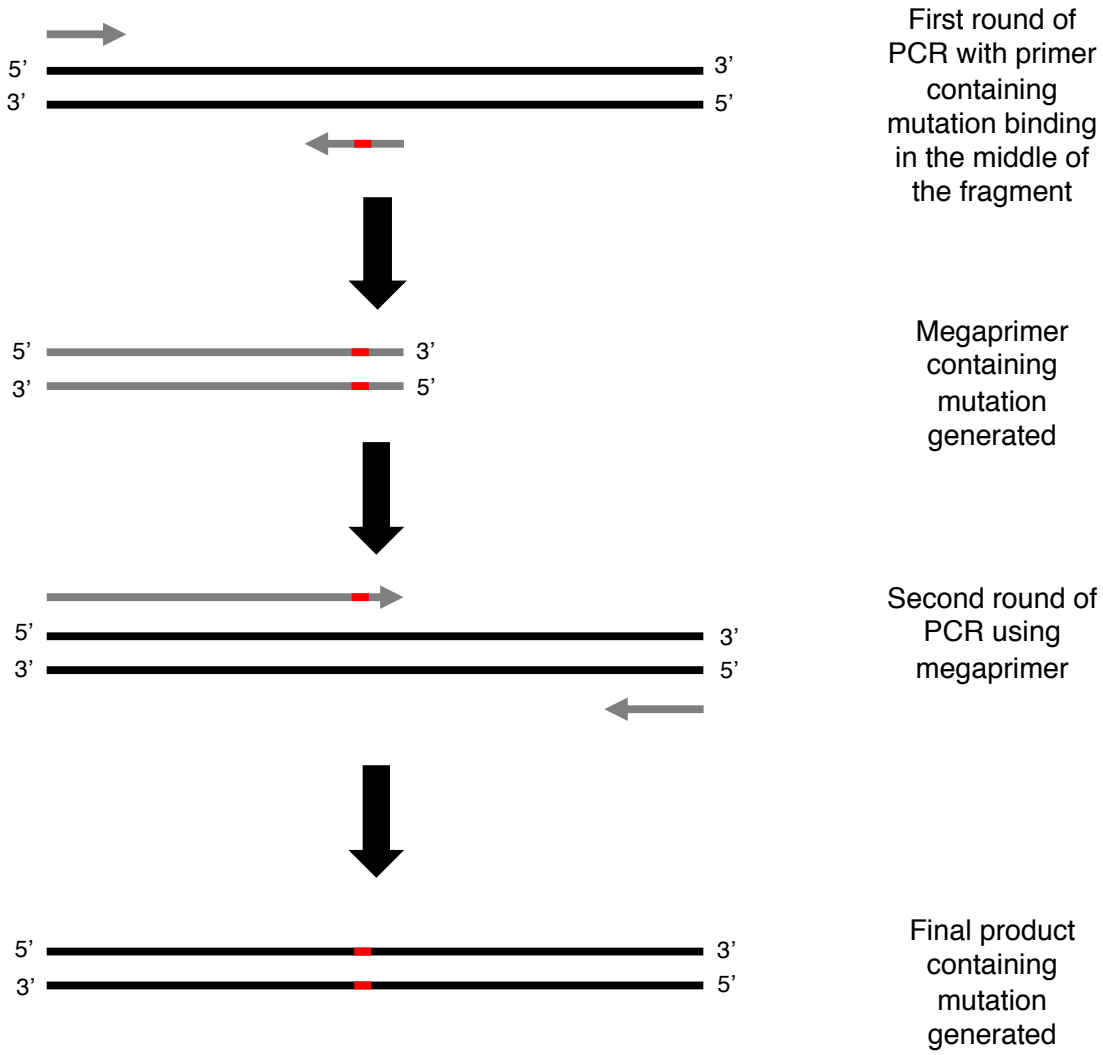

Figure 2.1 Megaprimer PCR

The figure shows a schematic of the megaprimer PCR procedure. Double stranded DNA is shown by pairs of black lines, with oligonucleotide primers shown by grey arrows. Introduced mutations are shown in red.

loading dye, gels were run at 110 V for 45 minutes in 1 x TBE running buffer before visualisation using a UV transilluminator.

2.2.4 PCR purification using the Qiagen PCR Purification Kit

PCR products were purified using the Qiagen PCR Purification Kit according to the manufacturer's instructions, removing unwanted contaminants such as primers, enzymes and salts. DNA fragments under 100 bp, or larger than 10 kb, are removed by the kit.

2.2.5 Restriction digests

Restriction digests were done using enzymes supplied by New England Biolabs. For single digestion of fragments, 43.5 µl of DNA solution was digested using 1.5 µl of restriction enzyme in a 50 µl reaction; double digestions were done using 42 µl of DNA solution and 1.5 µl of each enzyme, again in a 50 µl reaction. Double digestions of plasmid DNA maxipreps were done in a 90 µl reaction using the same ratios. All restriction digests were done in 1 x CutSmart® buffer at 37 °C for 3 hours. For plasmid vectors, 4 µl of Calf Intestinal Alkaline Phosphatase (New England Biolabs) was added for the last 30 minutes of the restriction digest, to prevent self-ligation of the plasmid.

2.2.6 Gel extraction using the Qiagen Gel Extraction Kit

Gel extraction was used to further purify DNA, such as to remove enzymes after restriction digestion or PCR. After separation of DNA bands on a 1.5 % agarose gel, the correct band was excised using a razor blade and DNA extracted from the gel slice using the kit, according to the manufacturer's instructions.

2.2.7 Phenol-chloroform extraction

For plasmid vectors larger than 10 kb (such as pRW50), phenol chloroform extraction was used to purify the vector after restriction. Equal volumes of DNA solution and phenol-chloroform were vortexed for 15 seconds before centrifugation at 17,000 x g for 3 minutes. The aqueous phase was transferred to a fresh tube containing a 3 x volume of ice-cold 100 % ethanol and a 0.1 x volume of 3 M sodium acetate. The sample was incubated at -80 °C for at least 30 minutes, prior to centrifugation at 17,000 x g for 30 minutes at 4 °C. The supernatant was removed and the pellet washed with ice-cold 70 % ethanol, before centrifugation as before for 20 minutes. The supernatant was removed again and the pellet dried using a vacuum before resuspension in ddH_2O.

2.2.8 Ligation of DNA fragments into cloning vectors

DNA fragments were ligated with plasmid vectors with complementary 5' and 3' overhangs. Ligations were done in a 20 µl reaction comprising 2 µl 10 x T4 DNA ligase buffer, 1 µl T4 DNA ligase (New England Biolabs) and a typical vector:insert ratio of 1:3. A vector-only reaction was included as a negative control. Reactions were left at room temperature for 2 hours, or overnight at 17 °C.

2.2.9 Plasmid DNA extraction

Minipreps and maxipreps were done with the relevant Qiagen kits, according to the manufacturer's instructions. 5 ml overnight cultures were used for miniprep extraction, whilst 100 ml (high copy number plasmids such as pSR and pBR322) or 250 ml (low copy number plasmids such as pRW50) cultures were used for the maxiprep extraction.

2.2.10 Sequencing of plasmids and DNA fragments

Sequencing was done by the Functional Genomics and Proteomics Facility at the University of Birmingham. 10 µl reactions contained 3.2 pmol of primer and variable amounts of DNA template, according to the facility guidelines. Typically, sequencing of a miniprep required 200 ng of DNA; sequencing of PCR products varied from 1-100 ng, depending on size.

2.2.11 Gene deletion using gene doctoring

Genes were deleted from *E. coli* strains using the method outlined by Lee *et al.* (2009), shown in

Figure 2.2. The kanamycin cassette was amplified from the pDOC-K plasmid, using primers complementary to the K-FWD and P-REV regions flanked by homology to the regions directly upstream and downstream of the gene to be deleted. This fragment was cloned via the *Eco*RI/*Hin*dIII sites into the pDOC-C plasmid, which along with the pACBSR plasmid was used to co-transform the strain of choice.

Strains were treated with 0.4 % arabinose, shaking at 37 °C for 2.5 hours. This induces I-SceI, encoded on pACBSR, to cleave the donor plasmid, providing linear DNA for λ-Red to recombine with the recipient chromosome. Recombinants were screened on LB + 5 % sucrose + 50 mg/ml kanamycin plates grown at room temperature for 72 hours. Successful recombinants were screened for loss of the pDOC-C and pACBSR plasmids, and recombination was verified by colony PCR and subsequent sequencing.

The kanamycin cassette was removed from verified recombinant strains. Strains were transformed by the pCP20 plasmid, using a recovery and overnight growth temperature

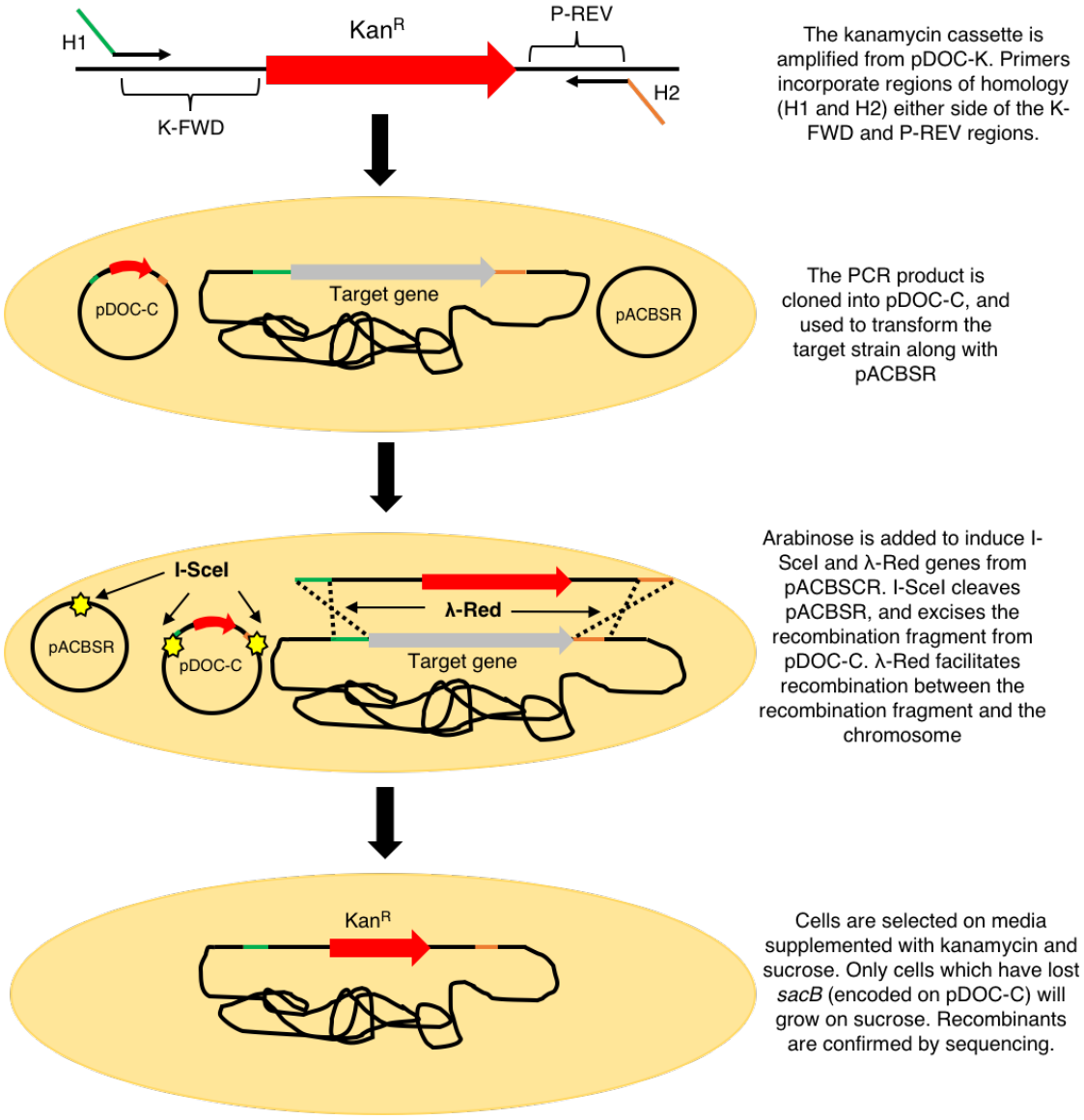

Figure 2.2 Deletion of genes by gene doctoring

The schematic shows the gene doctoring protocol developed by Lee *et al.* (2009). Genes are shown as block arrows, with Kan^R in red and the gene to be deleted in grey. Thick black lines indicate DNA; the bacterial genome is shown as a tangled mass of DNA. Regions of homology upstream and downstream of the target gene are shown in green (H1, upstream) and orange (H2, downstream). Recombination is shown by dotted lines. Cleavage by I-SceI is shown by yellow stars.

of 30 °C. The pCP20 FLP recombinase genes were then induced by streaking onto non-selective LB plates and growing overnight at 37 °C. Excision of the kanamycin cassette was checked by colony PCR and sequencing.

2.2.12 Growth of bacterial cultures

Bacterial strains used in this study are listed in Table 2.1. Unless stated otherwise, all cultures were grown at 37 °C, shaking at 200 rpm. Typically, LB was used, with the exception of MacConkey agar for screening of promoter-*lacZ* fusions.

2.2.13 Preparation of chemically competent cells

1 ml of an overnight bacterial culture was used to inoculate 50 ml of fresh media and grown to an OD_{600} of 0.3-0.6. The culture was then chilled on ice for 10 minutes before centrifugation at 1,600 x g for 5 minutes at 4 °C. Cells were resuspended in 25 ml ice-cold calcium chloride and incubated on ice for 20 minutes, before centrifugation again at 1,600 x g for 5 minutes at 4 °C. The cells were resuspended in 3.3 ml ice-cold calcium chloride and incubated overnight on ice. Cells were then stored at -80 °C in 15 % glycerol.

2.2.14 Transformation of chemically competent bacterial cells

100 µl of competent cells were mixed with either 100 ng of plasmid DNA or an entire ligation reaction and left to incubate on ice for one hour. Cells were then heat shocked at 42 °C for 2 minutes, before the addition of 900 µl of LB media. The reaction was incubated at 37 °C for 45 minutes, shaking at 200 rpm. Cells were then pelleted by centrifugation at 2,400 x g for 3 minutes, and the resulting pellet resuspended in 100 µl LB and plated on selective agar (as outlined in Table 2.2). Exceptions were made for

the temperature-sensitive plasmid pCP20; where recovery and growth on agar were done at 30 °C.

2.2.15 End-labelling of fragments for EMSA with T4 polynucleotide kinase

DNA fragments were prepared for 5' end labelling by PCR amplification, clean up (Qiagen PCR Purification Kit), digestion with *Eco*RI, and gel extraction. To label, fragments were incubated for 30 minutes at 37 °C in a 20 µl reaction comprising 16 µl of DNA digested by *Eco*RI, 1 µl T4 polynucleotide kinase, 2 µl of the supplied 10x T4 polynucleotide kinase buffer, and 1 µl [γ-^{32}P]-ATP. Labelled DNA was passed through a G-50 column for 3 minutes at 2,400 g to remove unincorporated radioactivity; the eluate was then collected and passed again through a fresh column, under the same conditions.

2.2.16 Electrophoretic mobility shift assay (EMSA)

[γ-^{32}P]-ATP labelled DNA was used for electrophoretic mobility shift assays (EMSAs). For each reaction, 20-30 counts of labelled DNA was mixed with 1 x TNSC buffer and 12.5 µg/ml Herring sperm DNA (as a non-specific competitor), to a final volume of 10 µl. The labelled DNA mix was incubated with 10 µl of protein/1 x TNSC mix at 37 °C for 20 minutes. The reactions were loaded on a 7.5 % polyacrylamide gel (10 ml 5 x TBE, 16 ml ProtoGel, plus 1 ml 10 % APS and 200 ul TEMED, made to 100 ml with ddH_2O). This was run at 150 V for approximately 1.5 hours in 0.5 x TBE running buffer. The gel was then vacuum dried and exposed overnight to a phosphor screen before visualisation using a Biorad FX® phosphoimager.

2.2.17 *In vitro* transcription assays

pSR derivatives with promoter fragments fused upstream of *oriT* were used for *in vitro* transcription experiments (Figure 2.3. For each reaction, 335 ng of a pSR maxiprep was mixed with 1 x TNSC buffer, as well as 100 µg/ml BSA, NTP mix (providing 200 µM ATP/GTP/CTP and 10 µM UTP), and 4 µCi [α-^{32}P]-UTP. ddH_2O was added to make a final reaction volume of 11 µl. This mix was then incubated with 5 µl of diluted transcription factor at 37 °C for 10 minutes. RNAP core enzyme and σ^{70} cofactor were incubated at 37 °C for 5 minutes, then 4 µl of the mixture was added at timed intervals to each DNA-protein mix. After incubation at 37 °C for 10 minutes, 20 µl STOP solution was added at timed intervals. Reactions were loaded onto a 6 % denaturing sequencing gel, which consisted of 24 ml UreaGel Concentrate, 10 ml UreaGel Buffer, 66 ml UreaGel Diluent, plus 800 µl 10 % APS and 40 µl TEMED. Electrophoresis was done at 60 W for approximately 1 hour in 1 x TBE running buffer. The gel was dried by vacuum and exposed to a phosphor screen overnight. Images were then scanned using a Bio-Rad FX® phosphoimager.

2.2.18 β-galactosidase assay

Promoter fragments were introduced upstream of *lacZ* in pRW50 and confirmed by sequencing (Figure 2.4). Resulting plasmids were used to transform *E. coli* JCB387. Three overnight cultures were set up for each construct, with each replicate made from a separate colony. 200 µl of each was then used the following day to inoculate a fresh 5 ml culture, and cultures were grown to an OD_{650} of 0.3-0.5. Cells were lysed with 1 drop each of toluene and 1 % sodium deoxycholate and incubated at 37 °C for 20 minutes to allow for toluene evaporation. 100 µl of lysate was then assayed for β-galactosidase activity; 2.5 ml ONPG solution was added at timed intervals, and tubes

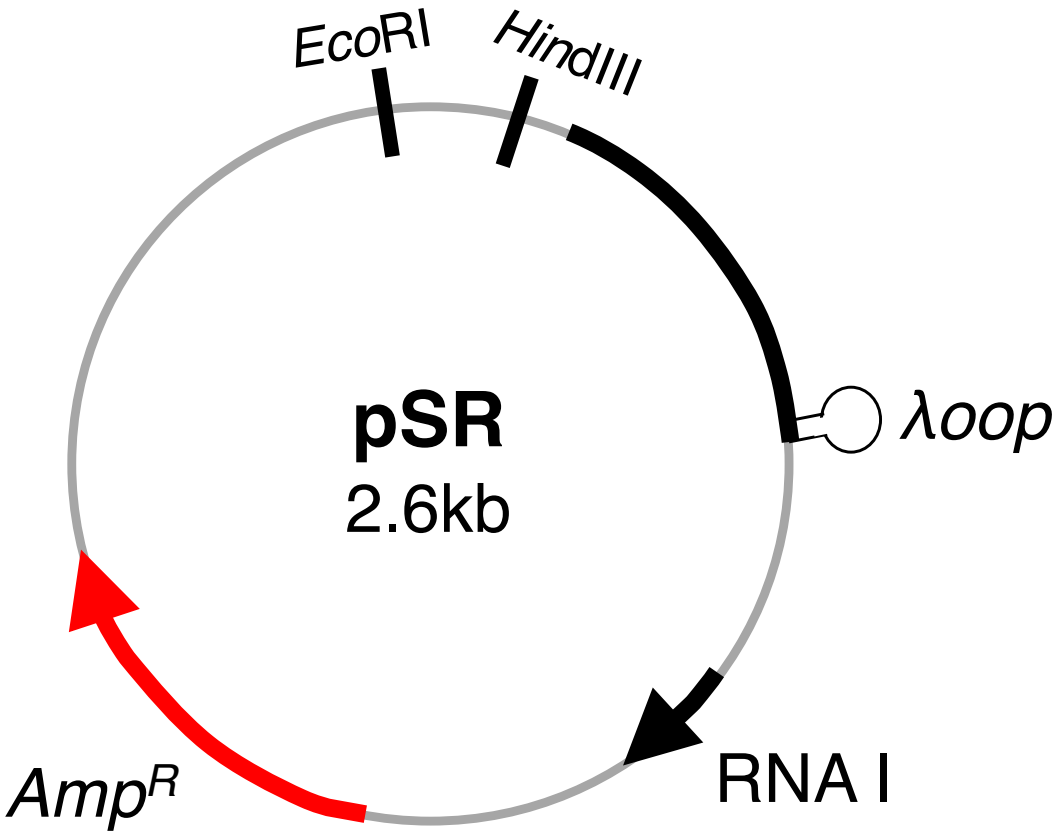

Figure 2.3 The pSR plasmid

A schematic of the pSR plasmid. This is a high copy number plasmid derived from pBR322 which can be used as a template for *in* vitro transcription assays. The ampicillin resistance gene is shown in red. Short transcripts can be derived from promoter fragments cloned between the *Eco*RI and *Hin*dIII sites, due to the presence of an λ*oop* transcription terminator. RNA I functions as an internal control.

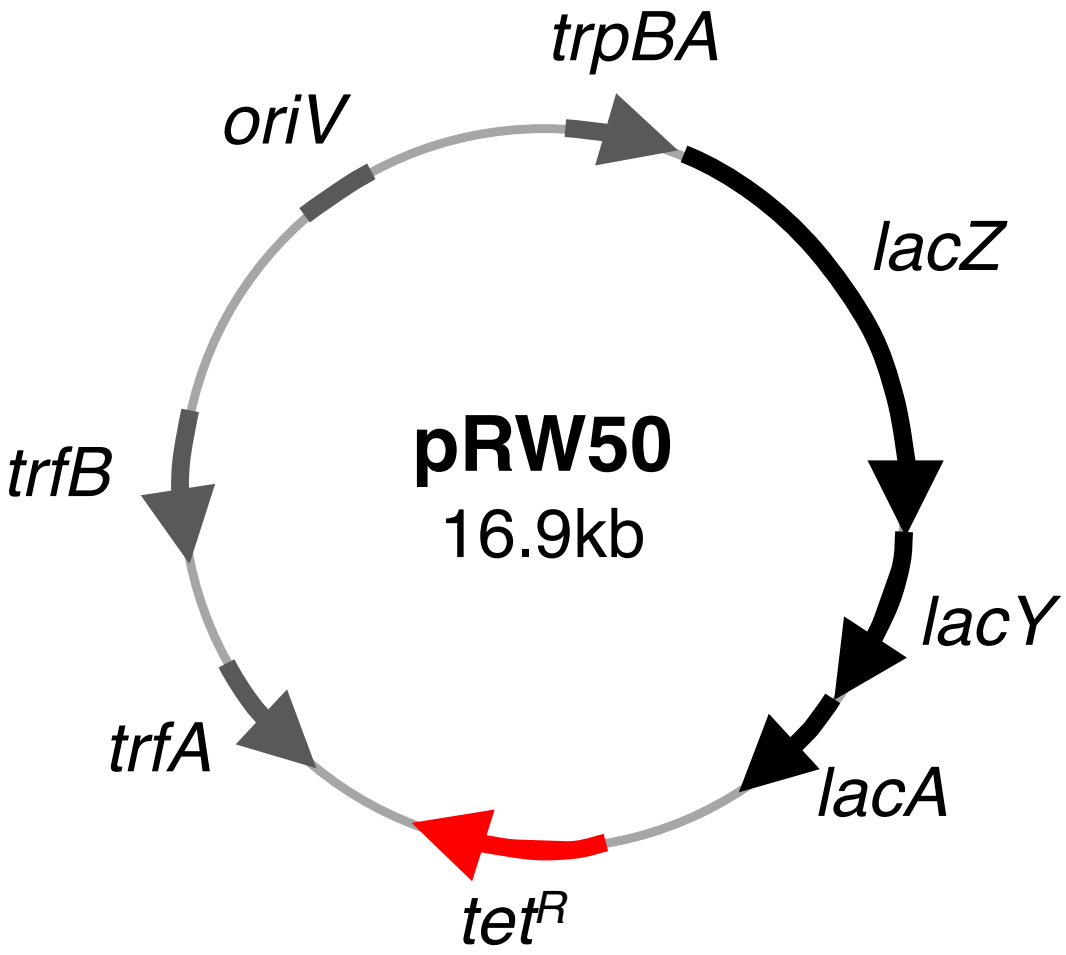

Figure 2.4 The pRW50 plasmid

The tetracycline resistance gene is shown by a red arrow; the *lacZYA* operon is shown by black arrows; all other genes are shown in grey. Promoter DNA fragments can be cloned using the multiple cloning region upstream of *lacZ* to place these genes under the control of the selected promoter fragment, allowing quantification of promoter activity in β-galactosidase assays.

were incubated at 37 °C for 10-20 minutes until a yellow colour had formed. The reactions were stopped at timed intervals by adding 1 ml of 1 M sodium carbonate, and the absorbance at OD_{420} was measured. The following formula was used to calculate promoter activity in Miller units:

$$Promoter\ activity\ = 1000\ \times \frac{Abs_{420} \times \text{ total reaction volume}}{Abs_{650} \times \text{ volume lysate } \times \text{ reaction time}}$$

A media-only control was included as a blank, and empty pRW50 was used as a control for background β-galactosidase activity.

2.2.19 Crystal violet biofilm staining assay

The crystal violet assay described in Baugh *et al.* (2014) was used to quantify biofilm production. Two overnight cultures (set up from individual colonies) per strain were diluted in LB to an OD_{600} of 0.1. 200 µl of this was aliquoted into a flat-bottomed 96-well polystyrene microtitre plate, with four replicate wells per culture. The plate was incubated at 30 °C for 48 hours. Wells were washed with water to remove unattached cells, and 200 µl of 0.1 % crystal violet added for 15 minutes. Wells were washed with water again to remove unbound crystal violet, and 200 µl of 70 % ethanol was added to solubilise the remaining dye. The OD_{600} was measured using a CLARIOstar® to give a quantitative measure of biofilm formation.

2.2.20 Determination of minimum inhibitory concentration (MIC)

Four overnight cultures were set up per strain, from individual colonies. The next day, these were diluted to an OD_{650} of 0.05 in sterile distilled water, and further diluted 1 in

20 in LB. A 96-well round bottomed microtitre plate was set up using the double dilution method as advised in Andrews (2001). Each well contained 50 µl of diluted culture in a final volume of 100 µl per well with antibiotic and LB. An LB + culture well was included as a growth control, and an LB only well as a sterility control. The plate was incubated for 24 hours at 37 °C, and the lowest antibiotic concentration which prevented bacterial growth recorded. The *E. coli* strains NCTC 10418 and ATCC 25922 were included as controls; results were rejected if the MIC was not within one double dilution of the expected for these strains.

2.2.21 Growth curves at pH 7 and pH 4

Three overnight cultures were set up per strain in LB (pH 7) from individual colonies. The following day, these were used to inoculate 10 ml of LB (pH 7) and LB (pH 4), to a starting OD_{650} of 0.05. These were incubated at 37 °C shaking for 7 hours. Each hour, a 1 ml sample was taken and the OD_{650} measured. Once an OD_{650} of 0.8 was reached, samples were diluted 1 in 10 with sterile LB to account for spectrophotometer inaccuracy.

2.2.22 Analysis of proteins by SDS-PAGE

SDS-PAGE was used to check the sizes and presence of proteins. 8 µl of protein sample was mixed with 2 µl of 5x SDS loading dye and boiled at 100 °C for ten minutes. Samples were then loaded onto a NuPAGE™ 4-12 % Bis-Tris protein gel (Invitrogen) in 1X NuPAGE™ MES SDS Running Buffer (Invitrogen) for 1 hour at 150V. Gels were then treated with staining solution for 1 minute in a microwave, then destained with Fast Destain solution for 1 hour.

2.2.23 Bradford assay

Bradford assays were used to determine protein concentration using the Bio-Rad Quick Start™ Bradford Protein Assay, according to the manufacturer's instructions for the 2ml cuvette microassay protocol (Bio-Rad). In brief, 1 ml of 1x Bradford dye reagent was mixed with 1 ml sample or standard protein, incubated at room temperature for 5 minutes before measurement of OD_{595} using a spectrophotometer. BSA was used as a standard, with a linear range of 1.25-10 μg/ml.

2.2.24 Purification of recombinant proteins

MarA, SoxS, and MarA derivatives were all purified using a protocol adapted from Jair *et al.* (1995). The coding sequence for the gene was amplified by PCR and digested with *Nde*I and *Bam*HI before ligation with pET28a downstream of the IPTG-inducible T7*lac* promoter. After verification by sequencing, constructs were used to transform the *Escherichia coli* strain T7 Express. To overexpress recombinant protein, strains were grown in 2 litres of LB + 1 % glucose to an OD_{600} of 0.8. 0.4 mM IPTG was then added and the culture grown for a further 3 hours, before harvesting of cells by centrifugation at 1,600 x g for 10 minutes at 4 °C. The pellet was washed with 25 ml of lysis buffer and frozen overnight at -80 °C.

All subsequent steps were done at 4 °C, unless specified otherwise. The frozen pellet was thawed and resuspended into 40 ml of the same buffer; cells were then lysed using an Avestin Emulsiflex C3 high pressure motorised homogeniser. The cells were then collected by centrifugation at 75,000 x g for 30 minutes; the supernatant was discarded and the pellet resuspended in 40 ml of wash buffer prior to further centrifugation.

Again, the supernatant was discarded, and the pellet resuspended in 40 ml of denaturing buffer before centrifugation as before.

The supernatant from the final centrifugation step was loaded onto a HisTrap™ 1 ml precharged Ni Sepharose High Performance column. Unbound protein was washed from the column with Buffer A. Bound protein was then eluted with a linear gradient of Buffer B. An elution peak was seen at approximately 0.22 M imidazole; fractions were checked by SDS-PAGE and desired fractions dialysed against Buffer X overnight.

After dialysis, protein was concentrated to 1 mg/ml using a 5,000 MWCO (molecular weight cut-off) Vivaspin 20 column. Protein was then digested, to remove the His tag, using 15 µl of thrombin sepharose beads per mg protein, gently rocking at room temperature for 5 hours. Digestion was confirmed by SDS-PAGE. Thrombin beads were removed by centrifugation at 1,600 x g for 5 minutes, 3 times; digested His tags were then removed using the HisTrap™ column with flow-through retained and dialysed against Buffer X + 20 % glycerol overnight. Purified protein was stored at -80 °C until required.

Chapter 3

Regulation of the *ycgZ-ymgABC* Operon by MarA

3.1 Introduction

The complexity of the MarA regulon creates challenges in developing a comprehensive list of targets. There are 12 experimentally confirmed targets listed in Ecocyc, despite estimates of the regulon comprising up to 100 genes (Barbosa and Levy 2000, Keseler *et al.* 2013). Experimental validation is essential; Martin and Rosner (2002) found that, of 19 putative MarA targets identified by microarray analysis, only seven showed regulation by MarA in *lacZ* fusions.

A recent ChIP-seq experiment identified 33 MarA targets, of which only three were previously confirmed (Sharma *et al.* 2017). These new targets may unveil novel antibiotic resistance mechanisms. This chapter investigates one such target upstream of the *ycgZ-ymgABC* operon (Figure 3.1). Inactivation of these genes show small but significant changes in antibiotic tolerance (Nichols *et al.* 2011). However, the *ycgZ-ymgABC* operon is best known to be involved in the control of biofilm formation.

Biofilms are surface-attached communities of microorganisms, which display increased resistance to antibiotics, invasion by immune cells, and environmental stress (Rabin *et al.* 2015). Biofilm formation occurs in three stages: attachment, maturation, and dispersion. Attachment is mediated by components such as flagella, type IV pili, and curli fibres (O'Toole and Kolter 1998, Barnhart and Chapman 2006). Once attached, an extracellular polymeric substance (EPS) matrix is produced. The EPS matrix is made up of a scaffold of exopolysaccharides which supports the adherence of other macromolecules. In *E. coli*, this EPS is colonic acid, the production of which is induced by stress response (Prigent-Combaret *et al.* 1999, Danese, Pratt and Kolter 2000). The EPS matrix also includes extracellular proteins which can provide stability or

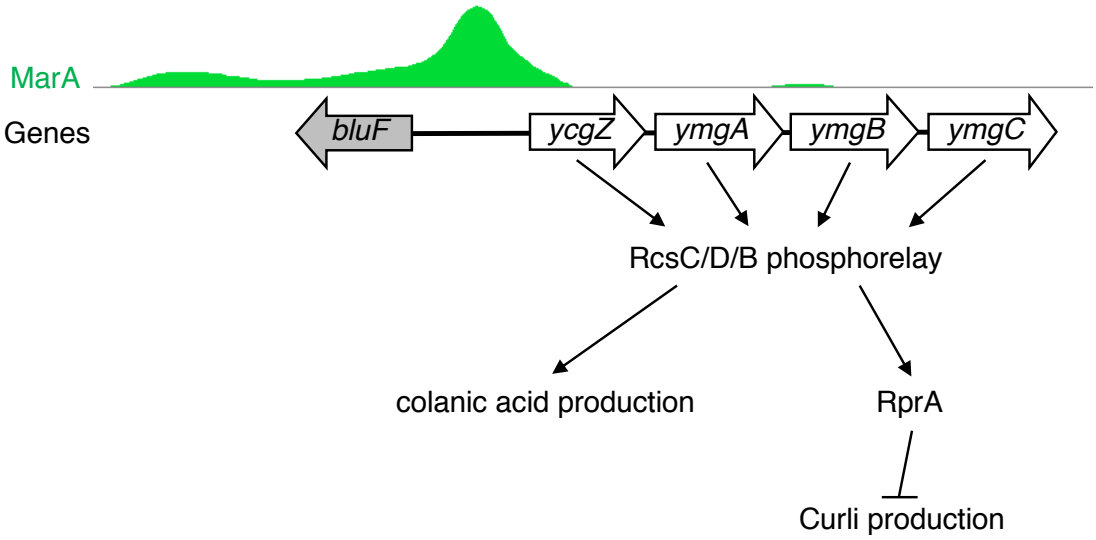

Figure 3.1 The MarA binding peak upstream of biofilm regulators *ycgZ-ymgABC.*

The MarA binding peak, from the Sharma *et al.* (2017) ChIP-seq experiment, is shown in green. The *ycgZ-ymgABC* operon is shown by white block arrows and a divergent gene, *bluF*, shown a grey block arrow. The thick black line indicates intergenic DNA. Black arrows signify activation of downstream genes/processes; black T-shapes indicate repression.

enzymatic functions, and extracellular DNA, which can facilitate adherence to surfaces (Zhang *et al.* 1999, Das *et al.* 2010). Further maturation of the biofilm involves growth of additional layers to form a 'mushroom' shape structure, with different communities of bacteria existing throughout the biofilm in accordance with their lifestyle requirements. Finally, dispersal of the biofilm may occur in response to nutritional stress or competition.

Regulation of biofilm formation by the *ycgZ-ymgABC* operon appears to be via components key in the early stages of the biofilm life cycle. YmgA and YmgB activate the RcsC/RcsD/RcsB two-component phosphorelay system (Lee *et al.* 2007, Majdalani and Gottesman 2007, Tschowri, Busse and Hengge 2009). In this system, the inner-membrane sensor kinase RcsC phosphorylates RcsD, a phosphotransferase, which in turn phosphorylates RcsB. RcsB then activates RprA, an sRNA which represses CsgD, an activator of curli production (Mika *et al.* 2012). Thus, YmgA and YmgB inhibit biofilm formation via this pathway. However, previous studies have only examined these genes individually and their roles appear contradictory; for example, YcgZ counteracts the action of YmgA and YmgB in an unknown manner (Tschowri, Busse and Hengge 2009). The overall effect of the entire operon on biofilm formation has not been studied and would elucidate the exact roles of this system.

The *ycgZ-ymgABC* operon has been linked with a number of other cellular functions. YcgZ has been shown to transcriptionally repress OmpF porin, which is key in the uptake of small hydrophilic molecules, including ß-lactam antibiotics (Duval *et al.* 2017). YmgB is likely a transcription factor; it has shown DNA-binding capabilities, and has structural similarity to Hha, another transcriptional regulator. A key role of

YmgB appears to be in downregulation of cellular motility and upregulation of acid tolerance; it is also known as AriR due to the latter role (Lee *et al.* 2007).

The *ycgZ-ymgABC* promoter is repressed by BluR at 37° C; BluR is in turn repressed by BluF which is activated by low temperature and blue light irradiation (Tschowri, Busse and Hengge 2009). This therefore leads to expression of the *ycgZ-ymgABC* operon in response to cold and blue light; the operon is also known to be triggered by starvation conditions (Duval *et al.* 2017). Additionally, *ycgZ-ymgABC* may be positively regulated by *fur* during iron depletion (Seo *et al.* 2014). Thus far, however, regulation of this operon by MarA has not been shown.

3.2 Binding and regulation of *ycgZ-ymgA-ariR-ymgC* by MarA

3.2.1 MarA recognises a marbox upstream of *ycgZ*

The DNA sequence of the regulatory region upstream of *ycgZ* is shown in Figure 3.2 (Panel A), alongside a schematic of the regulatory region. A putative marbox sequence occurs 60 bp upstream of the *ycgZ* transcription start site. To verify binding of MarA, derivatives of the regulatory region were prepared (Figure 3.2, Panel B). The 5' ends of the different fragments are shown by inverted triangles (Figure 3.2, Panel A). The derivatives were the full 119 bp DNA sequence containing the marbox (*ycgZ*.1), a truncated 90 bp sequence without the marbox (*ycgZ*.2), or the full sequence with a mutated marbox (*ycgZ*.1^{M}). Due to the degenerate nature of the marbox, the *ycgZ*.1^{M} mutations were introduced at four key residues. Within the marbox, the GCA motif at positions 1-3 (using the numbering system outlined in Figure 1.9) and the G at position 10 are well conserved, due to contacts made with amino acids R96 and T93 of MarA for the former and R46 for the latter (Rhee *et al.* 1998). Thus, mutations were

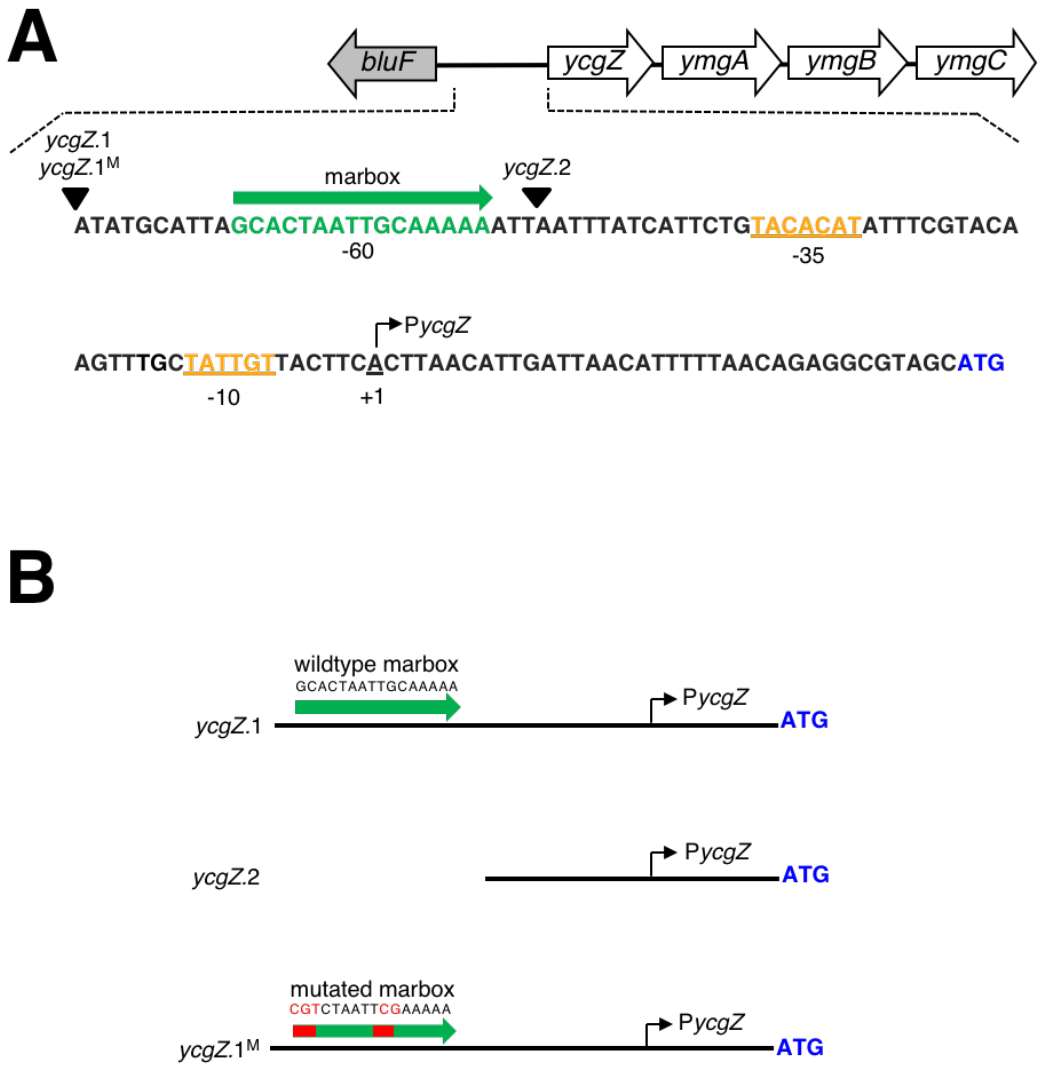

Figure 3.2 The P*ycgZ* regulatory region and derivatives.

Genes are shown as block arrows; white for the *ycgZ-ymgABC* operon, grey for the divergent gene *bluF*. The thick black line represents non-coding DNA regions. The sequence of the regulatory region upstream of *ycgZ* is shown; the dotted line indicates the location of this region. The marbox is indicated in green, with the direction of the green arrow indicating orientation. The *ycgZ* promoter -10 and -35 elements are shown in orange and underlined; the transcription start site is shown in black underline, with the right-angled arrow indicates the *ycgZ* transcription start site. The *ycgZ* start codon is shown in blue. Black triangles in Panel A indicate the 5' end of the promoter fragments generated in this study, shown in Panel B. Mutated bases of the marbox are indicated in red.

introduced at these positions. The *ycgZ* promoter derivatives were radiolabelled with [γ ^{32}P]-ATP and incubated with increasing concentrations of MarA, before separation of complexes on a 6 % polyacrylamide gel in an electrophoretic mobility shift assay (EMSA).

A DNA-protein complex was formed in experiments with the wildtype *ycgZ*.1 fragment (Figure 3.3, Panel i). More than 50 % of the free DNA was bound at the lowest concentration of MarA (0.4 μM), and no free DNA was observed with 1.2 μM MarA. However, for the *ycgZ*.2 fragment (Figure 3.3, Panel ii), complex formation was lost, with no reduction in free DNA even at the highest MarA concentration. The same is seen for *ycgZ*.1^{M} (Figure 3.3, Panel iii), indicating that the absence of DNA-protein complexes was specifically due to loss of binding in the region of the putative marbox.

3.2.2 MarA activates transcription from the *ycgZ* promoter *in vivo*

To examine the impact of the marbox on expression of *ycgZ-ymgABC*, the P*ycgZ* derivatives outlined in Figure 3.2 were fused to *lacZ* in the reporter plasmid pRW50. *E. coli* strain JCB387 was transformed with the pRW50 derivatives and assayed for β-galactosidase activity (Figure 3.4). Briefly, the cleavage of o-nitrophenyl-β-D-galactosidase (ONPG) by LacZ is measured to quantify promoter activity. A reduction in promoter activity was seen when the marbox was absent or mutated ($p < 0.01$). This suggests that MarA activates the *ycgZ-ymgABC* operon and is required for optimal *lacZ* expression from P*ycgZ*.

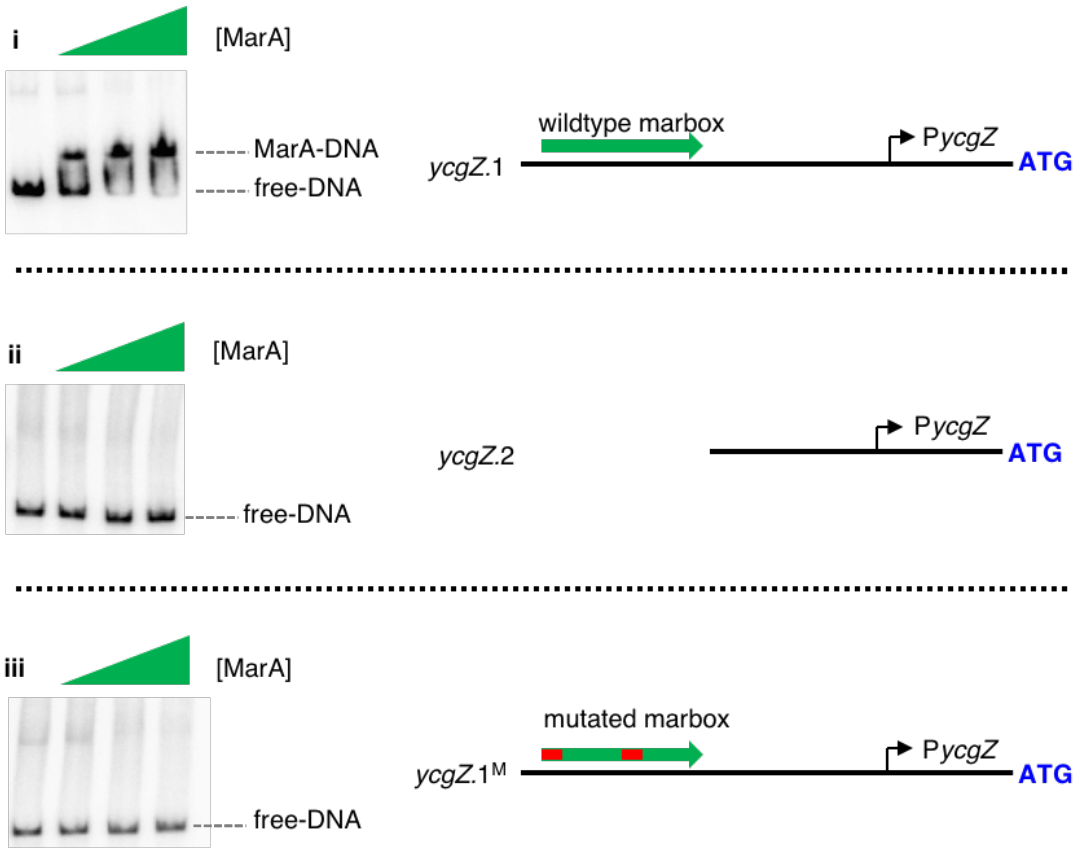

Figure 3.3 Binding of MarA to the P*ycgZ* marbox in an EMSA.

Images of 6 % polyacrylamide gels used to separate MarA:DNA complexes are shown. The panels show experiments for EMSA assays done with i) the *ycgZ*.1 promoter derivative with the wildtype marbox present, ii) the *ycgZ*.2 truncated derivative with the marbox absent, and iii) the *ycgZ*.1^{M} derivative with the marbox mutated. Increasing concentrations of MarA (0.4 µM – 1.2 µM - 2 µM) are shown by green triangles. Bands formed by free DNA and MarA-DNA complexes are indicated by dashed lines.

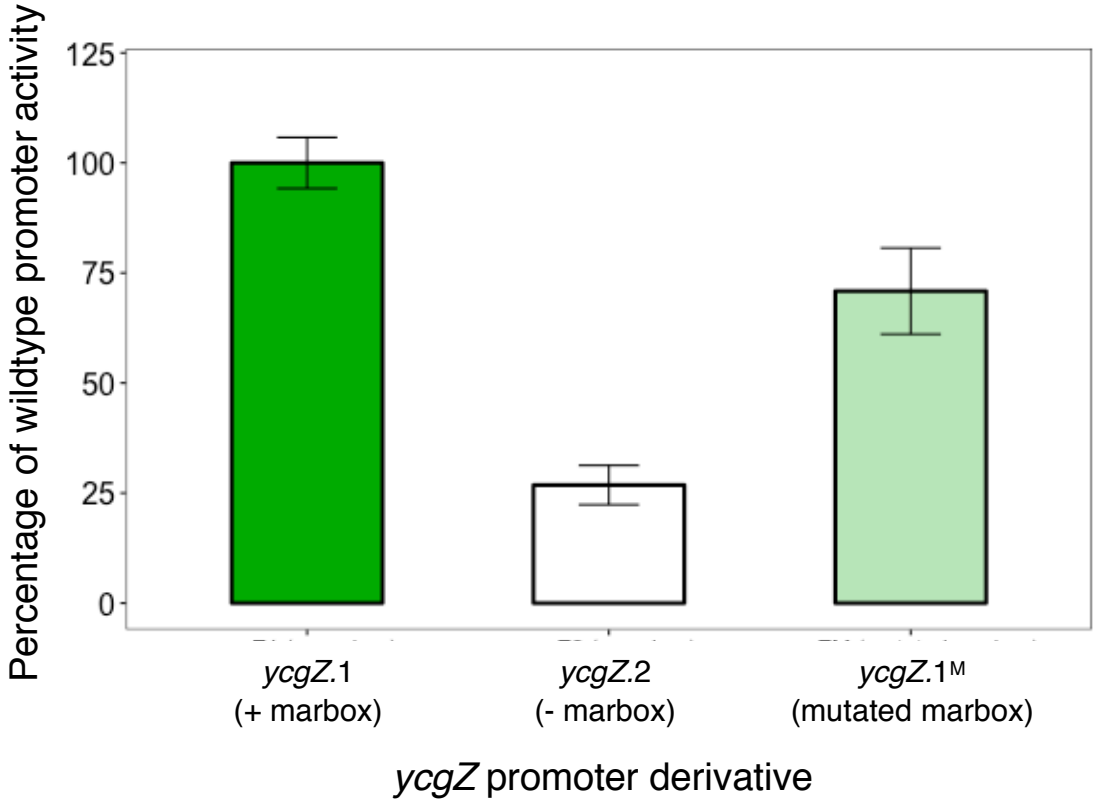

Figure 3.4 *In vivo* promoter activity from the *ycgZ* regulatory region derivatives at mid-log phase.

Expression of *lacZ* driven by various *ycgZ* regulatory region derivatives was assessed by β-galactosidase assay. Assays were done using lysates of *E. coli* JCB387 mid-log phase cultures. Cells containing empty pRW50 were used as a control (data not shown). Activities shown are from assays done on three separate days, with each assay comprising three biological replicates. The mean ± standard deviation relative to the average wildtype (*ycgZ*.1) promoter activity is shown. A one-way analysis of variance (ANOVA) was calculated with the promoter activities for the three constructs; the analysis was significant ($p < 0.00001$, F (2, 24) = 245.51). A post-hoc Tukey's HSD test showed that all groups were significantly different from each other, with a $p < 0.01$ for each comparison pair.

MarA-specific activation of P*ycgZ* was further validated by measuring β-galactosidase activity with and without the addition of 5 mM salicylate to the growth media (Figure 3.5). Salicylate is a known inducer of MarA expression. Induction is mediated through binding of salicylate ions to MarR. This causes a conformational change in MarR,reducing DNA binding, and relieving repression of *marRAB* (Alekshun and Levy 1999). In the presence of salicylate, *ycgZ* promoter activity increased 1.75-fold when the marbox was present but less when the marbox was absent or mutated, although due to inconsistent induction by salicylate this was not significant.

3.2.3 MarA activates transcription from the *ycgZ* promoter *in vitro*

Activation of P*ycgZ* by MarA was also tested using *in vitro* transcription. The *ycgZ.*1, *ycgZ.*2, and *ycgZ.*1^{M} promoter derivatives were cloned upstream of *λoop* in the plasmid pSR, which is a phage-derived transcription terminator. Therefore, when RNAP is added, transcription will initiate at P*ycgZ*, then terminate prematurely upon encountering *λoop,* thus producing short transcripts. A plasmid-encoded transcription factor-independent promoter acts as an internal control and produces the RNAI transcript. Transcripts were generated in the presence of increasing concentrations of MarA and the incorporation of [α ^{32}P]-UTP analysed on a denaturing gel (Figure 3.6). An increase in the intensity of a 140 nt transcript corresponding to that originating from P*ycgZ* was seen when MarA is added to *ycgZ.*1 (lanes 1-4). However, no increase was seen when MarA was added to *ycgZ.*2 (lanes 5-8) and *ycgZ.*1^{M} (lanes 9-12). Thus, MarA transcriptionally activates P*ycgZ* via the marbox -60 bp upstream of the transcription start site.

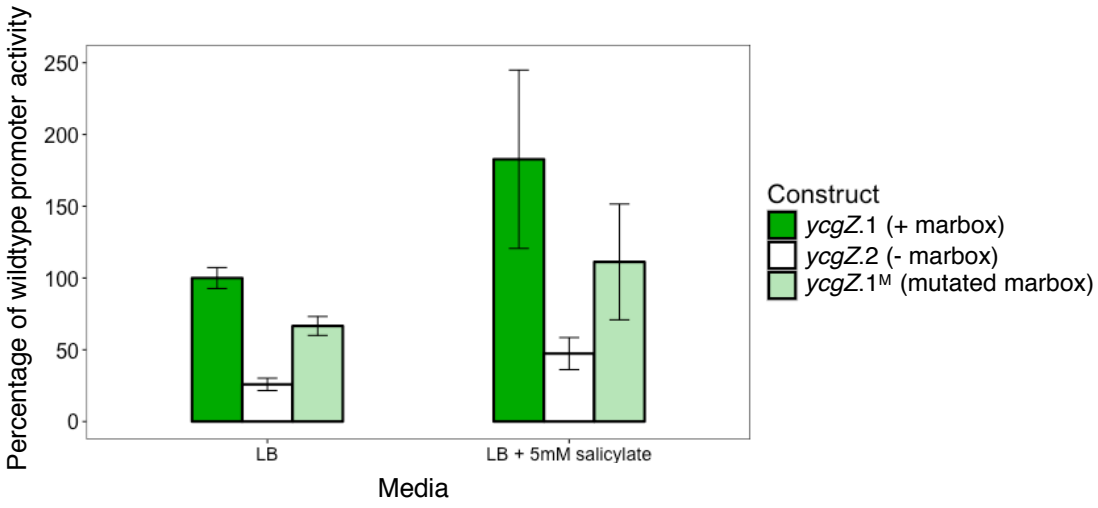

Figure 3.5 Effect of salicylate on *in vivo* promoter activity from *ycgZ* regulatory region derivatives.

Expression of lacZ driven by various *ycgZ* promoter derivatives was assessed using β-galactosidase assays, with and without the addition of 5 mM salicylate to LB media. Salicylate was added to fresh media after overnight growth, and *E. coli* JCB387 cultures grown to mid-log phase. Cells containing empty pRW50 were used as a control (data not shown). Activities shown are from assays done on three separate days, with each assay comprising three biological replicates. The mean ± standard deviation relative to the average wildtype (*ycgZ*.1 in LB only) promoter activity is shown. A one-way analysis of variance (ANOVA) was calculated with the fold-change between +/- salicylate for the three constructs; however, the analysis was not significant ($p > 0.05$) due to the variable expression seen in the + salicylate group.

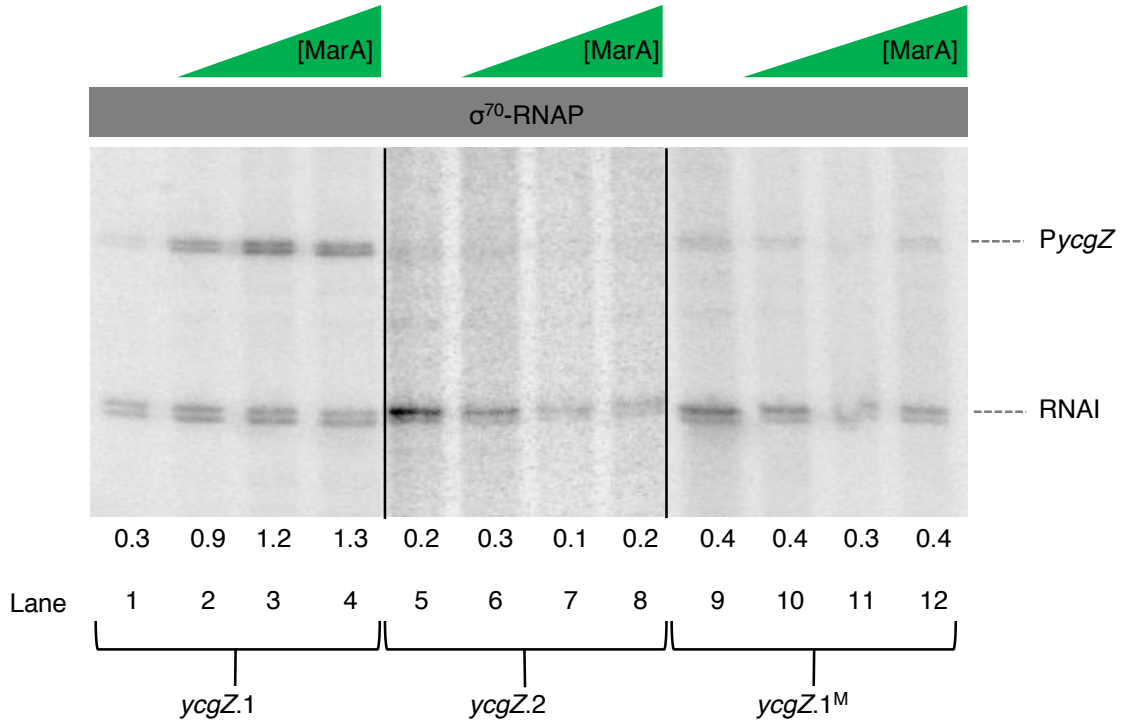

Figure 3.6 MarA activation of σ^{70}-dependent transcription from P*ycgZ*, modelled *in vitro*.

Images of denaturing sequencing gels used to separate transcripts generated *in vitro* using the *ycgZ*.1, *ycgZ*.2 and *ycgZ*.1^{M} fragments as templates. All assays were done with RNAP-σ^{70}. Green triangles show increasing concentrations of MarA (0.2 μM to 1 μM). Bands formed by transcripts originating from P*ycgZ* and RNAI are indicated by dashed lines. The image shown is from two different experiments, however the RNAI transcript shown allows for comparison between experiments. The ratio of transcript of P*ycgZ*:RNAI is shown.

3.3 The *ycgZ-ymgABC* promoter is recognised by σ^{70} and σ^{38}

Most genes in *Escherichia coli* are under the control of the housekeeping sigma factor, σ^{70} (Feklístov *et al.* 2014). However, the *ycgZ* promoter is predicted to be dependent on both σ^{70} and σ^{38}, although dependence has not been shown directly (Weber *et al.* 2005, Gama-Castro *et al.* 2008, White-Ziegler *et al.* 2008). This σ^{38} factor is triggered by environmental stress or entry into stationary phase growth (Lange and Hengge-Aronis 1991). Hence, an *in vitro* transcription experiment was done comparing the addition of RNAP in complex with σ^{70} or σ^{38}. Transcripts were generated using *ycgZ.*1 cloned in pSR as a template. Transcripts were then separated on a denaturing gel (Figure 3.7, Panel A). 140 nt transcripts from P*ycgZ* were generated under the direction of both σ^{70} and σ^{38}. However, the σ^{38}-dependent transcript is significantly more intense than that generated by σ^{70}. The *ycgZ-ymgABC* operon is thus induced by the stationary phase regulator σ^{38}.

Figure 3.6 showed that MarA activates transcription of P*ycgZ* when RNAP is in complex with σ^{70}. *In vitro* transcription experiments, using *ycgZ.*1 as a template with increasing concentrations of MarA, were repeated using RNAP in complex with σ^{38} (Figure 3.7, Panel B). Note that no increase in P*ycgZ*-derived transcript was seen when MarA was added, suggesting that MarA activates P*ycgZ* in a σ^{70}-dependent manner only. This effect can also be seen *in vivo*. Stationary phase cultures carrying pRW50 containing the *ycgZ* regulatory region derivatives were assayed for β-galactosidase activity (Figure 3.8). Whilst reduced activity was seen for the truncated *ycgZ.*2 ($p < 0.001$) fragment, no reduction was seen when the marbox was mutated (*ycgZ.*1^{M}, $p > 0.05$). This was in contrast to assays done at mid-log phase (Figure 3.4). Thus, MarA

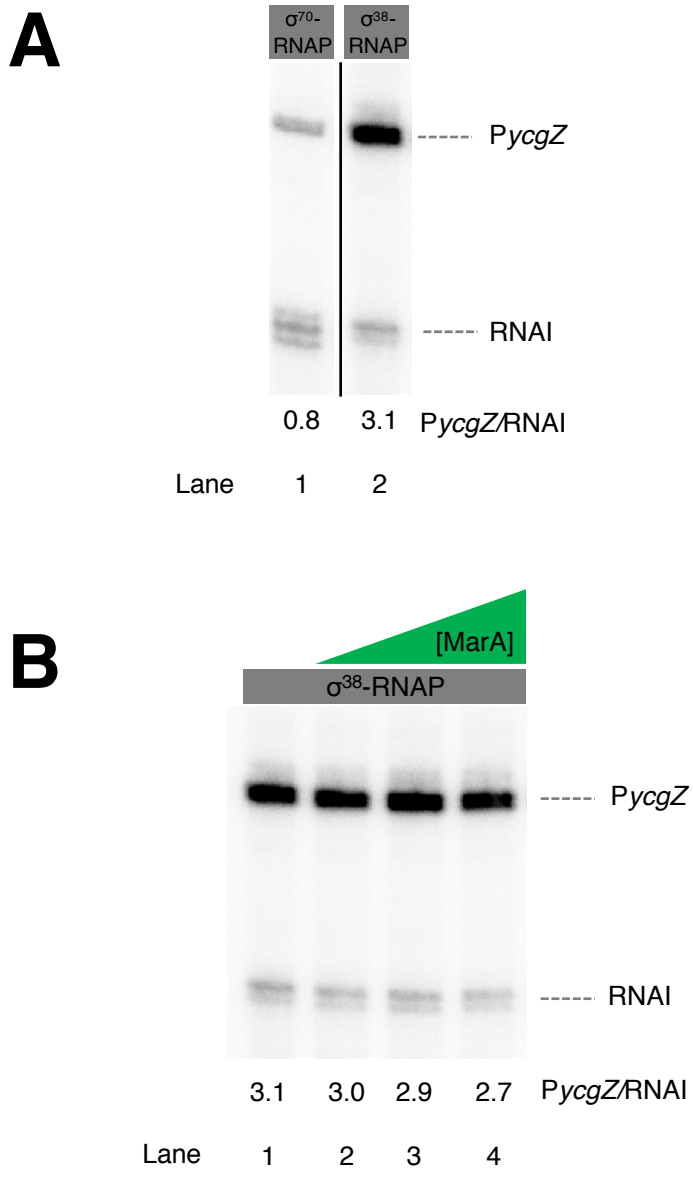

Figure 3.7 σ^{38}-dependent transcription from P*ycgZ*

Images of denaturing sequencing gels used to separate transcripts generated *in vitro* using the *ycgZ*.1 fragment as a template. Panel A shows an experiment comparing transcription with RNAP-σ^{70} (Lane 1) to RNAP-σ^{38} (Lane 2). Panel B shows an experiment with RNAP-σ^{38} and increasing concentrations of MarA (0.2 μM – 1 μM), shown by a green triangle. Bands formed by transcripts originating from P*ycgZ* and RNAI are indicated by dashed lines. Lanes in Panel A are from a single image, which has been rearranged for clarity. The ratio of transcript of P*ycgZ*:RNAI is shown.

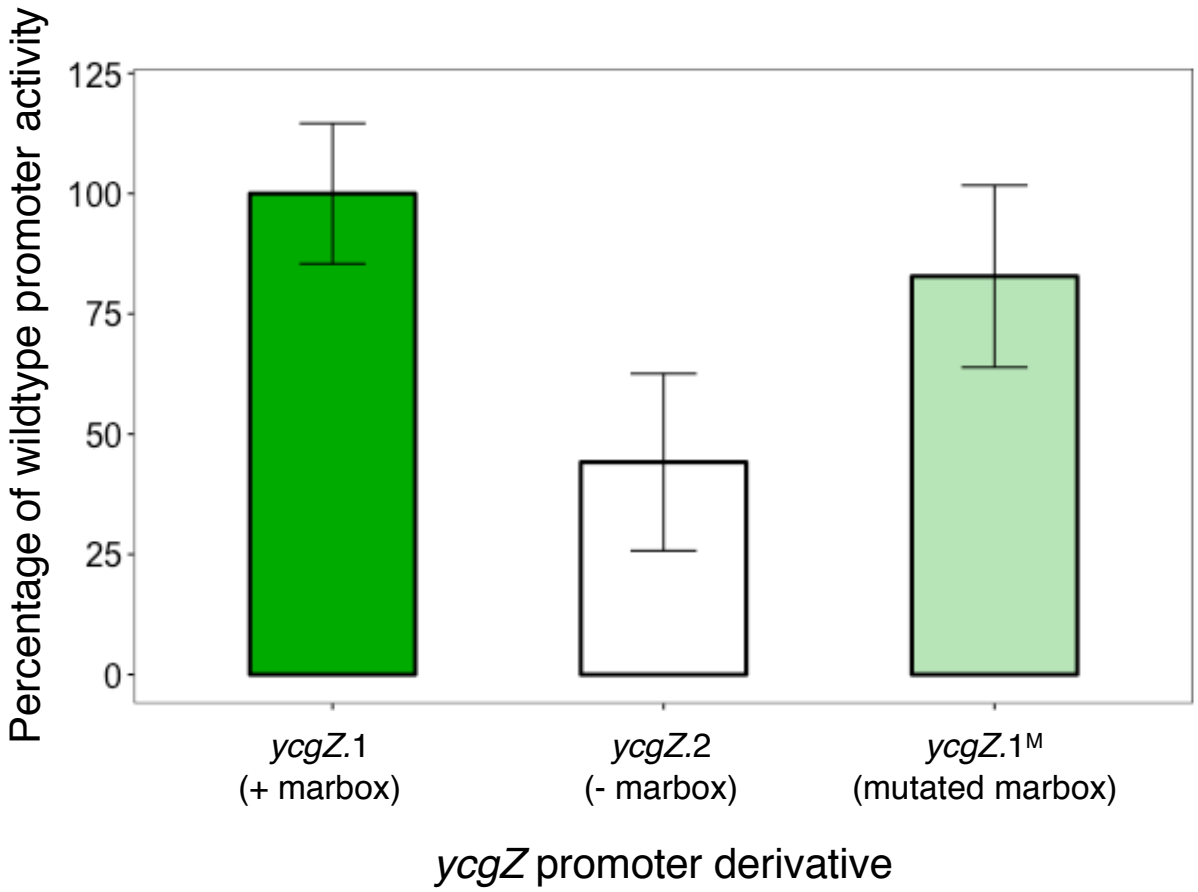

Figure 3.8 *In vivo* promoter activity of *ycgZ* regulatory region derivatives at stationary phase.

Expression of *lacZ* driven by the various *ycgZ* regulatory region derivatives was assessed using β-galactosidase assays. Assays were done using lysates of *E. coli* JCB387 grown overnight to stationary phase, otherwise known as the point at which no further increases in cell number are seen; here, this was typically an OD_{600} of 4, after 18 hours of growth. Cells containing empty pRW50 were used as a control (data not shown). Activities shown are from assays done on three separate days, with each assay comprising three biological replicates. The mean ± standard deviation relative to the average wildtype (*ycgZ*.1) promoter activity is shown. A one-way analysis of variance (ANOVA) was calculated with the promoter activities for the three constructs; the analysis was significant ($p < 0.00001$, F (2, 24) = 18.36). A post-hoc Tukey's HSD test showed a significant difference between *ycgZ*.1 and *ycgZ*.2 ($p < 0.001$), and between *ycgZ*.2 and *ycgZ*.1^M ($p < 0.01$) but not between *ycgZ*.1 and *ycgZ*.1^M ($p > 0.05$).

regulates the *ycgZ* promoter via σ^{70}-dependent transcription at mid-log, but does not regulate via σ^{38}-dependent transcription at stationary phase.

3.4 MarA activation of P*ycgZ* requires a contact with the alpha subunit of RNAP

The location of the P*ycgZ* marbox indicates that MarA activates this promoter in a Class I manner, requiring MarA to make contact with the α-CTD of RNAP (Jair *et al.* 1996, Dangi *et al.* 2004). To investigate this, residue W19 of MarA was mutated to an alanine, disrupting proposed the α-CTD surface contact (Dangi *et al.* 2004). The W19A mutant was purified and used in an *in vitro* transcription assay with *ycgZ*.1 (Figure 3.9). W19A was incapable of activating transcription by RNAP-σ^{70} (Panel A, lanes 5-7) or RNAP-σ^{38} (Panel B, lanes 5-7); no increase in the intensity of the P*ycgZ* transcript is seen. Thus, MarA requires the W19 contact with the α-CTD of RNAP to activate transcription, as would be expected of a Class I activator.

3.5 Activation of *ycgZ-ymgABC* controls biofilm formation

To elucidate the phenotypic effects of *ycgZ-ymgABC* activation by MarA, the *ycgZ-ymgABC* operon was deleted from *E. coli* JCB387 genome using gene doctoring. We intended to clone the *ycgZ-ymgABC* operon in plasmid pBR322 for complementation experiments. However, we noticed the presence of pBR322 alone reduced biofilm formation (Figure 3.10, Panel B). This was likely due to the presence of a β-lactamase (*bla*) gene in the pBR322 plasmid. β-lactamases may reduce biofilm formation by interfering with peptidoglycan remodelling and thus adhesion to surfaces (Gallant *et al.* 2005). To counteract this, an alternative plasmid was generated. Hence, the pBR322 *bla* gene was excised by digestion with *Aat*II and *Vsp*I and a

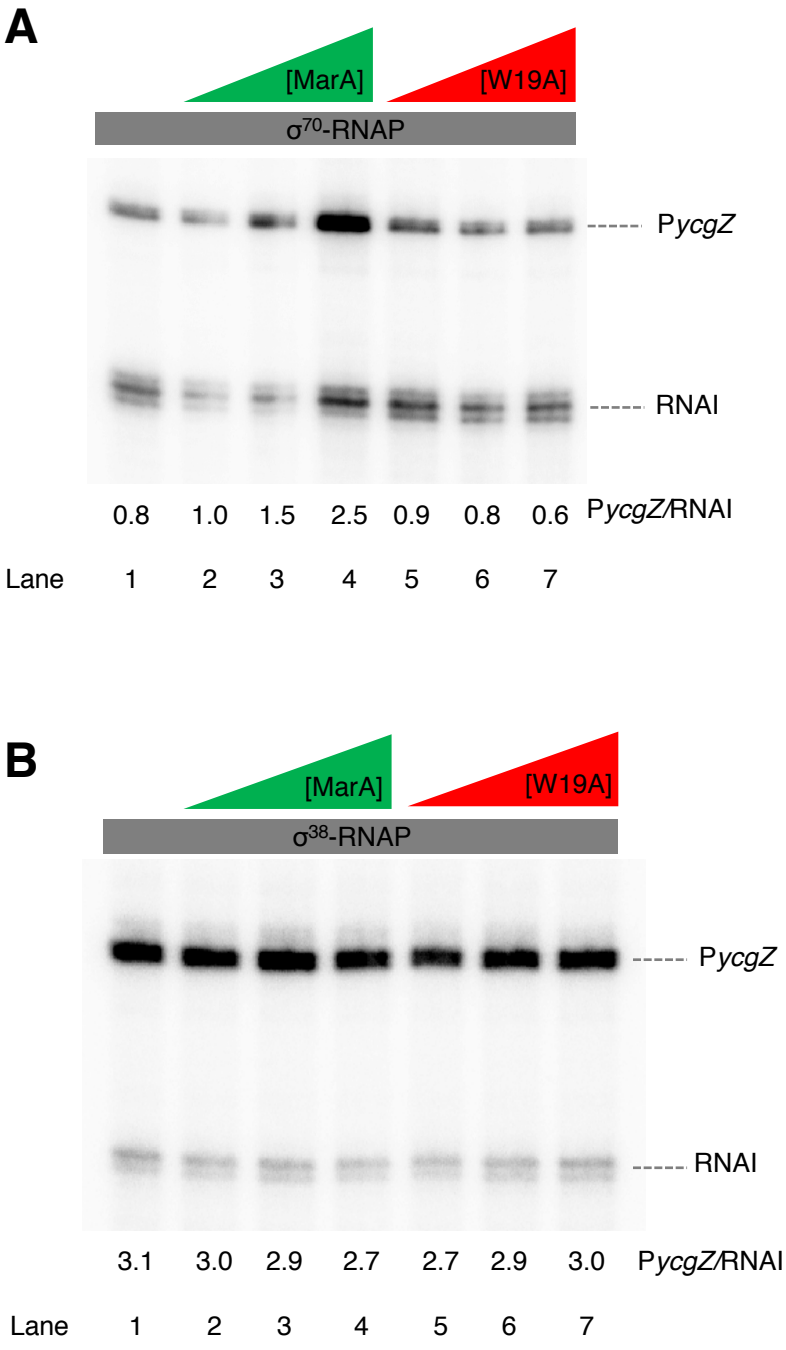

Figure 3.9 Activation of transcription by MarA-W19A.

Images of denaturing sequencing gels used to separate transcripts generated *in vitro* from the *ycgZ*.1 fragment. Increasing concentrations (0.2 μM – 1 μM) of wildtype (green triangles) and W19A (red triangles) MarA were used. Panels A and B show transcription with RNAP-σ^{70} and RNAP-σ^{38}, respectively. Bands formed by transcripts originating from P*ycgZ* and RNAI are indicated by dashed lines. The ratio of transcript of P*ycgZ*:RNAI is shown.

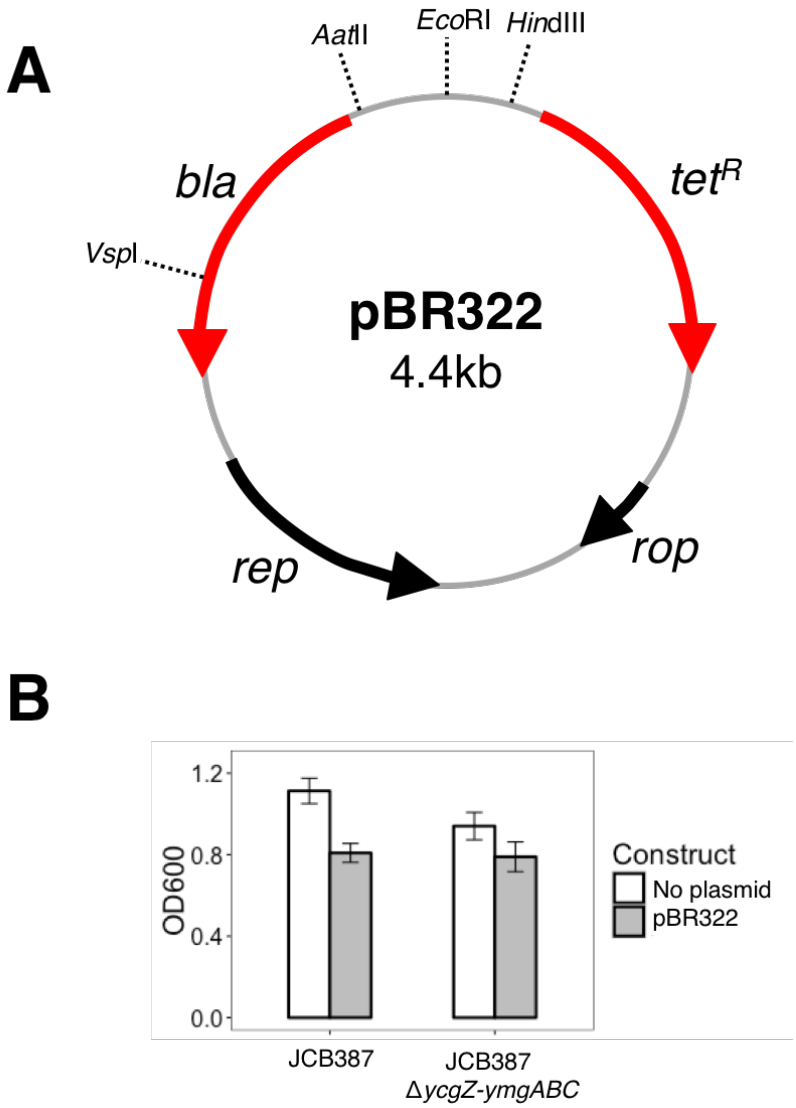

Figure 3.10 Disruption of biofilm formation by pBR322

Panel A shows the plasmid pBR322. Black arrows indicate genes. Positions of key restriction sites are shown by black dotted lines. The tetracycline and ampicillin resistance genes are shown by red arrows. Panel B shows wildtype and Δ*ycgZ-ymgABC* strains with and without the pBR322 plasmid, grown in a 96-well polystyrene plate for 48 hours and assayed for biofilm formation using the crystal violet assay. OD_{600} is shown as the mean ± standard deviation of 8 replicates (2 biological, 4 technical).

small linker cloned into the region, making pBR322Δ*bla* (Figure 3.11, Panel A). Reduction of biofilm formation was no longer seen when using this amended plasmid (Figure 3.11, Panel B).

The *ycgZ-ymgABC* operon was cloned into pBR322Δ*bla* under the control of the wildtype promoter or the *ycgZ* promoter derivates, via the *Eco*RI/*Aat*II sites (to prevent disruption of the Tet^R promoter). The complementation fragments are shown in Figure 3.12, Panel A. The new constructs were used to transform *E. coli* JCB387 and JCB387 Δ*ycgZ-ymgABC* and assayed for biofilm formation (Figure 3.12, Panel B). Knockout of the *ycgZ-ymgABC* operon caused an increase in biofilm formation, due to loss of negative biofilm regulation by these genes. Upon complementation with the *ycgZ-ymgABC*.1 fragment, crystal violet binding decreased, due to induction of the operon by MarA ($p < 0.01$). This decrease was then recovered with deletion (*ycgZ-ymgABC*.2) or mutation (*ycgZ-ymgABC*.1^M) of the marbox ($p < 0.01$ for both). This effect was seen both for wildtype JCB387 and JCB387 Δ*ycgZ-ymgABC.* Thus, MarA inhibits biofilm formation through the activation of the *ycgZ-ymgABC* operon.

3.6 Role of the *ycgZ-ymgABC* operon in acid tolerance and antibiotic resistance

Unlike biofilm formation, acid tolerance is a well characterised *mar* phenotype (Rosner and Slonczewski 1994, Ruiz, McMurry and Levy 2008). YmgB is a known regulator of acid resistance, binding the DNA of downstream genes in response to indole (Lee *et al.* 2007). To investigate this, growth of wildtype and Δ*ycgZ-ymgABC* JCB387 was measured at pH 4 and pH 7 (Figure 3.13). We selected pH 4 as it was the lowest pH at which growth could still be observed. At pH 7, the wildtype and Δ*ycgZ-ymgABC*

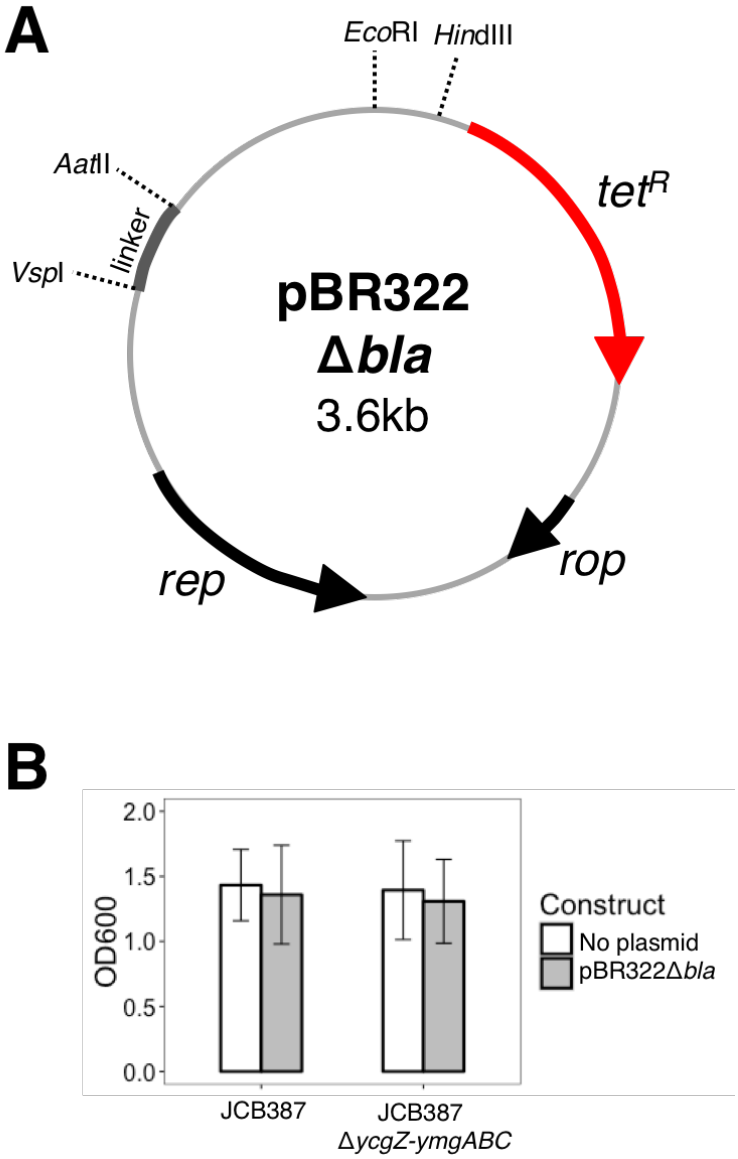

Figure 3.11 The pBR322Δ*bla* plasmid

Panel A shows the plasmid pBR322Δ*bla*. Black arrows indicate genes. Positions of key restriction sites are shown by black dotted lines. The tetracycline resistance gene is shown by a red arrow; all other genes are shown by black arrows. Key restriction sites are shown by black dotted lines. The *bla* gene of pBR322 has been excised by digestion with *Vsp*I and *Aat*II, and a 117 bp linker with terminal *Vsp*I and *Aat*II sites cloned into the region. Panel B shows wildtype and Δ*ycgZ-ymgABC* strains with and without the pBR322Δ*bla* plasmid, grown in a 96-well polystyrene plate for 48 hours and assayed for biofilm formation using the crystal violet assay. OD_{600} is shown as the mean ± standard deviation of 8 replicates (2 biological, 4 technical).

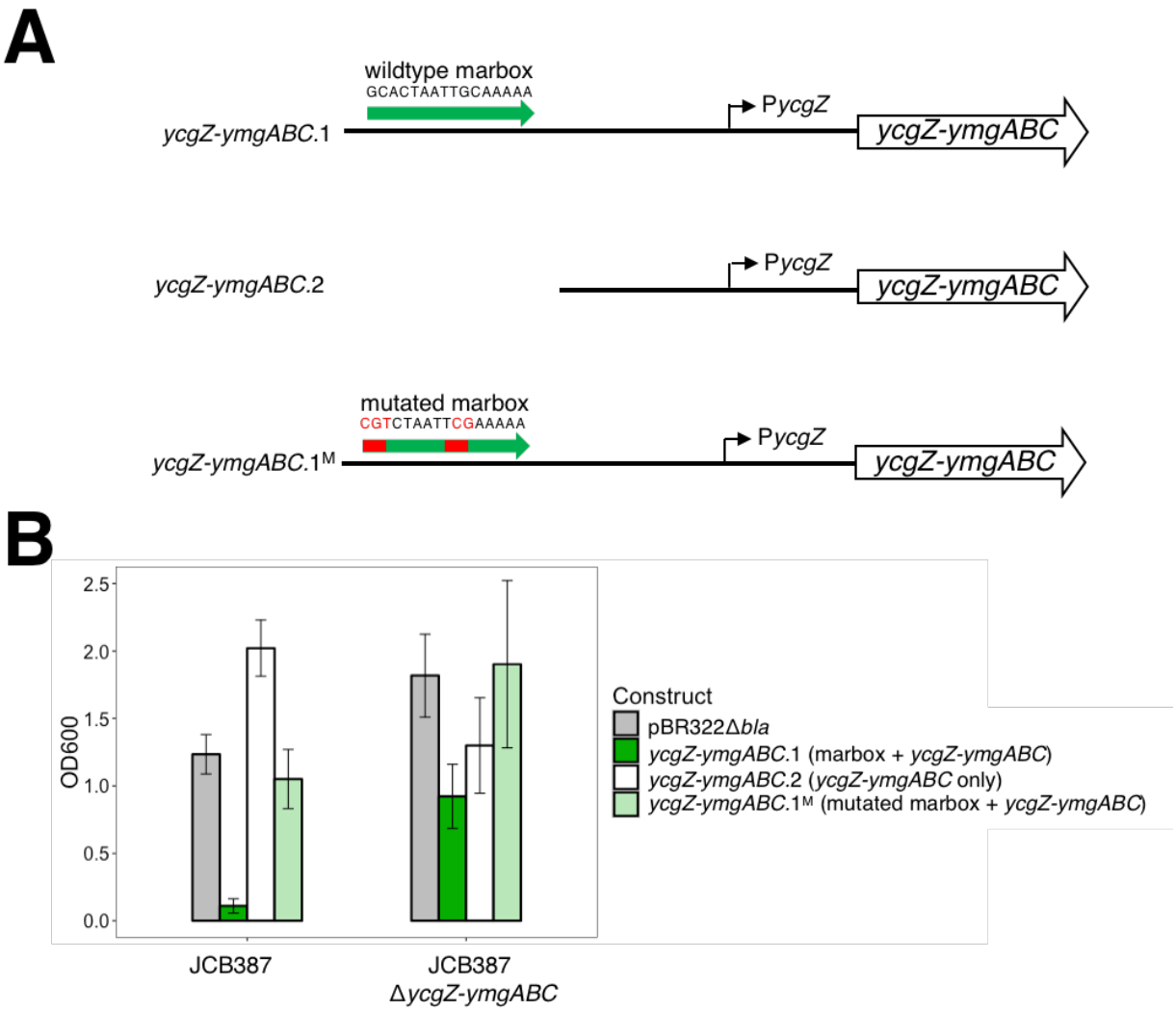

Figure 3.12 Regulation of biofilm formation by MarA-dependent activation of *ycgZ-ymgABC*.

Panel A is a schematic showing the *ycgZ-ymgABC* complementation fragments. White block arrows show the genes; thick black lines represents non-coding DNA regions. The marbox is indicated in green, with the direction of the green arrow indicating orientation. Right-angled arrows indicate the *ycgZ* transcription start site. Panel B shows biofilm formation by wildtype and Δ*ycgZ-ymgABC* strains containing the *ycgZ* regulatory region derivatives fused to the *ycgZ-ymgABC* operon. Cells were grown in a 96-well polystyrene plate for 48 hours and assayed for biofilm formation using the crystal violet assay. OD_{600} is shown as the mean ± standard deviation of 8 replicates (2 biological, 4 technical). A one-way analysis of variance (ANOVA) followed by a post-hoc Tukey's HSD test showed significant differences between all constructs within each strain ($p < 0.01$ for all), except between pBR322 and *ycgZ-ymgABC*.1^{M} ($p > 0.05$).

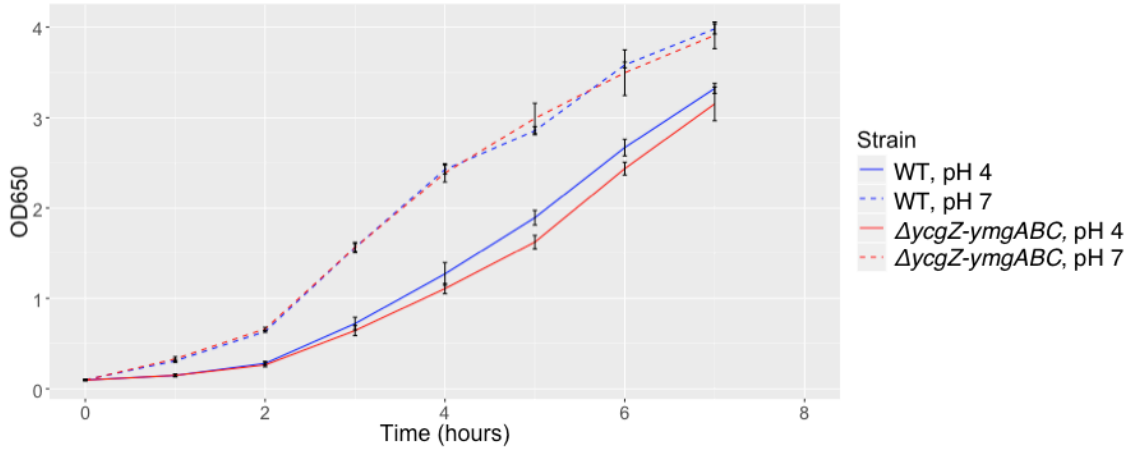

Figure 3.13 Growth of wildtype and Δ*ycgZ-ymgABC* JCB387 at pH 4 and pH 7.

Growth was assessed using a standard growth curve assay in LB adjusted to pH 7 and pH 4. Samples were taken hourly and the OD_{650} measured. Blue lines represent wildtype JCB387, whilst red lines represent JCB387 Δ*ycgZ-ymgABC*. Dashed lines and solid lines show growth curves done at pH 7 and pH 4, respectively. Points on the curve shown are the mean of three replicate flasks ± the standard deviation.

appeared similar. However at pH 4 a slight growth defect was seen for Δ*ycgZ-ymgABC*, emerging after approximately 3 hours. Unexpectedly however, this deficiency was small, questioning the role of the *ycgZ-ymgA-ariR-ymgC* operon in acid resistance. Further study is required to determine the function of MarA regulation on *ycgZ-ymgABC* mediated acid tolerance.

Finally, wildtype and Δ*ycgZ-ymgABC* JCB387 were investigated for sensitivity to seven unrelated antibiotics (Table 3.1). Novobiocin and nalidixic acid were expected to show changes in MIC, as single knockout of *ycgZ* shows reduced fitness in the presence of these drugs, with scores of -2.68 and -2.13, respectively (Nichols *et al.* 2011). However no changes in MIC were seen for Δ*ycgZ-ymgABC* across all antibiotics tested. This does not necessarily mean that Δ*ycgZ-ymgABC* has no involvement in antibiotic tolerance, as changes may be below the level detectable in this assay. Growth curves in sub-lethal concentrations of antibiotic may be more appropriate, as this will highlight additional parameters in the bacteria-antibiotic relationship.

Table 3.1 Minimum inhibitory concentration of 7 antibiotics for JCB387 and JCB387 Δ*ycgZ-ymgABC*.

96-well MIC assays were done for *E. coli* strains JCB387 and JCB387 Δ*ycgZ-ymgABC* across seven antibiotics, using the method outlined by Andrews (2001). MIC is shown as the minimum concentration of antibiotic (mg/L) required to inhibit growth of the strain. Assays were done in quadruplicate and repeated on three separate days. Results were rejected if not in line with the control strains ATCC 25922 and NCTC 10418. Assays were also carried out with the addition of 5 mM salicylate, but showed no changes (data not shown).

Antibiotic	MIC (mg/L)	
	WT	Δ*ycgZ-ymgABC*
Ampicillin	4	4
Tetracycline	1	1
Doxycycline	4	4
Sulfamonomethoxine	2	2
Nalidixic acid	8	8
Novobiocin	128	128
Kanamycin	16	16

3.7 Discussion

The aim of this chapter was to characterise control of the *ycgZ-ymgABC* operon by MarA. Previous work identified a putative marbox upstream of *ycgZ* by ChIP-seq analysis, but did not investigate regulation by MarA (Sharma *et al.* 2017). The data here confirm that MarA activates transcription from P*ycgZ* via a marbox 60 bp upstream of the transcription start site. This explains a report of unknown regulation within the literature in which *ycgZ-ymgABC* was reported to accumulate in Lon$^-$ strains (Duval *et al.* 2017). Lon protease is known to rapidly degrade MarA (Griffith, Shah and Wolf 2004). Increased levels of MarA in Lon$^-$ strains would thus explain the results seen by Duval *et al.* (2017).

Activation of P*ycgZ* by MarA appears to be Class I, requiring residue W19 of MarA to make contact with the C-terminal domain of the α subunit of RNAP. Interestingly, the *ycgZ* marbox is in the forward orientation (Figure 3.2), positioning MarA incorrectly for Class I activation (Martin *et al.* 1999). The flexible linker joining the two α subunits may allow for non-traditional orientation of the marbox, but this relationship of MarA with the promoter has only been reported in the literature for *zwf*. This chapter has confirmed predictions that the *ycgZ* promoter is both σ^{70} and σ^{38} dependent, with strong induction by RpoS upon entry to stationary phase (Gama-Castro *et al.* 2008). However, MarA appears to activate transcription in a σ^{70}-dependent manner only and does not activate via σ^{38}. This is unsurprising, as MarA has never been shown to activate via σ^{38} dependent promoters. Regulation via only one σ factor at promoters controlled by both σ^{38} and σ^{70} has been reported for other transcription factors, notably Fis and H-NS at the *dps* promoter (Grainger *et al.* 2008). However, it has not been demonstrated for MarA or other transcriptional regulators of the AraC family.

This chapter describes how activation of *ycgZ-ymgABC* by MarA results in inhibition of biofilm formation. The *mar* inducer, salicylate, has previously been reported to repress biofilm formation in uropathogenic *E. coli* via inhibition of type I fimbriae expression (Vila and Soto 2012). The authors speculated that this was through repression of *fimB* by MarA. However as there is no marbox sequence present in the *fimB* promoter, this cannot be via direct regulation. Instead, changes in type I fimbriae expression may be an additional consequence of MarA activation of the *ycgZ-ymgABC* operon.

Biofilm inhibition appears counterintuitive for an antibiotic stress regulator, as the biofilm environment provides a number of advantages: reduced antibiotic penetration, cell dormancy, and an increased level of mutations (Hoiby *et al.* 2010). However, certain environmental conditions may make the biofilm environment suboptimal. For planktonic cells which have not yet established a biofilm, forming a biofilm provides a long-term survival strategy but will not offer immediate protection against antibiotic challenge. Repression of biofilm formation may allow cellular resources to be focused on other mechanisms of antibiotic resistance, such as drug efflux and metabolic changes.

Additional regulators may also be involved in regulation of this pathway. ß-galactosidase assays showed a 4-fold drop in promoter activity for *ycgZ*.2, but only a 2-fold drop for *ycgZ*.1^{M} (Figure 3.4). The upstream location of the marbox and the high activity of the *ycgZ*.2 fragment relative to the pRW50 control indicate that loss of the core promoter elements did not occur. Partial binding to the mutated fragment may have occurred, although this was not demonstrable at the MarA concentrations used in

EMSAs (Figure 3.3). Thus, binding sites for other regulators may be present between positions -50 and -78 relative to the transcription start site.

Unusually, ß-galactosidase assays shown here suggest that the normally transcriptionally silent *mar* operon is expressed at high levels in *E. coli* JCB387. One would expect, in the absence of *mar* induction by salicylate, to see no effect of marbox deletion or mutation on promoter activity; however, a marked difference was seen between *ycgZ*.1 and *ycgZ*.1^{M}/*ycgZ*.2. Testing of MarA levels in *E. coli* JCB387 would be required to explain the unusual MarA-dependent results seen here. Additionally, experiments in *marA, rob, and soxS* knockout strains could serve to further verify the dependence of regulation *in vivo* on MarA rather than its close relatives.

Conflicting results were also seen here regarding the interplay between *ycgZ-ymgABC* and MarA in acid tolerance (Lee *et al.* 2007). YmgB is known to upregulate acid resistance via activation of the *gadABCE* and *hdeAB* operons. However, our *ycgZ-ymgABC* knockout created here showed minimal changes in acid sensitivity. Additionally, the inclusion of *ycgZ-ymgABC* within the MarA regulon is somewhat unusual given that MarA is a known repressor of *hdeAB* (Schneiders et al. 2004). However, repression of *hdeAB* by MarA has been shown to be highly dependent on growth phase and other regulators; opposing regulation of *hdeAB* by MarA and YmgB could therefore allow for varied expression of *hdeAB* under different cellular conditions (Ruiz, McMurry and Levy 2008). Further experiments with both *ycgZ-ymgABC* and *marRAB* knockouts could elucidate the points within the *E. coli* life cycle at which these two systems regulate *hdeAB*.

In summary, this chapter has identified a new mechanism for MarA in the regulation of biofilm formation and has elucidated an unexpected role of biofilms within an antibiotic resistance context. As a global stress regulator, this provides MarA with an additional route to manage challenges within the cell.

Chapter 4

Spacing Requirements for Transcriptional Activation by MarA at the *mlaF* Intergenic Region

4.1 Introduction

Previously, MarA had been thought to control antibiotic resistance primarily through OmpF porin and the AcrAB-TolC efflux pump (Cohen, McMurry and Levy 1988, Cohen *et al.* 1989, Ma *et al.* 1996, Okusu, Ma and Nikaido 1996). However, ChIP-seq experiments identified novel mechanisms utilised by MarA to tolerate antibiotic stress (Sharma *et al.* 2017). One target identified was the *mlaFEDCB* operon. MarA activates transcription of the operon, which encodes a lipid trafficking ABC transport system. Hence, by regulating encoded the *mlaFEDCB* operon, MarA controls outer membrane permeability and sensitivity to antibiotics such as tetracyclines (Sharma *et al.* 2017).

The *mlaFEDCB* operon is under the control of three promoters (P1, P2 and P3) with overlapping -35 and -10 elements and a putative UP element sequence (Figure 4.2, Panel A). The promoters produce transcripts of 128, 148, and 157 nucleotides in length, respectively. As transcription can be modelled *in vitro* from this region without the need for any additional transcription factors, it is a good candidate for examining the mechanisms of MarA activation.

The aim of this chapter is to understand the spacing and orientation requirements for the different promoter elements and the marbox at the *mlaF* intergenic region. The *mlaF* marbox is correctly positioned and orientated for Class II activation by MarA, which would require contact with region 4 of the σ^{70} subunit of RNAP. In MarA, the residue forming this contact (Y81) diverges from the equivalent residue in Rob and SoxS, which are known to contact region 4 of σ^{70} in order to occlude its binding to the -35 element at Class II promoters (Gallegos *et al.* 1997, Zafar, Sanchez-Alberola and Wolf 2011, Taliaferro *et al.* 2012). Thus, Class II promoters regulated by MarA may show

flexibility in spacing requirements. Orientation, meanwhile, may not be fixed; as seen with *ycgZ* and *zwf*, MarA can still activate at these promoters despite the marbox being incorrectly orientated for Class I activation (Martin *et al.* 1999). Thus, orientation requirements may not be fixed at Class II promoters such as that seen upstream of *mlaF*.

4.2 Activation of P2*mlaF* by MarA

A derivative of the 135 bp region immediately upstream of *mlaF* was prepared. This fragment, named *mlaF.1,* was cloned in pSR and used as a template for *in vitro* transcription (Figure 4.2). MarA induces activation of transcription from P2*mlaF*.

4.3 Activation of P2*mlaF* by MarA is orientation specific

The marbox upstream of P*mlaF* is correctly positioned for Class II activation by MarA, with the marbox in the forward orientation immediately adjacent to the P2 -35 element (Figure 4.2). Activation of transcription by MarA is reported to be orientation specific, with inversion of the marbox resulting in total loss of activation (Jair *et al.* 1996, Martin *et al.* 1999, Gillette, Martin and Rosner 2000). However, Chapter 3 highlighted how MarA is able to activate transcription from P*ycgZ* despite the non-traditional orientation of the marbox. Thus, specific marbox orientation may not be essential at all promoters.

To investigate this, a derivative of the *mlaF*.1 fragment with the marbox inverted was cloned in pSR and named *mlaF*.1.inv (Figure 4.3, Panel A). Transcripts originating from this region were compared to *mlaF*.1 in an *in vitro* transcription experiment, with the addition of 2 μM MarA (Figure 4.3, Panel B). Activation of the transcript initiating from *mlaF* P2 no longer occurred when the marbox is inverted (lanes 3-4). Thus, the forward orientation of the marbox is essential at the *mlaF* promoter.

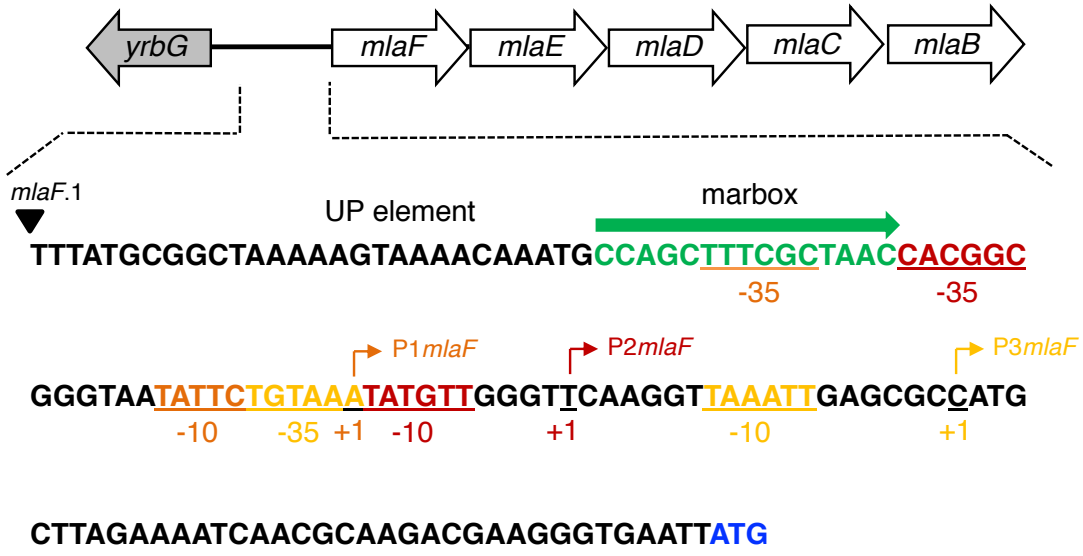

Figure 4.1 The regulatory region upstream of *mlaF*

The diagram shows the *mlaFEDCB* operon and its upstream regulatory region. -10 and -35 elements are indicated in underline for P1 (orange), P2 (red) and P3 (yellow). Transcription start sites are shown by right-angled arrows. The start codon is shown in blue. The UP element is indicated by a dotted black line, and the marbox by a green arrow. The black triangle indicates the beginning of the *mlaF*.1 derivative.

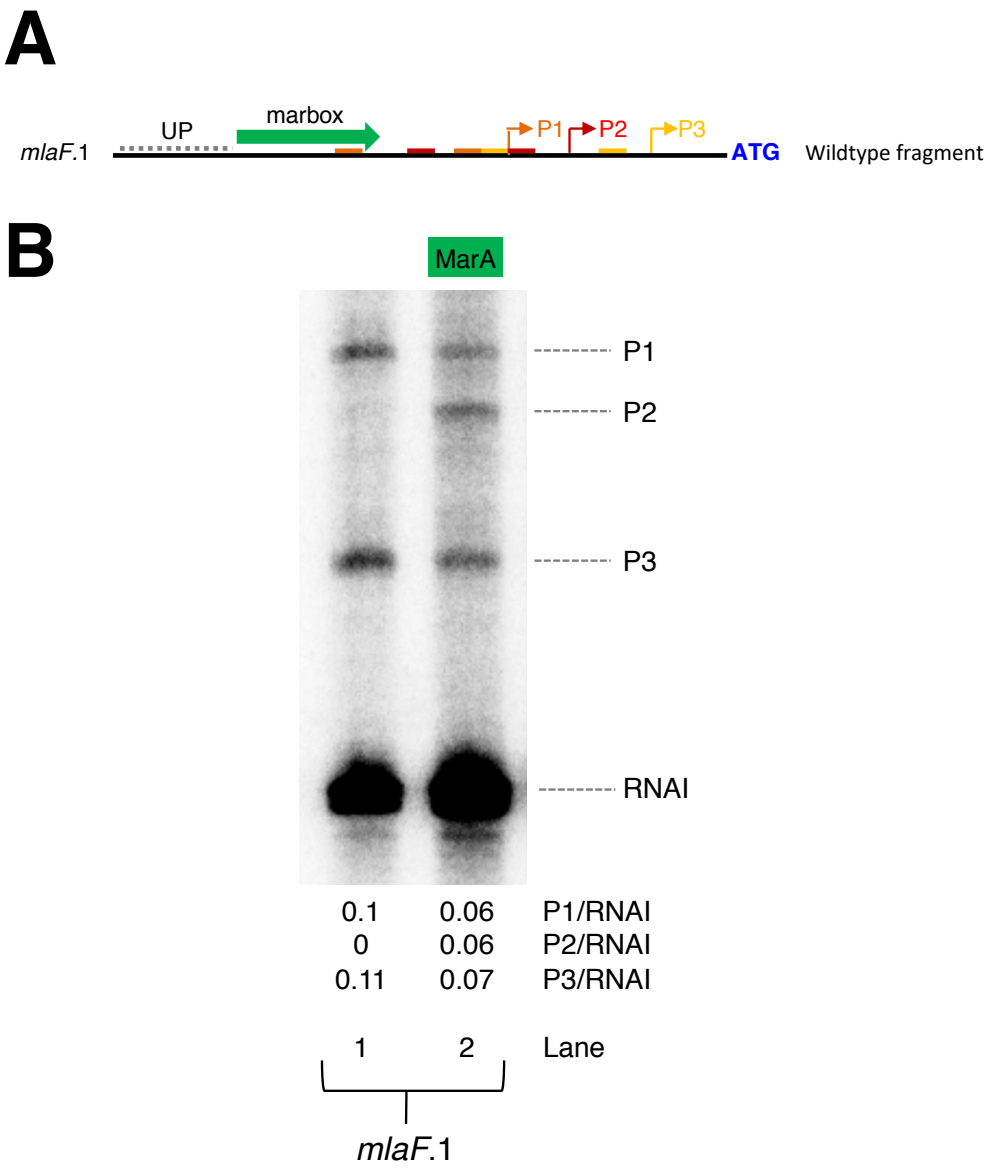

Figure 4.2 Activation of P2*mlaF* by MarA.

Panel A shows the *mlaF*.1 fragment schematically; the beginning of the fragment is labelled in Figure 4.1. Coloured rectangles represent the P1 (orange), P2 (red) and P3 (yellow) -10 and -35 elements, with coloured right-angled arrows indicating the transcription start sites. The marbox is shown by a green arrow and the UP element by a grey dotted line. Panel B shows a gel image from an *in vitro* transcription experiment, using *mlaF*.1 cloned in pSR as a template. Transcripts initiating from P1, P2 and P3 and indicated by dashed lines, as is the RNAI internal control. The green rectangle represents addition of 2 μM MarA. Transcriptions were done with RNAP-σ70. Ratios of transcript to RNAI are shown.

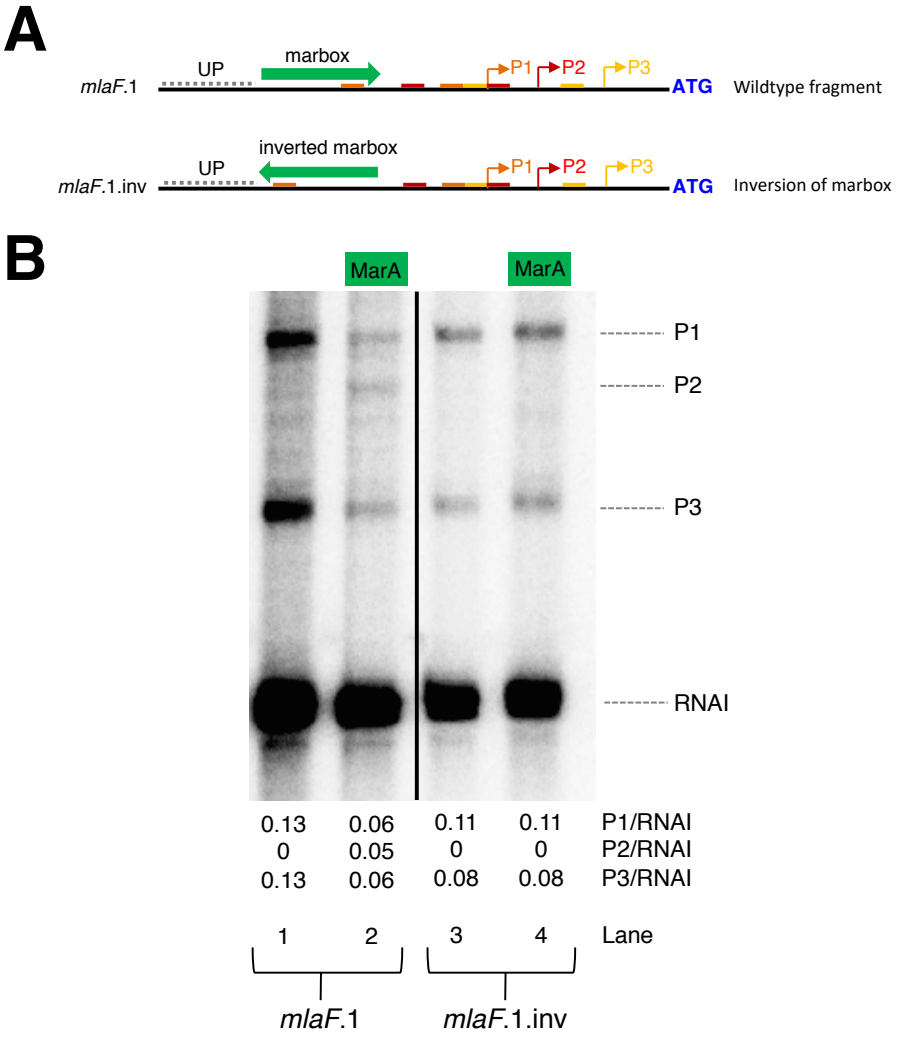

Figure 4.3 Effect of marbox inversion on MarA activation of transcription at P*mlaF.*

Panel A is a diagram of the *mlaF.*1 and *mlaF.1.*inv DNA fragments. Orange, red and yellow rectangles represent the -10 and -35 elements for P1, P2, and P3 respectively. Right-angled arrows show transcription start sites. Start codons are indicated in blue. UP elements are displayed as grey dotted lines, and the marbox is shown by green arrows. Panel B shows an image of a denaturing sequencing gel on which transcripts from an *in vitro* transcription experiment were compared. Transcripts were generated with the addition of RNAP-σ^{70} holoenzyme to the *mlaF.*1 and *mlaF.*1.inv fragments cloned in pSR. Transcription was done with and without the addition of 2 μM MarA, shown by green rectangles. Dashed lines indicate positions of transcripts originating from the *mlaF* promoters and from RNAI, an internal control. Ratios of transcript to RNAI are shown.

4.4 MarA activation of P*mlaF* requires contact with the alpha subunit of RNAP

MarA, Rob and SoxS are described as 'ambidextrous' transcriptional activators, requiring contact with the α-CTD of RNAP at certain promoters only (Jair *et al.* 1995, Jair *et al.* 1996, Jair *et al.* 1996). The α-CTD binds the UP element upstream of the -35 element to interact with activator proteins (Igarashi *et al.* 1991, Blatter *et al.* 1994, Estrem *et al.* 1998). An AT-rich region upstream of the *mlaF* marbox was identified as a putative UP element (Figure 4.2, Panel A).

A derivative of *mlaF*.1 was created with the UP element removed and named *mlaF*.upE (Figure 4.4, Panel A). This was cloned in pSR and used as a template for *in vitro* transcription assays in comparison to *mlaF*.1 (Figure 4.4, Panel B). In the absence of MarA, *mlaF*.upE showed reduced transcription from P1 (lane 3 vs lane 1). With the addition of 2 μM MarA, activation of P2 was present but reduced (lane 4 vs lane 2).

In vitro transcription assays were also done with the addition of the MarA W19A mutant, which has residue W19 mutated to an alanine to disrupt the α-CTD contact (Figure 4.5). Activation of the P2*mlaF* was not seen when the W19A mutant is added (lane 3 vs lane 1), confirming the role of the MarA α-CTD interaction. Thus, MarA requires an UP element and interaction with the α-CTD of RNAP for full activation of P2*mlaF*.

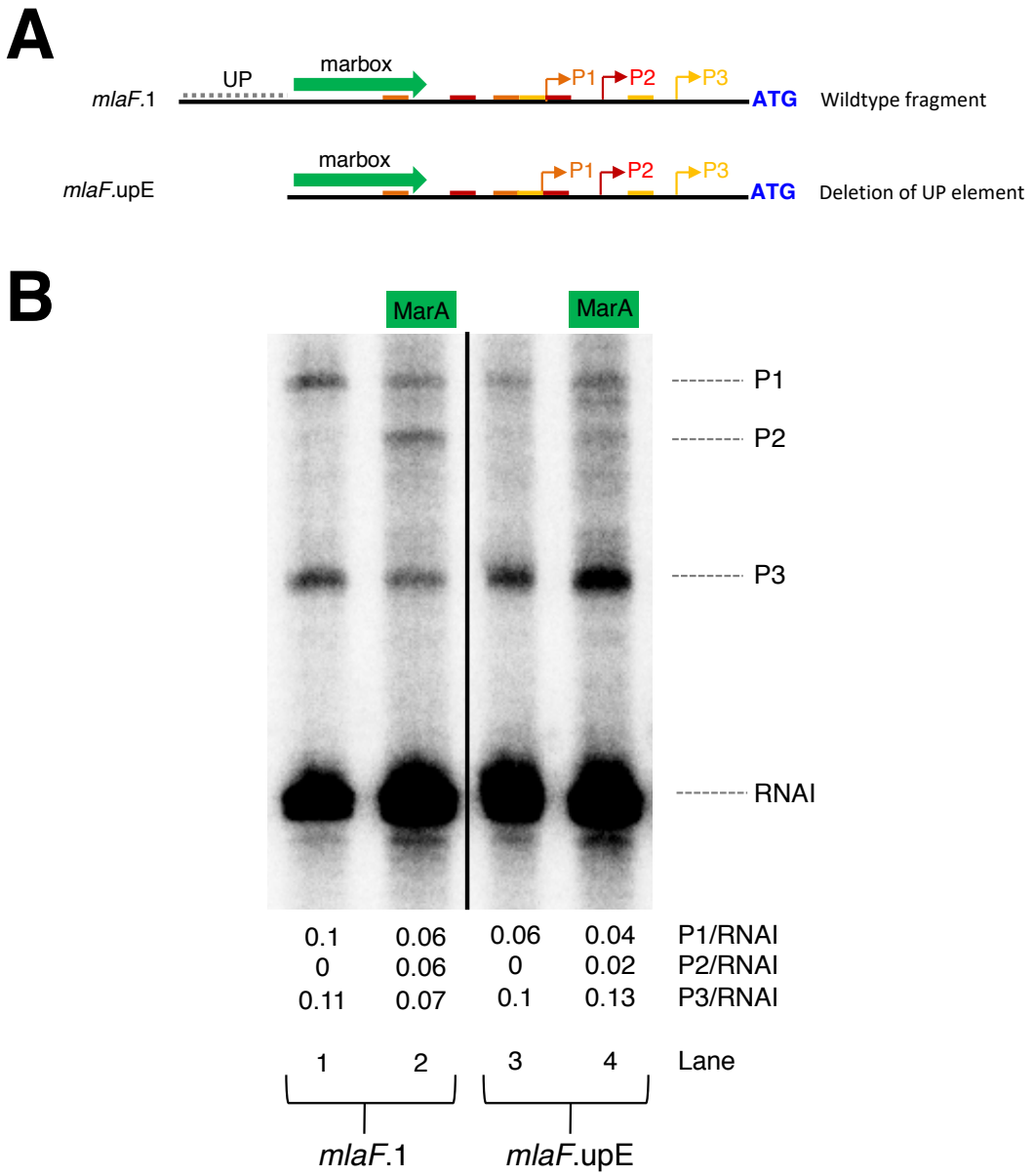

Figure 4.4 Role of the UP element in activation of P*mlaF* by MarA.

Panel A is a diagram of the *mlaF*.1 and *mlaF*.upE DNA fragments. Rectangles represent the -10 and -35 elements for P1 (orange), P2 (red), and P3 (yellow). Right-angled arrows show transcription start sites. Start codons are indicated in blue. The UP element is displayed as a grey dotted line, and the marbox is shown by green arrows. Panel B shows a gel image of transcripts generated in an *in vitro* transcription experiment. RNAP-σ^{70} holoenzyme was added to the *mlaF*.1 and *mlaF*.upE fragments cloned in pSR, with and without the addition of 2 μM MarA, shown by green rectangles. Dashed lines indicate positions of transcripts originating from P1, P2, P3 and the RNAI control. Ratios of transcript to RNAI are shown.

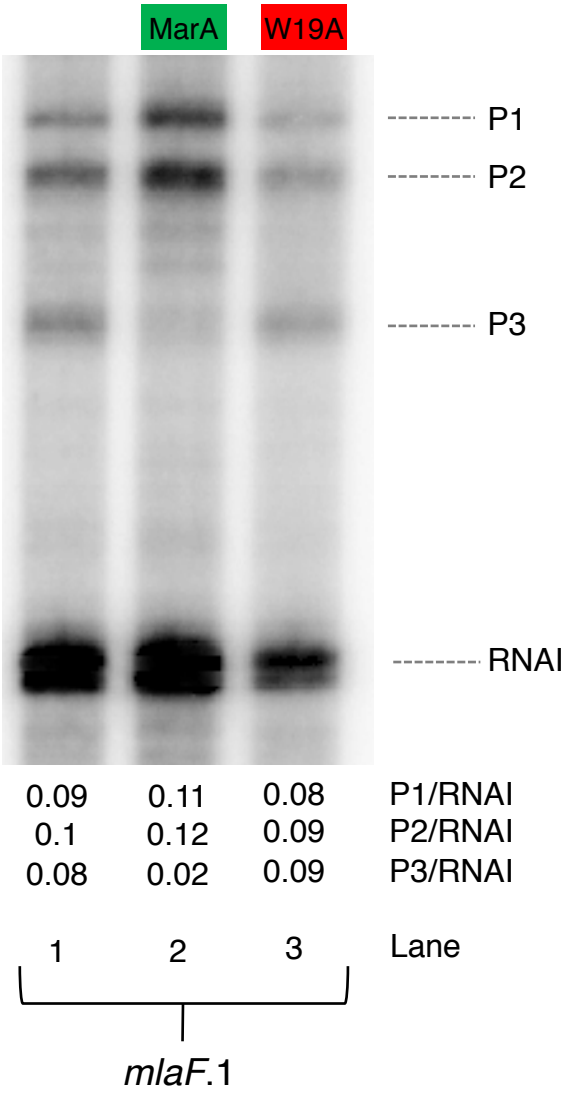

Figure 4.5 Requirement of the RNAP alpha contact for activation of P*mlaF* by MarA

The figure shows a sequencing gel image of transcripts generated in an *in vitro* transcription experiment. RNAP-σ^{70} holoenzyme was added to the *mlaF*.1 fragment cloned in pSR. 2 μM MarA (green rectangle) or W19A mutant (red rectangle) was then added. Dashed lines indicate positions of transcripts originating from P1, P2, and P3, and from the RNAI internal control. Ratios of transcript to RNAI are shown.

4.5 Activation of P2*mlaF* by Mar is highly specific relative to the -35 hexamer and transcription start site

The location of a transcription factor binding site positions the transcription factor to form specific interactions with RNAP. MarA is unusual however in its ability to activate transcription by binding marboxes at variable locations relative to the core promoter elements (Martin *et al.* 1999). We have shown though that MarA requires an UP element and contact with α-CTD of RNAP for full activation at P*mlaF*, and thus MarA may have strong location preferences at this locus.

Derivatives of *mlaF*.1 with insertions between the marbox and the P2 -35 element were created (Figure 4.6, Panel A). These fragments, named *mlaF*.1.U1-10 (the number referring to the number of nucleotides inserted) were cloned in pSR for use as templates for *in vitro* transcription experiments (Figure 4.6, Panel B). In the absence of MarA, movement of the marbox showed no effect on transcription initiating from P1 and P3 (lanes 1-10). When the marbox was moved 1 bp further from the -35 element, activation of P2 by MarA was reduced (compare lanes 11 and 12). Further than 1 bp, activation could not be seen (lanes 13-20 vs lane 11), even at 10 bp (lane 20) with MarA returned to the same face of the DNA. Assays were repeated for derivatives with the marbox moved 1-2 bp closer to the -35 element (Figure 4.7). Again, these derivatives (named *mlaF*.1.D1-2) showed partial loss of activation of the P2 transcript when the marbox was moved 1 bp (lanes 3-4), and total loss when moved 2 bp (lanes 5-6). These results indicate that movement of the marbox 1 bp in either direction allows MarA to maintain contacts with RNAP, but further than this contacts cannot be maintained due to MarA and RNAP residing on separate faces of the DNA.

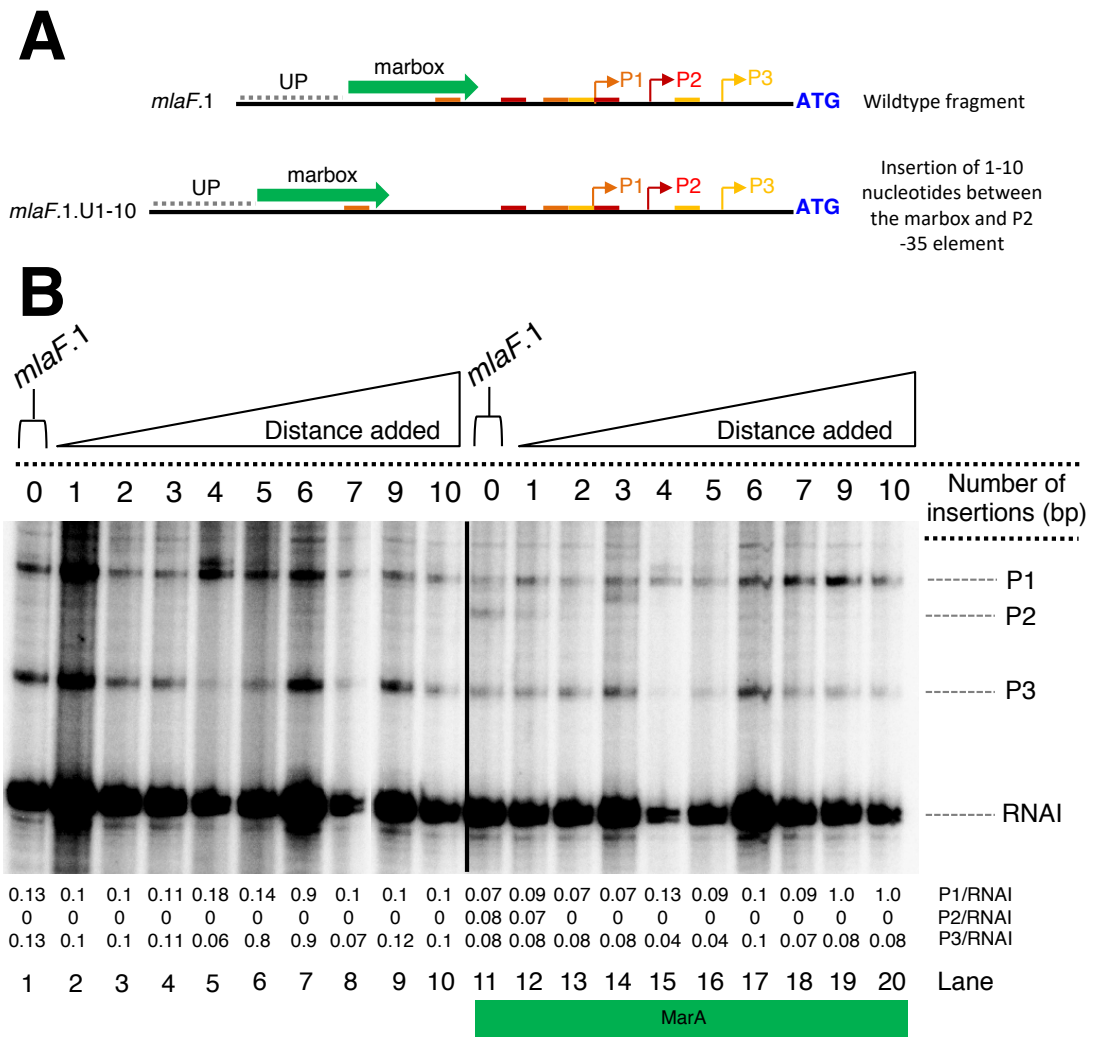

Figure 4.6 *In vitro* transcription from P*mlaF* with increasing distance of the marbox from the P2 -35 element

Panel A is a diagram of the *mlaF*.1 and *mlaF*.1.U1-U0 fragments. Rectangles represent the -10 and -35 elements for P1 (orange), P2 (red), and P3 (yellow). Right-angled arrows show transcription start sites; start codons are indicated in blue. The UP element is displayed as a grey dotted line, and the marbox is shown by green block arrows. Panel B shows sequencing gel images comparing transcripts generated in an *in vitro* transcription experiment. RNAP-σ^{70} holoenzyme was added to the *mlaF*.1 and *mlaF*.1.U1-10 fragments cloned in pSR, with and without the addition of 2 μM MarA, shown by a green rectangle. Dashed lines indicate positions of transcripts originating from P1, P2, P3 and the RNAI control. White triangles indicate the increasing number of nucleotides inserted between the marbox and the -35 element; the exact number are listed above each lane. Ratios of transcript to RNAI are shown.

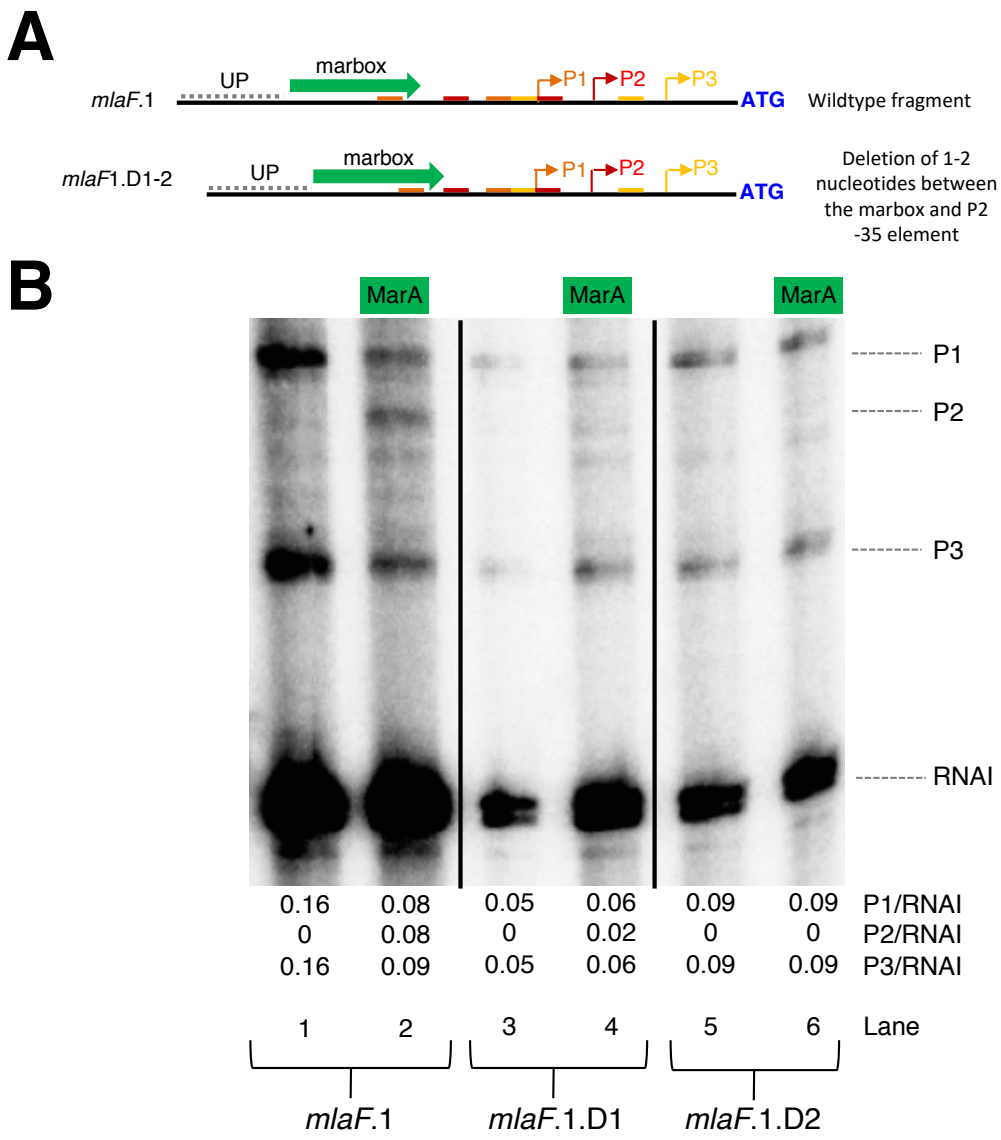

Figure 4.7 *In vitro* transcription from P*mlaF* with reduced distance between the marbox and the P2 -35 element

Panel A is a diagram of the *mlaF*.1 and *mlaF*.1.D1-2 fragments. Rectangles represent the -10 and -35 elements for P1 (orange), P2 (red), and P3 (yellow). Right-angled arrows show transcription start sites; start codons are indicated in blue. The UP element is displayed as a grey dotted line, and the marbox is shown by green block arrows. Panel B shows sequencing gel images comparing transcripts generated in an *in vitro* transcription assay. RNAP-σ^{70} holoenzyme was added to the *mlaF*.1 and *mlaF*.1.D1-10 fragments cloned in pSR, with and without the addition of 2 μM MarA, shown by green rectangles. Dashed lines indicate positions of transcripts originating from P1, P2, P3 and the RNAI control. Ratios of transcripts to RNAI are shown.

To further confirm this, the *mlaF*.1, *mlaF*.1.U1-10 and *mlaF*.1.D1-2 fragments were cloned upstream of *lacZ* in pRW50. Constructs were used to transform *E. coli* JCB387, grown to mid-log phase, and assayed for β-galactosidase activity (Figure 4.8). Reduced expression was seen regardless of how far the marbox was moved ($p < 0.01$). Thus, both *in vivo* and *in vitro* assays show that the marbox is highly location specific and cannot activate transcription when the marbox is moved.

4.6 Activation of P2*mlaF* by MarA is less efficient when P1 is mutated

MarA control of the *mlaF* regulatory region has been shown to be via activation of transcription from P2 (Sharma *et al.* 2017). However, two further *mlaF* promoters are located immediately adjacent to P2 with overlapping -10 or -35 elements. The P1 promoter is also well positioned for interaction with MarA in a Class II manner, as the P1*mlaF* -35 element is embedded within the marbox. Consequently, movement of the marbox in Figure 4.6 also results in movement of the P1 -35 element. Interestingly, transcription originating from P1*mlaF* is still apparent when the marbox is moved, with no reduction. Therefore, P1*mlaF* cannot require a -35 hexamer. Presumably, this is because this element is a very poor match to the consensus; TTTCGC opposed to the consensus TTGACA, giving a 2/6 match.

To assess the dependence of P1*mlaF* on its -10 element, a derivative of *mlaF*.1 was created with the P1 -10 element mutated from TATTCT to GGTTCT, and named *mlaF*.1.P1 (Figure 4.9, Panel A). This was cloned in pSR and used as a template for *in vitro* transcription experiments (Figure 4.9, Panel B). Mutation of the P1 -10 element

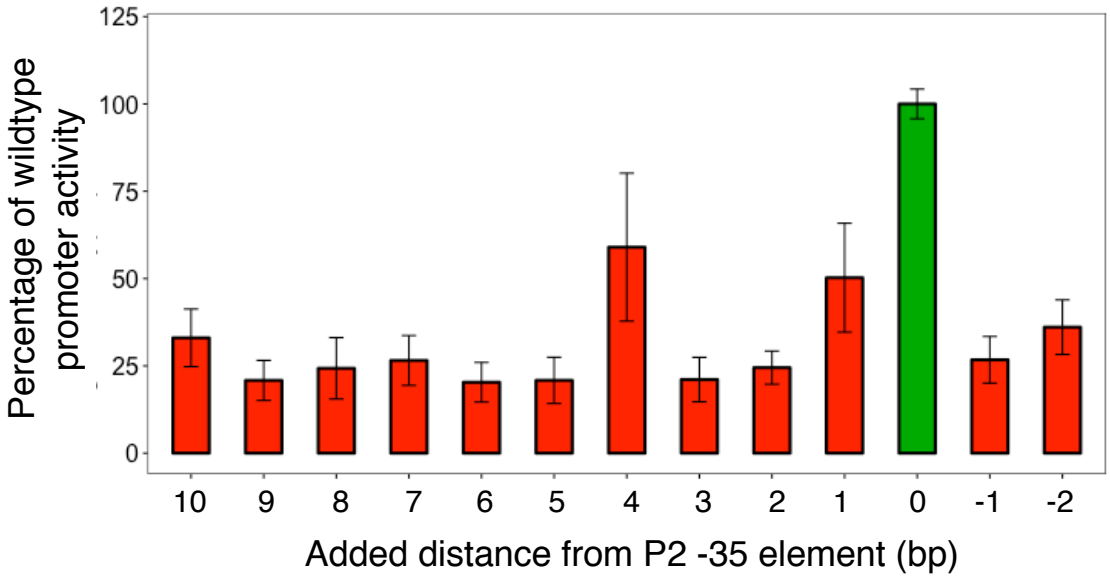

Figure 4.8 *In vivo* effect of moving the marbox on *mlaF* expression

The graph shows the β-galactosidase activity of pRW50 constructs containing the *mlaF*.1, *mlaF*.1.U1-10, and *mlaF*.1.D1-2 promoter derivatives. The green bar shows the wildtype *mlaF*.1 fragment; red bars show mutant fragments with the marbox moved closer or further from the P2 -35 element. All assays were done in JCB387 at mid-log phase, with cells containing empty pRW50 used as a control (data not shown). Activities shown are from assays done on three separate days, with each assay comprising three biological replicates. The mean ± standard deviation relative to the average wildtype (*ycgZ*.1) promoter activity is shown A one-way analysis of variance (ANOVA) was calculated with the promoter activities for the constructs; the analysis was significant ($p < 1 \times 10^{-15}$, F (12, 116) = 60.442). A post-hoc Tukey's HSD test showed that all mutants were significantly different from the *mlaF* wildtype promoter, with a $p < 0.01$ for each comparison pair.

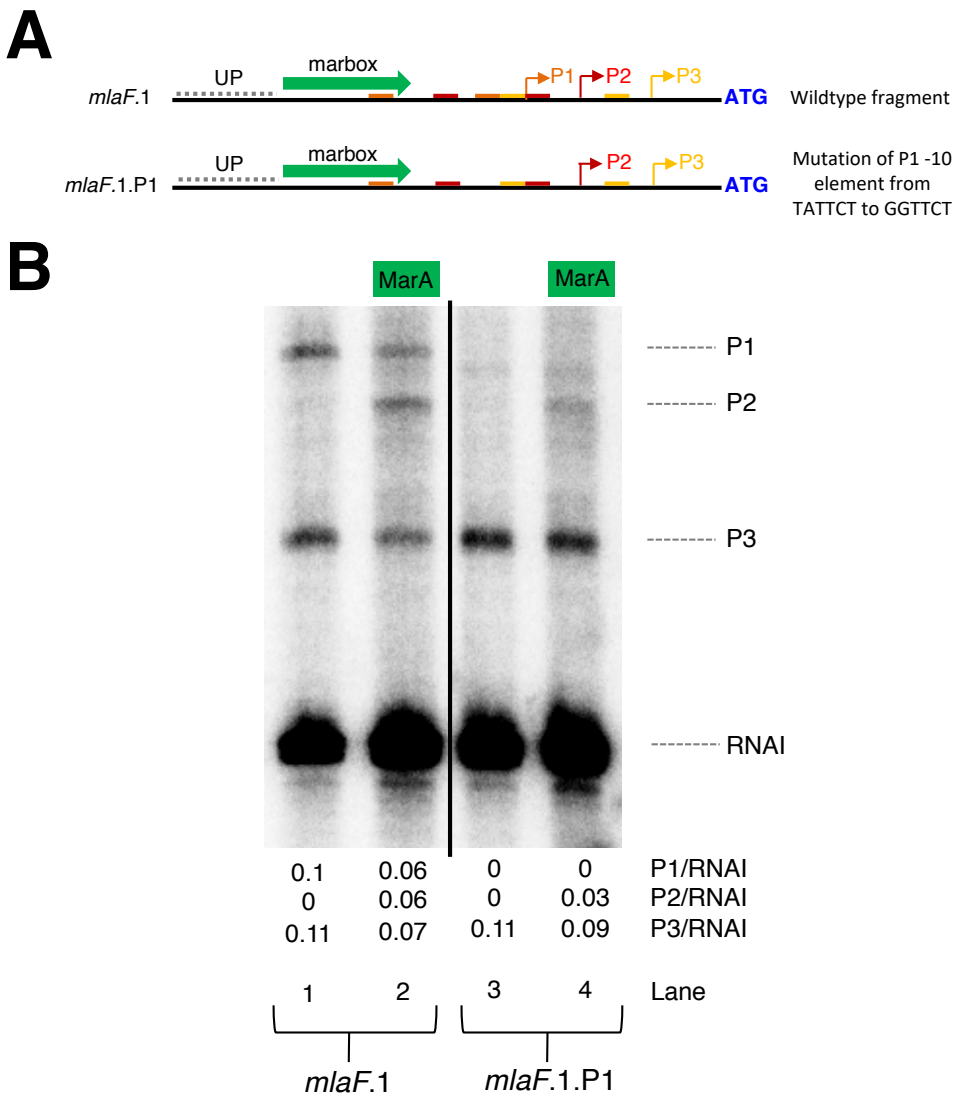

Figure 4.9 Effect of P1 mutation on *in vitro* transcription from the *mlaF* regulatory region

Panel A is a diagram of *mlaF*.1 and the *mlaF*.1.P1 derivative. Rectangles represent the -10 and -35 elements for P1 (orange), P2 (red), and P3 (yellow). Right-angled arrows show transcription start sites. Start codons are indicated in blue. The UP element is displayed as a grey dotted line, and the marbox is shown by green arrows. Panel B is an image of a sequencing gel used to analyse transcripts generated in an *in vitro* transcription experiment. RNAP-σ^{70} holoenzyme was added to the *mlaF*.1 and *mlaF*.1.P1 fragments cloned in pSR, ± 2 μM MarA (green rectangles). Dashed lines indicate positions of transcripts originating from P1, P2, P3 and the RNAI control. Ratios of transcript to RNAI are shown.

resulted in total loss of the P1 transcript (lane 3); P1*mlaF* is therefore presumably dependent on its -10 element. Consequently, loss of P1 resulted in increased transcription from P3 compared to *mlaF*.1 (compare lane 3 to lane 1). With the addition of MarA, activation of P2 was still seen for the *mlaF*.1.P1 fragment, but to a lesser extent (lane 4 vs lane 2). The P1 -10 element is therefore required for full activation of transcription from P2 by MarA.

4.7 Discussion

The work of Sharma *et al.* (2017) identified *mlaFEDCB* as a target of MarA in a ChIP-seq experiment, and verified that MarA activates this operon via the second of three overlapping promoters. This chapter aimed to characterise the spacing requirements for activation of the *mlaF* P2 promoter by MarA. The *mlaF* P2 marbox is positioned for Class II activation, and we have shown here that MarA requires an UP element and contact with α-CTD of RNAP for full activation of P2.

There are strict requirements in regards to orientation of the marbox, as MarA binds as a monomer to a non-palindromic site (Gillette, Martin and Rosner 2000). Previous studies have shown complete loss of activation when the marbox is inverted (Martin *et al.* 1999, Gillette, Martin and Rosner 2000). Unsurprisingly, the marbox upstream of *mlaF* functioned only in the forward orientation.

This study showed that MarA activation is stringent in regards to marbox location; whilst it could be moved 1 bp relative to the -35 element with only partial loss of activation, any further completely eliminated activation. The contacts made by MarA with α-CTD of

RNAP at the *mlaF* promoter may restrict its ability to activate at non-traditional locations. This is seen for the cyclic-AMP receptor protein-cAMP complex (CRP-cAMP), which requires positioning on the same face of the DNA helix as RNAP in order to interact with the α-CTD (Gaston *et al.* 1990). Movement of the CRP site results in a sharp reduction in activation, but this is restored when the site is moved a full turn of the DNA helix (10 bp) as this places CRP on the same face as RNAP. These stringent spacing requirements are relaxed if an UP element is present (Zhou *et al.* 2014). Interestingly, activation by MarA was not restored for the 10 bp insertion mutant. As *mlaF* does not appear to be a classic Class I promoter, there may be other contacts, such as with region 4 of the σ^{70} subunit of RNAP, which further restrict marbox movement.

Martin *et al.* (1999) described the possible locations and orientations marbox, indicating that the MarA-DNA-RNAP ternary complex can exist in a number of conformations. This chapter has characterised marbox orientation and spacing requirements relative to the -35 hexamer and has identified how these requirements are critical to activation, confirming that whilst a number of orientations are possible, MarA-DNA-RNAP interactions have limited flexibility.

Chapter 5
Differential Marbox Binding by MarA, Rob and SoxS

5.1 Introduction

Although MarA, Rob, and SoxS are all capable of binding the marbox, and share many of their targets, the extent to which they activate target promoters differs. This is due to way the factors bind the marbox. In general, Rob is better able to bind degenerate sequences, whilst MarA is the most specific (Martin, Gillette and Rosner 2000). Martin and Rosner (2011) suggest, based on crystal structures, that differences in the flexibility of the two helix-turn-helix motif regions between the proteins may partially account for this.

Several bases within the marbox confer discrimination between MarA and SoxS. Mutation of residues at positions 1, 3, 9, 10 and 11 (positioning as defined in Figure 1.9) alters SoxS specificity, and MarA specificity is altered by mutations at positions 1 and 9. In particular, a thymine at position 9 is thought to form Van der Waals interactions with Arg-96 of MarA, improving MarA specificity (Martin, Gillette and Rosner 2000). Mutation of amino acids within MarA, Rob and SoxS also impacts specificity. For instance, alanine substitution of Glu89 causes MarA to behave more like SoxS, showing improved binding and activation at a number of Class I superoxide responsive promoters (Martin and Rosner 2011).

The different abilities of MarA, Rob and SoxS to recruit RNAP may also result in regulon variation; MarA and SoxS activate by prerecruitment, whilst Rob activates by traditional recruitment (Gillette, Martin and Rosner 2000). Differences in transcription factor-RNAP are also key. For example, SoxS and Rob occlude binding of domain 4 of σ^{70} at Class II promoters, whilst this has not been reported for MarA (Zafar, Sanchez-Alberola and Wolf

2011). SoxS and Rob have also been shown to differ in the contacts they require with the α-CTD of RNAP (Taliaferro *et al.* 2012). Thus, polymerase contacts, in combination with varying binding affinities for the marbox, and vastly different protein concentrations within the cell, are key for these similar transcription factors to show phenotypic variation, as is seen by the reduced abilities of Rob and SoxS to activate the *mar* phenotype, and vice-versa (Jair *et al.* 1996).

5.2 Affinity of MarA, Rob and SoxS for the marbox correlates to strength of activation at P2*mlaF*

The intergenic region upstream of *mlaFEDCB* contains three promoters, with overlapping -35 and -10 elements. MarA is known to bind a marbox upstream of the *mlaF* operon to activate transcription from P2*mlaF* promoter (Sharma et al. 2017). The *mlaF* operon is also likely targeted by Rob and SoxS that can bind the marbox (Ariza *et al.* 1995). To test this, an *in vitro* transcription experiment was done with increasing concentrations of MarA, Rob or SoxS (Figure 5.1, Panel A). The DNA template was the *mlaF*.1 DNA fragment cloned in the pSR plasmid. In the absence of any transcription factor, two transcripts were seen corresponding to those originating from P1*mlaF* (157 nt) and P3*mlaF* (128 nt). Upon the addition of MarA (lanes 2-5), P1*mlaF* and P3*mlaF* reduced in intensity, whilst transcription from P2*mlaF* (148 nt) is also observed. The reduction in P1 and P3 is likely due to transcriptional interference between P1/P3 and P2. Addition of Rob (lanes 7-10) activated P2*mlaF* more efficiently than MarA, and also blocked transcription from P1*mlaF* and P3*mlaF.* Conversely, SoxS activated P2*mlaF* poorly and the P1*mlaF* and P3*mlaF* transcripts do not disappear.

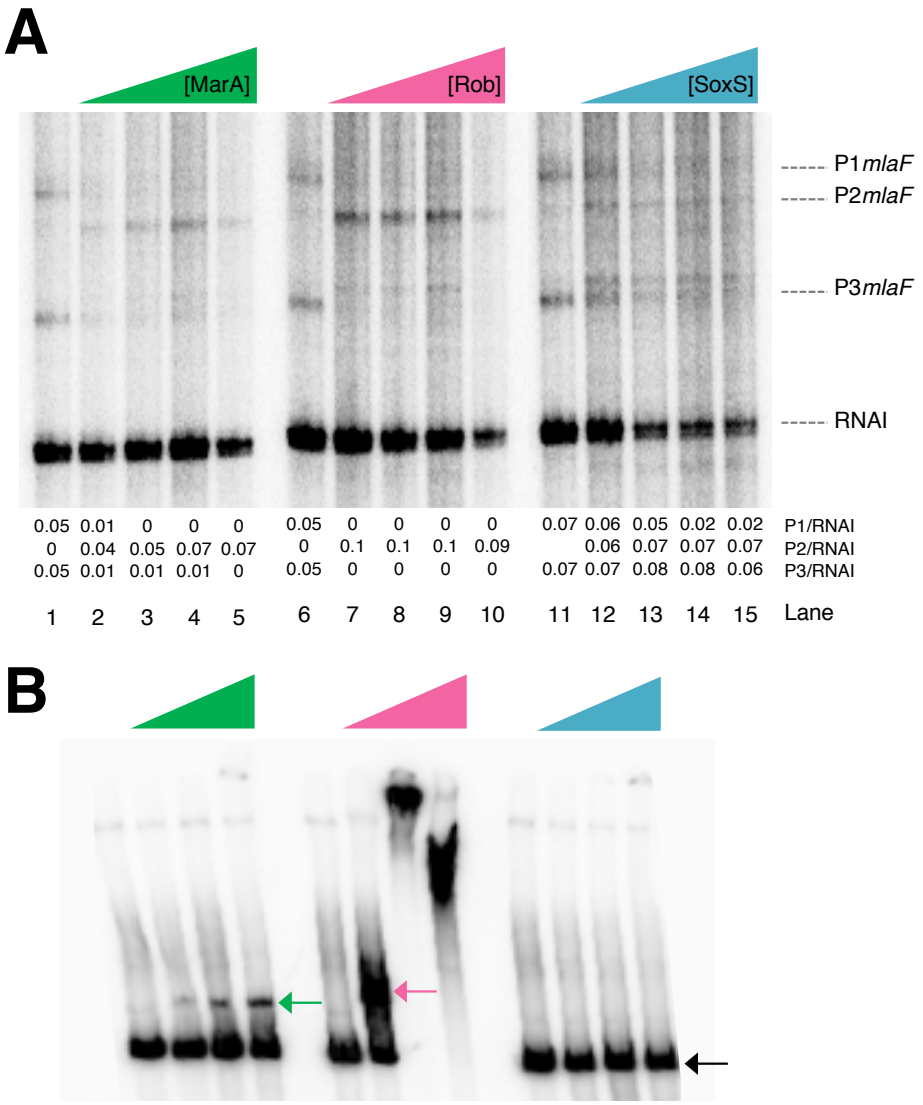

Figure 5.1 *In vitro* binding and activation of the regulatory region upstream of *mlaF* by MarA, Rob and SoxS

Panel A shows an image of a denaturing sequencing gels used to separate transcripts generated *in vitro* using the *mlaF*.1 fragment as a template. All assays were done with RNAP-σ^{70}. Triangles show increasing concentrations (0.4 µM to 2 µM) of MarA (green), Rob (pink) and SoxS (blue). Bands formed by transcripts originating from P1*mlaF*, P2*mlaF*, P3*mlaF* and RNAI are indicated by dashed lines. Ratios of transcripts to RNAI are shown. Panel B shows an image of a 6 % polyacrylamide gel used to separate protein:*mlaF*.1 complexes. Coloured triangles show increasing protein concentrations (0.4 µM – 1.2 µM - 2 µM), as for Panel A. Bands formed by free DNA are indicated by a black arrow. Protein-DNA complexes are indicated by coloured arrows (MarA – green; Rob – pink).

Binding of MarA, Rob and SoxS to *mlaF*.1 was assessed by EMSA (Figure 5.1, Panel B). Addition of MarA resulted in the formation of a single DNA-protein complex (green arrow, lanes 2-4). At low concentrations Rob formed a complex of similar mobility to that formed by MarA (pink arrow, lane 6). At higher concentrations Rob formed very low mobility complexes (lanes 7-8). This is probably because Rob can bind DNA as a dimer (Gallegos *et al.* 1997). Rob also bound more tightly than MarA, with over 50 % of the DNA bound at the lowest concentration of Rob. SoxS was unable to form complexes with the *mlaF*.1 fragment in this assay (lanes 10-12). Thus, the affinity of the regulators for the *mlaF* marbox is SoxS < MarA < Rob. This correlates with the activation of P2*mlaF* (Figure 5.1, Panel A).

5.3 Binding of MarA, Rob and SoxS to MarA ChIP-seq and SoxS ChIP-exo targets *in vitro*

As evaluated by the *mlaF* regulatory region (Figure 5.1), MarA, Rob and SoxS bind targets with different affinities (Martin, Gillette and Rosner 2000, Martin and Rosner 2011, Chubiz, Glekas and Rao 2012). To better understand these differences, binding of MarA, SoxS and Rob to a larger number of sites was tested. The sites to be tested were gathered from genome-wide assays of MarA or SoxS binding (Seo *et al.* 2015, Sharma *et al.* 2017). Briefly, the Sharma *et al.* (2017) MarA ChIP-seq identified targets for MarA and targets for SoxS were identified by the Seo *et al.* (2015) ChIP-exo.

The binding of MarA, Rob and SoxS to 29 of the targets identified in the MarA ChIP-seq experiment was assessed by EMSA. The data are shown in Appendix 1 and a summary is shown in Table 5.1. Analysis of MarA, Rob and SoxS binding to 16 SoxS sites

Table 5.1 Summary of binding of MarA, Rob and SoxS to MarA ChIP-seq targets

29 targets from the Sharma et al. (2017) ChIP-seq were assessed for MarA, Rob and SoxS binding by EMSA (images shown in Appendix 1). '+++' indicates binding observed at 0.4uM. '++' indicates binding observed at 1.2uM. '+' indicates binding observed at 2uM only. '-' indicates no clear binding seen even at 2uM. *estA* is a negative control fragment containing no marbox. ETECp9480770 is a gene found on the ETEC p948 plasmid.

Number	Target	Marbox sequence	MarA binding	Rob binding	SoxS binding
1	*thrL*	gcacagacagataaa	+++	+++	+++
2	*leuL<>leuO*	gcacaattagctaat	+++	+++	++
3	*degP*	gcgttatctgttaat	++	+++	-
4	*lacZ*	gcataaagtgtaaag	++	+++	-
5	*ybaO*	gcacaaaatgacaaa	+++	+++	+++
6	*pheP*	gcactaaatgttaaa	+++	+++	+++
7	*modE<>acrZ*	ccacgcaaagctgac	+++	+++	++
8	*ybiV*	cctatgagcgtaaaa	++	+++	-
9	*grxA/ybjC*	gcattaattgctaaa	+++	+++	++
10	*ycgF<>ycgZ*	gcactaattgcaaaa	+++	+++	+++
11	*fnr*	gcacaaattgtttaa	+++	+++	-
12	*yneO*	gcactaattgctaaa	+++	+++	+++
13	*marC<>marR*	ccacgttttgctaaa	+++	+++	+++
14	*yeeF*	gcactatttgctaaa	+++	+++	-
15	*ompC<>micF*	gcactgaatgtcaaa	+++	+++	++
16	*ypeC*	gcatttttgctaaa	+++	+++	+++
17	*yfeS><cysM*	gcaacaactgttaaa	++	+++	+
18	*guaB<>xseA*	gcatttttgcaaaa	+++	+++	+
19	ETEC3200	ccaatatccggcaaa	-	++	-
20	*nudF<>tolC*	gcacgtaacgccaac	+++	+++	-
21	*yhbV*	gcacaatctgcttac	+++	+++	+
22	*mlaF<>yrbG*	ccagctttcgctaac	+++	+++	-
23	*ibpA<>yidQ*	gcacgaaacgttaaa	++	+++	-
24	*yihT*	ccgctttacggtaaa	+++	+++	-
25	ETEC4304	aggctaatcgtataa	+	+++	-
26	ETEC4307	ccaaaaacaggtaaa	++	+++	-
27	ETEC4702	ccgataaatgcgaaa	+++	+++	+
28	*deoB*	gcaggaagcggcgaa	+++	+++	++
29	ETECp9480770	gcattttctgtcaaa	+++	+++	++
30	*estA*	No marbox (negative control)	-	++	-

identified by ChIP-exo is shown in Appendix 2 and summarised in Table 5.2 Note that Rob was used at 5-fold lower concentrations than MarA and SoxS, due to the strong non-specific binding of this protein.

At all targets, Rob bound with the highest affinity and required less than 0.24 μM of protein for complex formation. MarA bound to 28 of the MarA targets and all of the SoxS targets. SoxS bound poorest, to 17 of the MarA targets and 11 of the SoxS targets. The lack of binding seen by SoxS to the ChIP-exo targets is surprising. Seo *et al.* (2015) did not confirm their targets experimentally, which could explain this, although binding by MarA suggests that these marboxes are genuine.

5.4 SoxS poorly tolerates deviations from the consensus marbox

Although MarA and SoxS bind the same consensus DNA site, SoxS is not capable of binding all MarA targets; Table 5.1 showed that SoxS was not capable of binding all MarA targets. Analysis of the marbox sequences at differentially recognised targets could identify residues which are key for SoxS binding but not for MarA. Hence, the MarA ChIP-seq targets were grouped according to their ability to be bound by MarA and SoxS. Group I comprised targets which bind both MarA and SoxS tightly; Group II targets which bind MarA tightly but SoxS poorly; and Group III targets which bind MarA but not SoxS. Marboxes from each group aligned and the overall sequence properties of the group were visualised using WebLogo (Figure 5.2).

Table 5.2 Summary of binding of MarA, Rob and SoxS to SoxS ChIP-exo targets

16 targets from the Seo *et al.* (2015) ChIP-exo were assessed for MarA, Rob and SoxS binding by EMSA (images shown in Appendix 1). '+++' indicates clear binding observed at 0.4uM. '++' indicates binding observed at 1.2uM. '+' indicates binding observed at 2uM only. '-' indicates no binding seen even at 2uM.

Number	Target	MarA binding	Rob binding	SoxS binding
1	*lpxC*	+++	+++	+++
2	*acrAB*	+++	+++	+++
3	*uof-fur*	++	+++	-
4	*acnA*	+++	+++	-
5	*ribA*	+++	+++	++
6	*ydbK*	+++	+++	+++
7	*nhoA*	+++	+++	++
8	*fumC*	+++	+++	++
9	*zwf*	++	+++	++
10	*nfo*	+	++	-
11	*aroF-tyrA*	++	+++	+
12	*yrbL*	+++	+++	++
13	*nepI*	+	++	-
14	*sodA*	++	++	-
15	*fpr*	++	+++	+++
16	*soxS*	++	+++	-

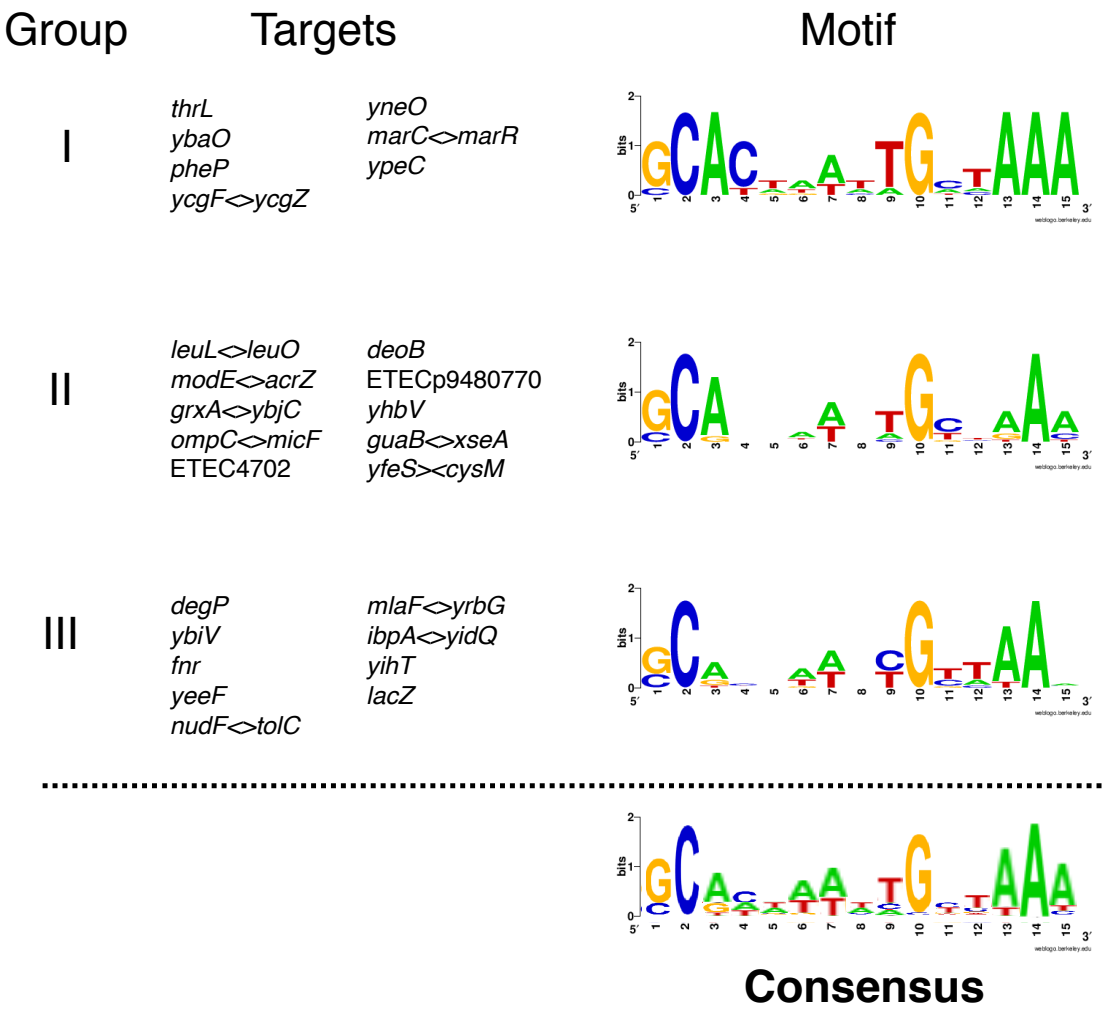

Figure 5.2 Grouping of the MarA ChIP-seq targets according to their ability to be bound by MarA and SoxS

MarA ChIP-seq targets were grouped according to their binding by MarA and SoxS, as assessed in Table 5.1. Group I comprised targets bound tightly by both MarA and SoxS; Group II was those bound tightly by MarA and poorly by SoxS; and Group III consisted of targets bound MarA but not SoxS. Marboxes for the targets were assembled using WebLogo (https://weblogo.berkeley.edu/logo.cgi) to generate a consensus motif. The MarA consensus motif generated from the Sharma *et al.* (2017) ChIP-seq is shown below for comparison.

No specific bases within the marbox appear key for SoxS binding. Instead, marboxes bound well by SoxS appear to have a closer overall match to the consensus marbox than those not bound by SoxS. MarA on the other hand binds well to marboxes across all groups. MarA is thus more able to tolerate deviations from the marbox consensus.

5.5 MarA and SoxS differ in their ability to form hydrogen bonding contacts with the DNA backbone

The crystal structure of MarA bound to DNA identified contacts made by MarA between the protein, marbox and the DNA backbone (Rhee *et al.* 1998). Contacts with bases utilise mainly van der Waals interactions, and contacts with the DNA backbone are all hydrogen bonds. The base specific contacts are shown in Figure 5.3, Panel A (i). All but one of the MarA residues forming base-specific contacts with the marbox are conserved in SoxS (Panel A (ii)). Figure 5.3 Panel B (i) shows MarA amino acid residues that form contacts with the DNA backbone, the majority of which are hydrogen bonds; 9 of these are lost in SoxS. This may explain why deviations from the consensus marbox are better tolerated by MarA relative to SoxS, as MarA utilise non-specific contacts with the DNA backbone to stabilise binding.

5.5.1 MarA is less able than SoxS to bind marboxes in low salt conditions

To test this model, binding of MarA and SoxS to the *ycgZ*.1 fragment was assessed. This target was selected as it binds MarA tightly and SoxS weakly *in vitro* (Appendix 1, Panel 10). To better understand the role of hydrogen bonding in favouring the binding of MarA, we tested different buffer conditions. Salts promote hydrogen bond interactions due to their ionic charge and the effects this has on solvation (Nucci and Vanderkooi 2008).

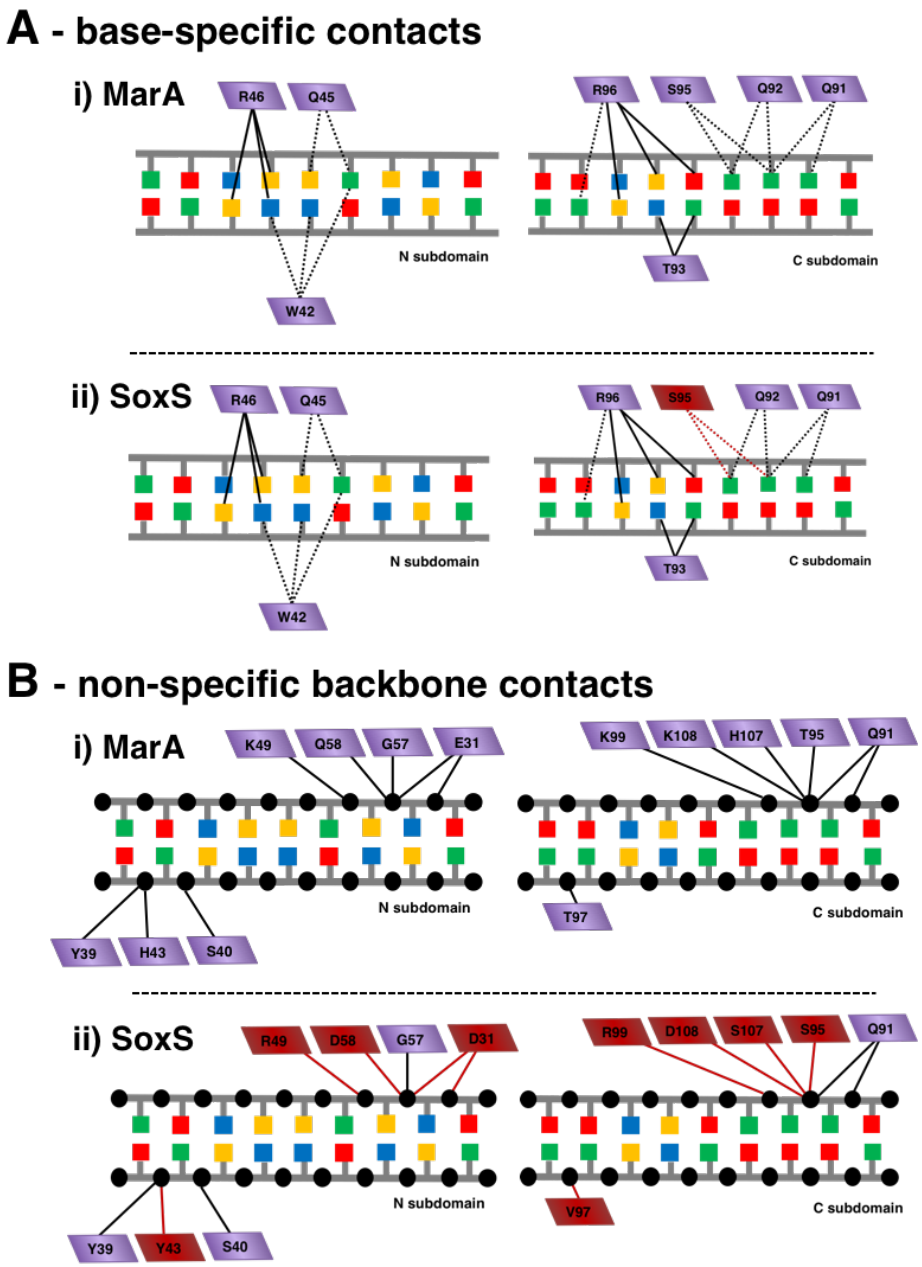

Figure 5.3 Contacts formed by MarA and SoxS with the marbox

Diagram of the base-specific and non-specific contacts formed by MarA and SoxS with the marbox, adapted from Rhee *et al.* (1998). Coloured squares represent bases OF THE DNA. Grey lines represent the sugar-phosphate backbone, with black circles representing the phosphates. Parallelograms represent amino acid residues, with purple indicating residues present in MarA and maroon indicating residues mutated in SoxS. Solid lines represent van der Waals interactions, whilst dashed represent hydrogen bonds.

Furthermore, it is more difficult for van der Waals interactions to overcome the energetic barrier to DNA binding, posed by association of water and salt ions with the DNA, at high salt concentrations (Misra *et al.* 1994).

To achieve a reduced-salt EMSA, the standard reaction buffer was replaced with ddH_2O. MarA and SoxS were also dialysed into the same storage buffer and diluted to the same concentration. DNA-protein complexes were loaded under tension (to prevent complex formation due to the salts provided by the gel running buffer) and separated on a 6 % polyacrylamide gel (Figure 5.4). In standard buffer, containing salt, the *ycgZ*.1 fragment is bound well by MarA (green arrow, lanes 2-4) and weakly by SoxS (blue arrow, lanes 5-7). In reduced salt buffer, the DNA migrates differently (black arrow, lane 8). Presumably this results from changes in DNA topology. No MarA-DNA complexes are formed in reduced-salt conditions (lanes 9-11). However, SoxS-DNA complexes do form (lanes 12-14). These complexes have the same mobility as SoxS:DNA complexes formed in the standard conditions. Thus, SoxS is more able than MarA to bind marboxes in very low salt conditions.

5.5.2 Relative binding affinities of MarA and SoxS can be changed in response to salt conditions

EMSAs were repeated in the reduced salt buffer with increasing concentrations of KCl (Figure 5.5). As expected, addition of KCl had no effect on DNA migration (lanes 1-5). At low KCl concentrations, SoxS is able to form a complex with *ycgZ*.1 (lanes 11-14), whilst MarA is not (lanes 6-10). At the highest KCl concentration the preference reverses and MarA binds more of the free DNA than SoxS (compare lanes 10 and 15).

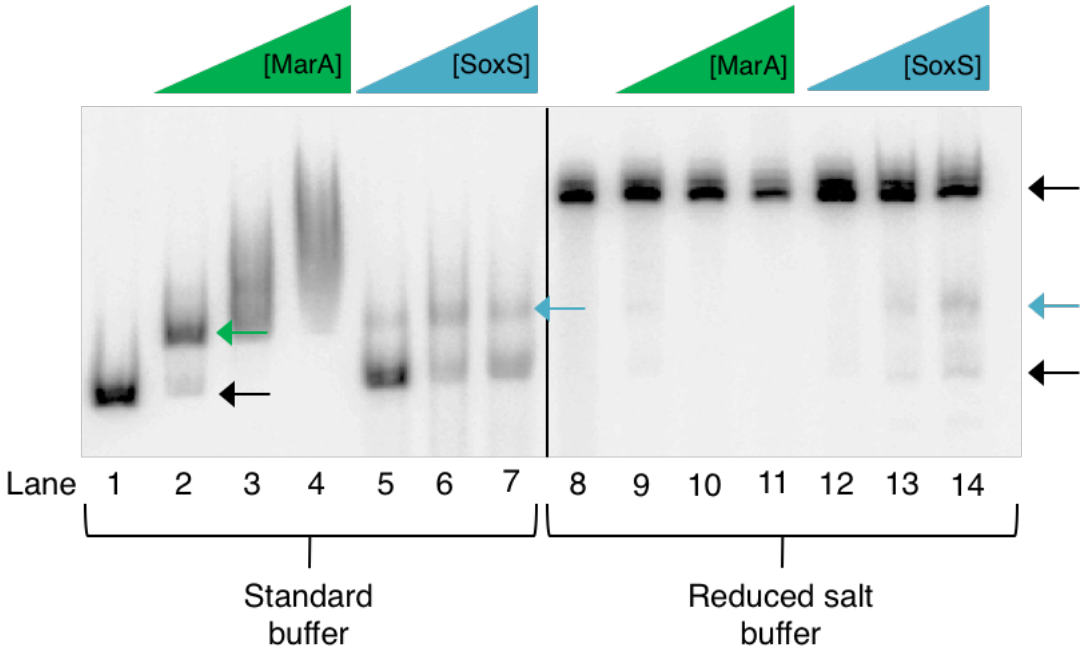

Figure 5.4 Binding of MarA and SoxS to P*ycgZ* in low salt conditions

An image of a 6 % polyacrylamide gel used to separate protein:DNA complexes is shown. [γ ^{32}P]-ATP labelled *ycgZ*.1 fragment was incubated with increasing concentrations (0.4 µM – 1.2 µM - 2 µM) of MarA (green triangles) and SoxS (blue triangles), in standard buffer or reduced salt buffer. Standard buffer comprised 1 x TNSC buffer (40 mM Tris acetate (pH 7.9), 1 mM $MgCl_2$, 100 mM KCl, 1 mM DTT) and 12.5 µg/ml Herring sperm DNA. Reduced salt buffer comprised 12.5 µg/ml Herring sperm DNA in ddH_2O only. Bands formed by free DNA are indicated by black arrows. MarA:DNA Complexes are indicated by green arrows, and SoxS:DNA complexes by blue arrows.

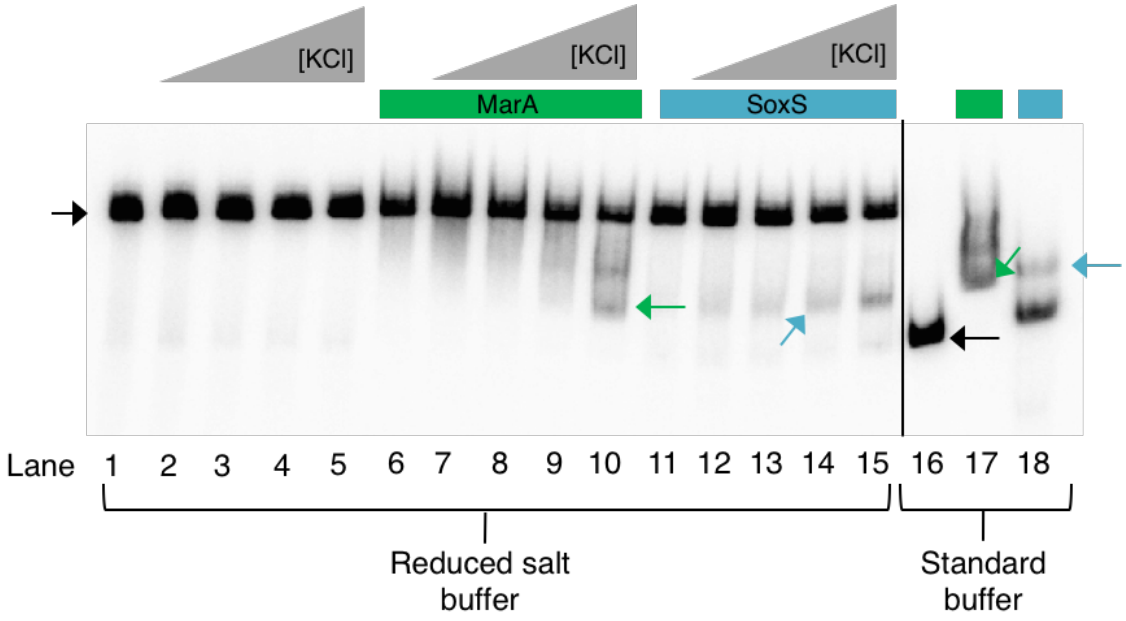

Figure 5.5 Binding of MarA and SoxS to *ycgZ*.1 with increasing concentrations of KCl

An image of a 6 % polyacrylamide gel used to separate protein:DNA complexes is shown. [γ ^{32}P]-ATP labelled *ycgZ*.1 fragment was incubated with 1.2 μM of MarA (green rectangle) or SoxS (blue rectangle), in the presence or absence of salts. Increasing concentrations (2 – 20 mM) KCl was added, shown by grey triangles. Bands formed by free DNA are indicated by black arrows. MarA-DNA complexes are indicated by green arrows, and SoxS-DNA complexes by blue arrows.

Binding of MarA and SoxS to *ycgZ*.1 was also assessed with increasing concentrations of potassium glutamate (KGlu). KGlu is the primary cytoplasmic salt in *Escherichia coli* (Richey *et al.* 1987, Cayley *et al.* 1991). Within the Hofmeister series it is placed above KCl, meaning it contributes more to protein stability and solubility (Cheng *et al.* 2016, Sengupta *et al.* 2016). Figure 5.6 shows that MarA is unable to form complexes with the DNA even at the highest KGlu concentration (lanes 6-10), whilst SoxS complex formation increases substantially with KGlu addition (lanes 11-15). Thus, changes in salt conditions can change relative binding affinities of MarA and SoxS and therefore alter target preference.

5.5.3 Impact of molecular crowding agents on DNA binding by MarA and SoxS

Reduced-salt EMSAs were repeated with the addition of molecular crowding agents. Crowding agents occupy a large amount of space and reduce solvent availability, thus increasing the effective concentration of local macromolecules (Minton 2001). They have been shown to stabilise DNA-protein interactions (Ganji *et al.* 2016). EMSAs were repeated with increasing concentrations of PEG, a crowding agent (Figure 5.7). At low PEG concentrations, SoxS forms a faint complex with the DNA (lanes 11-13), whilst MarA is unable (lanes 6-7). At high PEG concentrations, complex formation by MarA and SoxS is similar (lanes 9-10 vs lanes 14-15. Thus, molecular crowding agents can also alter target preference of MarA and SoxS.

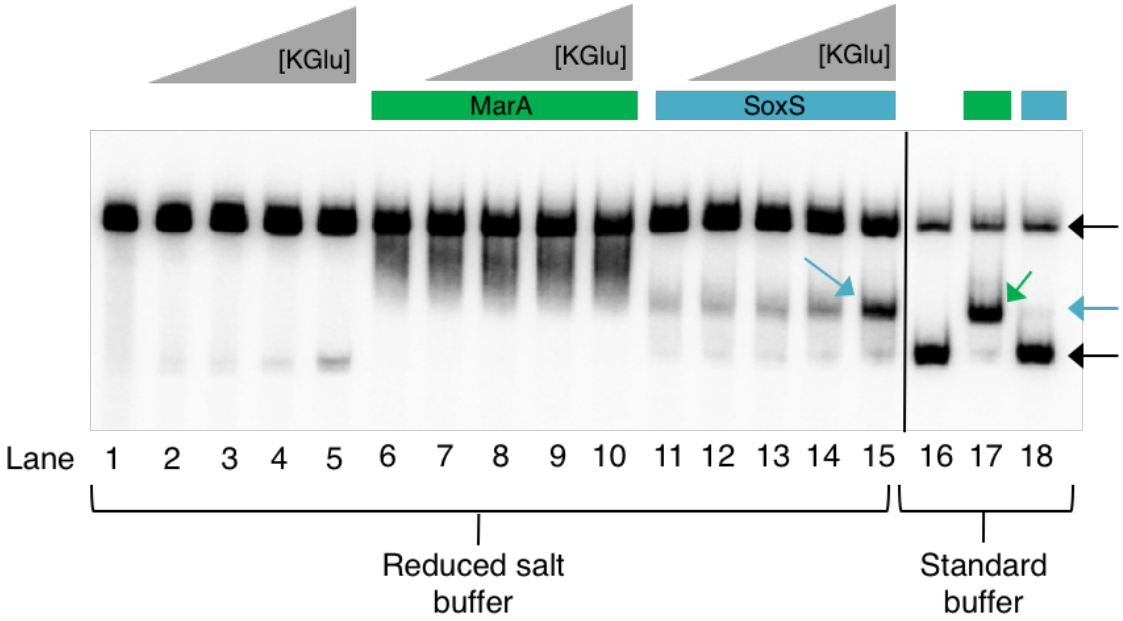

Figure 5.6 Effect of increasing KGlu concentration on MarA and SoxS binding to *ycgZ*.1

An image of a 6 % polyacrylamide gel used to separate protein:DNA complexes is shown. [γ ^{32}P]-ATP labelled *ycgZ*.1 fragment was incubated with 1.2 μM of MarA (green rectangle) or SoxS (blue rectangle), in the presence or absence of salts. Increasing concentrations (2 – 20 mM) KGlu was added, shown by grey triangles. Bands formed by free DNA are indicated by black arrows. MarA-DNA complexes are indicated by green arrows, and SoxS-DNA complexes by blue arrows.

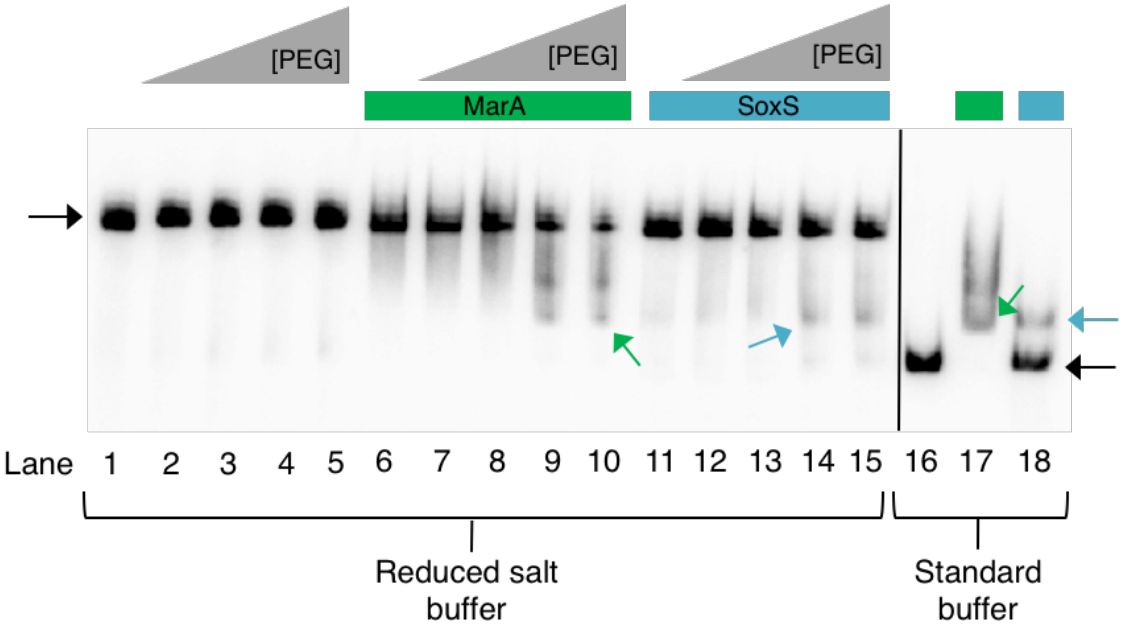

Figure 5.7 Binding of MarA and SoxS to *ycgZ*.1 with increasing concentrations of PEG

An image of a 6 % polyacrylamide gel used to separate protein:DNA complexes is shown. [γ ^{32}P]-ATP labelled *ycgZ*.1 fragment was incubated with 1.2 μM of MarA (green rectangle) or SoxS (blue rectangle), in the presence or absence of salts. Increasing concentrations (1 – 10 %) PEG was added, shown by grey triangles. Bands formed by free DNA are indicated by black arrows. MarA-DNA complexes are indicated by green arrows, and SoxS-DNA complexes by blue arrows.

5.6 Residues E31 and Q58 of MarA are key for MarA:marbox hydrogen bond formation

To further investigate differences between MarA and SoxS, with respect to DNA backbone contacts, key MarA residues were replaced with equivalent residues from SoxS. Thus, the Glu at position 31 of MarA was replaced with the Asp of SoxS, resulting in a predicted loss of a hydrogen bond. Additionally, the Gln at position 58 of MarA was replaced with the Asp seen in SoxS. This is predicted to result in a clash between the side chains of Asp and the backbone of the DNA.

MarA derivatives were assessed for binding to *ycgZ*.1 in an EMSA in standard buffer conditions (Figure 5.8). Both mutations reduced the affinity of MarA for the DNA, but the impact of the Q58D mutation was much more pronounced. Binding of the various proteins was then assessed in reduced-salt buffer with titration of KCl (Figure 5.9, Panel A), and in 7.5 mM KCl with titration of protein (Figure 5.9, Panel B). Panel A shows that, as expected, MarA did not bind the DNA target in reduced-salt buffer and only weakly upon addition of KCl (lanes 4-6). Conversely, SoxS binding was observed (lanes 7-9). MarA E31D and MarA Q58D behaved more like SoxS than MarA and bound the DNA fragment (lanes 10-15). Panel B shows that in reduced-salt buffer + 7.5 mM KCl, MarA binds *ycgZ*.1 at a similar affinity to standard buffer (compare lanes 15-17 with lanes 2-4). SoxS however shows improved binding in the reduced salt + 7.5 mM KCl buffer (lanes 5-7 versus lanes 18-20). MarA E31D and MarA Q58D again behave more like SoxS, showing improved binding in the reduced salt + 7.5 mM KCl conditions (lanes 8-10 and 21-23, and lanes 11-13 and 24-26, respectively). These data show thus show that the binding defects seen for E31D and Q58D under normal salt conditions are not prominent

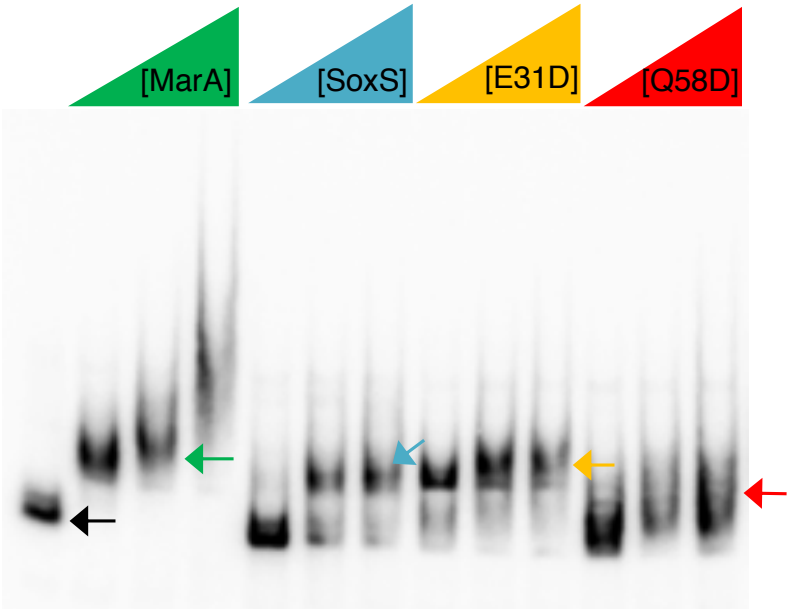

Figure 5.8 Binding of MarA mutants to *ycgZ*.1

An image of a 6 % polyacrylamide gel used to separate protein:DNA complexes is shown. [γ ^{32}P]-ATP labelled *ycgZ*.1 fragment was incubated with 0.4 - 2 μM of MarA (green triangle), SoxS (blue), E31D (yellow) or Q58D (red), under normal salt conditions. Bands formed by free DNA are indicated by black arrows. Protein-DNA complexes are indicated by coloured arrows.

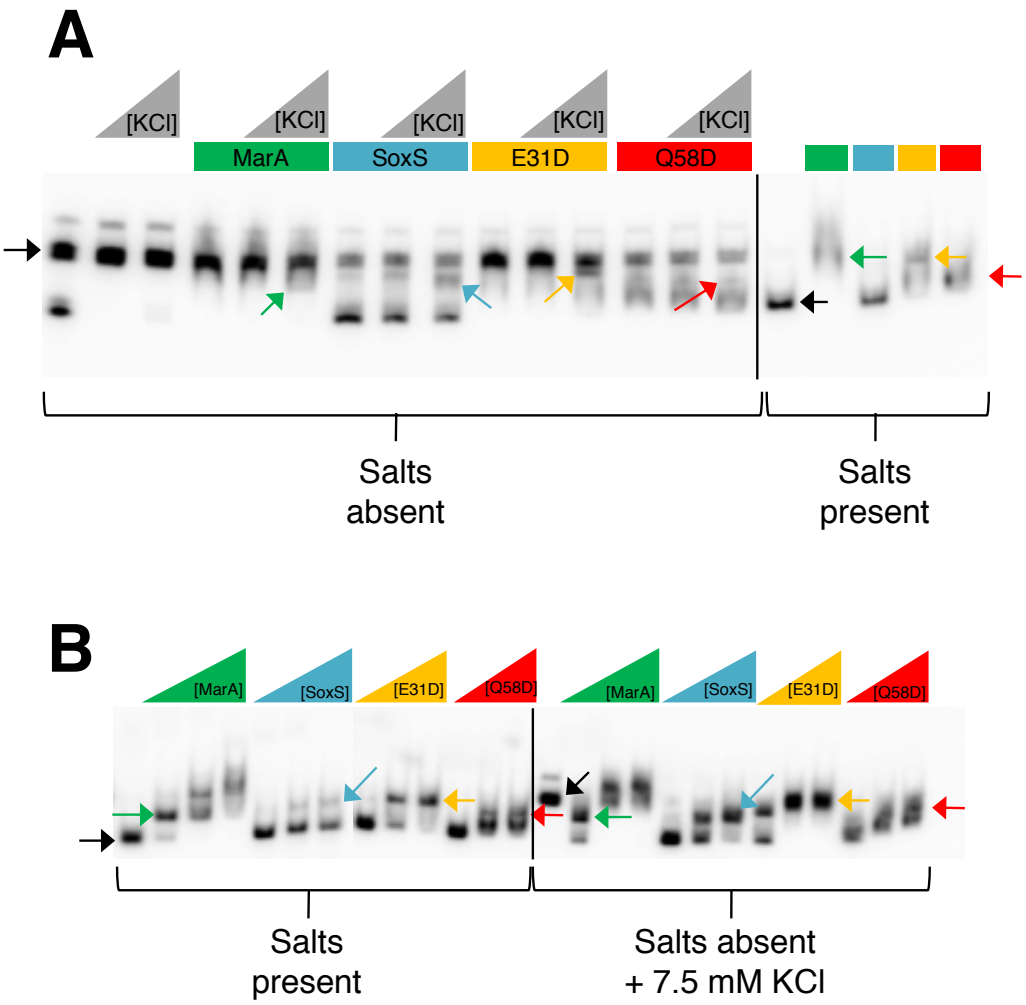

Figure 5.9 Binding of MarA mutants under different salt conditions

Image of 6 % polyacrylamide gels used to separate protein:DNA complexes are shown. Panel A shows an experiment in which [γ ^{32}P]-ATP labelled *ycgZ*.1 fragment was incubated with 1.2 µM of MarA (green rectangle), SoxS (blue), E31D (yellow) or (Q58D), in the presence or absence of salts, with increasing KCl concentrations (5 – 10 mM) shown by grey triangles. In panel B [γ ^{32}P]-ATP labelled *ycgZ*.1 fragment was incubated with 0.4 - 2 µM of MarA (green triangle), SoxS (blue), E31D (yellow) or Q58D (red), under normal or minimal + 7.5 mM KCl conditions. Bands formed by free DNA are indicated by black arrows. Protein-DNA complexes are indicated by coloured arrows. The images in Panel B are from two separate gels, run concurrently and pasted together for clarity.

in low salt conditions, and these mutants are affected in a manner more similar to SoxS by changes in salt levels. Thus, E31 and Q58 are important for binding of the marbox under regular salt conditions but not under low salt conditions.

5.7 Discussion

MarA, Rob, and SoxS control overlapping but distinct phenotypes, through the binding of shared sites (Chubiz, Glekas and Rao 2012, Duval and Lister 2013). This chapter aimed to identify how these regulators are able to show preferential binding for certain targets. Extent of transcription factor binding usually, but not always, correlates to the degree of transcriptional activation (Nuzhdin, Rychkova and Hahn 2010, Gao and Stock 2015). Binding of MarA to the marbox has been shown to not correlate with the extent of promoter stimulation (Martin, Gillette and Rosner 2000, Wall *et al.* 2009). However, the relative binding of MarA, Rob and SoxS to a marbox does correlate with activation (Martin, Gillette and Rosner 2000, Martin and Rosner 2011). Here, we showed that the *mlaF* promoter is bound by the MarA/Rob/SoxS proteins in the order SoxS < MarA < Rob. The same order is seen when looking at the extent of activation *in vitro*.

We have shown here that MarA, Rob, and SoxS bind at different affinities to 45 targets studied. For all targets, Rob bound at the highest affinity, generally requiring less than a fifth of the concentration of MarA or SoxS to achieve similar binding of free DNA. This creates an interesting paradox however; as Rob is constitutively expressed at high levels within the cell, binding of all MarA targets at high affinity would lead to a permanent *mar* phenotype. However, *in vitro* Rob has only been reported to activate *marRAB* and *micF* (Martin, Gillette and Rosner 2000). This is likely due to the traditional recruitment

of RNAP by Rob, as opposed to the prerecruitment model proposed for MarA and SoxS (Martin *et al.* 2002). MarA and SoxS are capable of forming stable complexes with RNAP without DNA present, allowing them to form a 'promoter scanning' machinery which efficiently locates viable marboxes amongst the >10,000 marboxes within the cell (Griffith *et al.* 2002). Therefore *in vivo,* Rob is less able to activate transcription despite binding at higher affinity. Sequestration also means that much of the Rob within the cell is inactive (Griffith *et al.* 2009). Rob is thus incapable of outcompeting MarA and SoxS for their targets, despite binding with a higher affinity.

Of the MarA targets studied here, roughly half (17/29) were bound by SoxS. Previous studies have indicated that the increased flexibility of the SoxS helix-turn-helix enables binding of more degenerate sequences than MarA (Gillette, Martin and Rosner 2000). The data here show the opposite: SoxS displays a reduced tolerance to deviations from the marbox due to loss of non-specific contacts with the DNA backbone, which remain present in MarA. Under regular salt conditions MarA binds P*ycgZ* at a higher affinity than SoxS, due to the ability of MarA to form additional non-specific interactions with the DNA backbone. In low salt conditions, the binding preference is reversed. SoxS, being dependent almost solely on base-specific contacts, is minimally affected by low-salt conditions, whilst MarA binding is eliminated.

We have identified two residues in MarA key for these interactions: E31 and Q58. Mutation of these residues results in significant decrease in binding under regular salt conditions, but minimal effect in low-salt conditions. Thus, E31 and Q58 are key residues for stabilisation of the MarA:marbox complex and allow MarA to tolerate deviations from

the marbox consensus. These residues are mutated in SoxS (D31 and D58, respectively) and thus their contacts disrupted. This results in increased dependence on the marbox sequence by SoxS, but also allows SoxS to respond differently to MarA in response to changes in salt conditions. However, it should be considered that in all low-salt assays shown here, the effects seen may also be due to MarA, SoxS and the MarA mutants precipitating out of solution at different salt concentrations. Whilst differences in solvability could be interesting and also provide grounds for differential regulatory properties of MarA and SoxS, further study is needed to determine exactly how these proteins behave in low salt conditions. Thus, these results should be taken with a 'pinch of salt'.

Transcription factors provide an essential link between cellular conditions and gene expression to allow a variable phenotypic response to environmental triggers. Control of transcription factors can occur through ligand binding, covalent modification, changes in abundance and availability, or control by additional transcription factors (Martínez-Antonio and Collado-Vides 2003, Martinez-Antonio *et al.* 2006). MarA is controlled by MarR, which can be inactivated through direct binding by salicylate; SoxS transcriptionally regulated by SoxR, which is converted into an activator through oxidation by redox-cycling drugs (Hidalgo, Leautaud and Demple 1998, Alekshun and Levy 1999). Here we have identified how two highly similar transcription factors can show vastly different preferences for the same binding site and have proposed a theory that differences in hydrogen bonding contacts may allow this. In combination with the existing mechanisms of regulation of MarA and SoxS, this may provide an additional mechanism for these proteins to fine-tune the transcriptional output of the cell.

Chapter 6
Final Conclusions

Regulation of gene expression allows the cell to respond appropriately to external signals, improving cell fitness during environmental challenge. The majority of this regulation occurs at the level of transcription initiation; transcriptional regulators respond to external cues and modulate recruitment of RNAP to the promoter, thus providing the link between the environment and transcriptional output (Browning and Busby 2016).

Here, we have investigated multiple aspects of the role of transcription in linking extracellular and intracellular cues to phenotypic output, specifically looking at MarA, the activator of multiple antibiotic resistance. MarA binds a marbox upstream of *ycgZ-ymgABC*, activating transcription from P*ycgZ* in a σ^{70}-dependent manner. Expression of *ycgZ-ymgABC* results in reduction of biofilm formation. This may provide protection to cells in the advent of antibiotic attack; biofilm formation can be considered a long-term survival strategy, and cells which are not already within a biofilm may find better use of cellular resources. The most well characterised target of MarA is *acrAB*, which encodes the AcrAB-TolC efflux pump (Okusu, Ma and Nikaido 1996). MarA could be considered as a short-term regulator, due to its use of pre-recruitment to activate transcription and its rapid degradation by Lon protease; thus, under short-term antibiotic stress, cellular resources may be better spent on the resource-heavy AcrAB-TolC pump than on a long-term biofilm survival strategy (Griffith *et al.* 2002, Griffith, Shah and Wolf 2004).

Further work would be required to further characterise the need for biofilm inhibition by MarA via the *ycgZ-ymgABC* operon. Interestingly, uropathogenic *E. coli* (UPEC) strains lacking *marA, soxS* and *rob* show a significant loss of virulence in murine models of ascending pyelonephritis; virulence is restored upon complementation of the genes

(Casaz *et al.* 2006). A key feature of UPEC pathogenesis is the formation of biofilms on the mucosal lining of the bladder (Costerton, Stewart and Greenberg 1999). It is therefore surprising that MarA induces increased virulence in these strains, given the inhibition of biofilm formation shown via *ycgZ-ymgABC*. Further studies are needed to identify if regulation of biofilm formation by MarA is solely via *ycgZ-ymgABC*, and indeed whether biofilm formation is a key feature of upregulation of UPEC pathogenesis by MarA.

This work has also identified the requirements for transcriptional activation by MarA at another target, upstream of the *mlaFEDCB* operon, which encodes a lipid trafficking ABC transport system (Sharma *et al.* 2017). The marbox at this site shows strict spacing and orientation requirements, functioning only in the forward direction and when moved no more than 1 bp from its original site. Although orientation specificity has been characterised for the marbox previously, spacing requirements have not. Here, we have shown the spacing requirements for the *mlaF* marbox which is positioned for Class II activation; whether the same requirements are necessary for other Class II marboxes, or for Class I, would be a question for future work. Additionally, orientation requirements may not be maintained at all marboxes; the marbox upstream of *ycgZ* is positioned for Class I activation, but orientated for Class II (Martin *et al.* 1999). This has previously been seen only for the marbox upstream of *zwf,* but is perhaps more common than previously thought and indicates a need for further study into the mechanisms of activation by MarA at these promoters.

Whilst this work has predominantly focused on role of MarA as an activator, MarA can also act as a repressor at the *hdeA*, *purA* and *rob* promoters (Schneiders *et al.* 2004,

Schneiders and Levy 2006, McMurry and Levy 2010). Interactions between MarA, the marbox, and RNAP are thus different at these promoters, with the marbox in the reverse orientation overlapping either the -35 element alone (*hdeA* and *purA*) or both the -35 and the -10 (*rob*). Spacing and orientation requirements of the marbox relative to the -35 hexamer may not be the same at these promoters, and therefore require further study. Given that repression at the *rob* promoter is thought to be via steric hindrance rather than by specific contacts with RNAP, promoters which are repressed by MarA may show much greater flexibility in spacing of the marbox (McMurry and Levy 2010). Orientation requirements may stand however, as changes in the marbox orientation at *hdeA* and *purA* would position the marbox correctly for Class II activation (Schneiders *et al.* 2004).

Finally, this work examined the regulatory overlap between MarA and two similar regulators, Rob and SoxS. These regulators respond to different signals (salicylate, decanoate, and paraquat, respectively) and activate distinct phenotypes, yet share a binding site and many of their targets (Duval and Lister 2013). They can thus be considered a single system, allowing for a fine-tuned transcriptional response by binding different subsets of genes in response to their respective environmental triggers. The work here has found another potential variable of control in this system. MarA, Rob and SoxS were shown to bind differentially to 45 known targets, verifying the 'distinct yet overlapping' nature of their respective regulons. SoxS was found to require a much closer match to the marbox consensus than MarA, which we have hypothesised here to be due to the presence of residues in MarA which form hydrogen bonding contacts with the DNA backbone, allowing MarA to tolerate divergences from the consensus. We have shown here how these differences in how MarA and SoxS interact with DNA can be exploited

to change relative binding affinities under different salt conditions. If this were to translate *in vivo*, this could allow the target preferences of MarA and SoxS to be altered according to intracellular salt conditions. Thus, changes in osmotic stress could regulate MarA and SoxS independently of induction by compounds such as salicylate and paraquat.

Appendices

Appendix 1 Binding of MarA, Rob and SoxS to MarA ChIP-seq targets

Images show EMSAs to assess the binding of MarA, Rob and SoxS to 29 MarA ChIP-seq targets, from Sharma *et al.* (2017). Increasing MarA, Rob and SoxS concentrations (0.4 – 2 μM for MarA and SoxS; 0.08 – 0.4 μM for Rob) are shown by green, pink and blue triangles, respectively. Arrows indicate free DNA (black), MarA:DNA complexes (green), Rob:DNA complexes (pink) and SoxS:DNA complexes (blue).

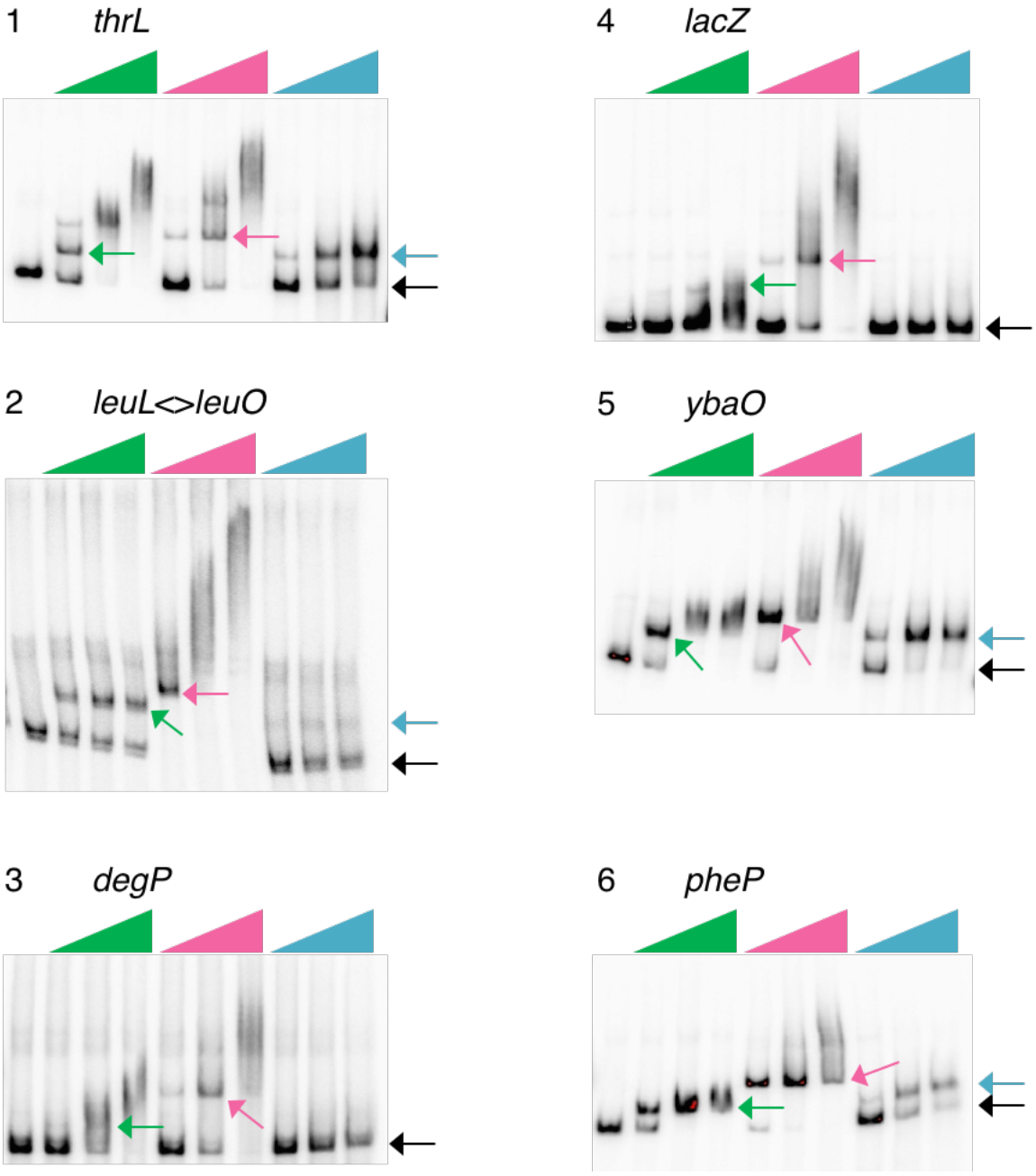

7 *modE<>acrZ*

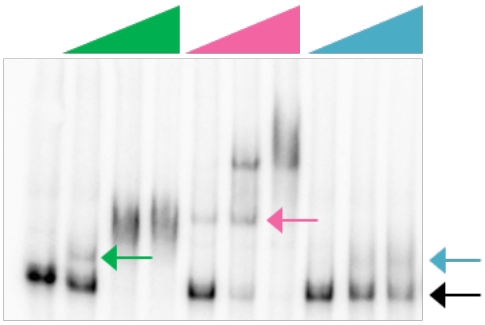

10 *ycgF<>ycgZ*

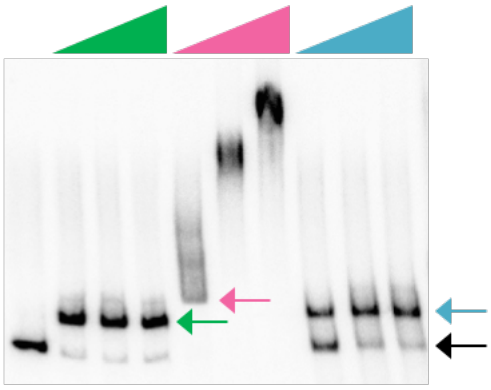

8 *ybiV*

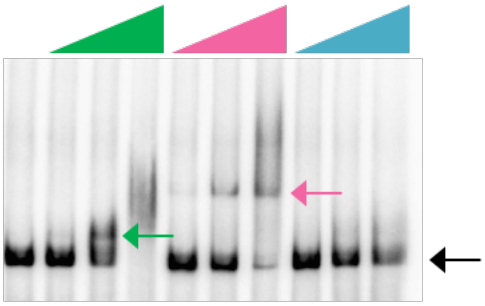

11 *fnr*

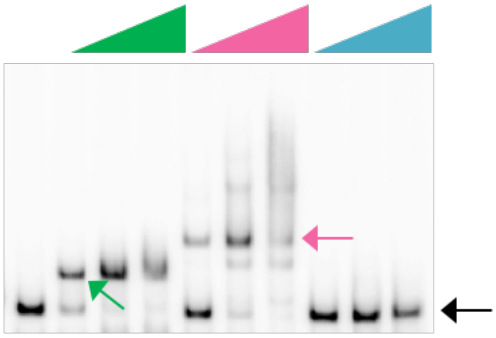

9 *grxA<>ybjC*

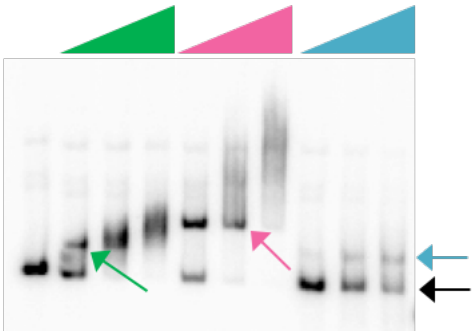

12 *yneO*

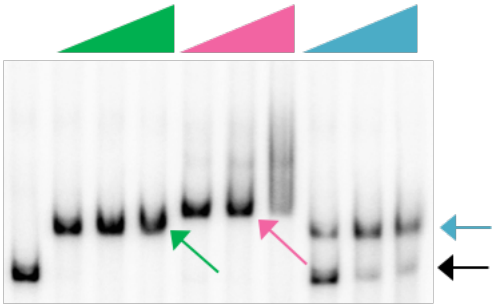

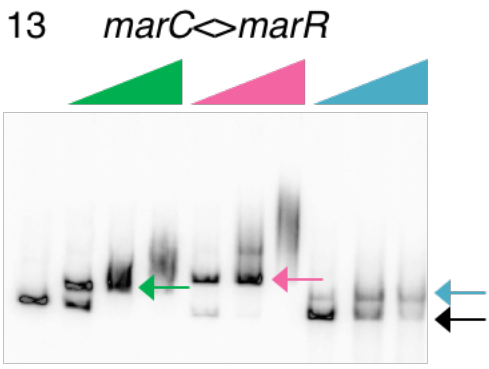
13 marC<>marR

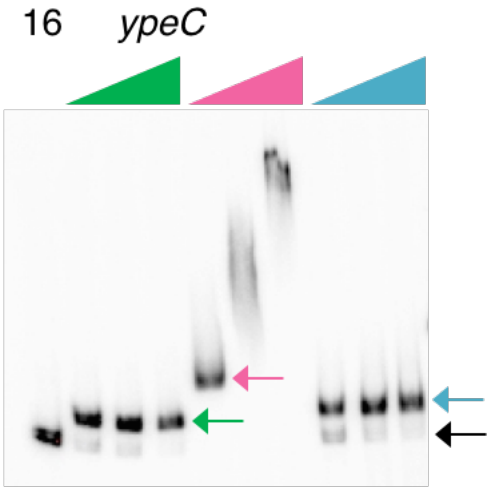
16 ypeC

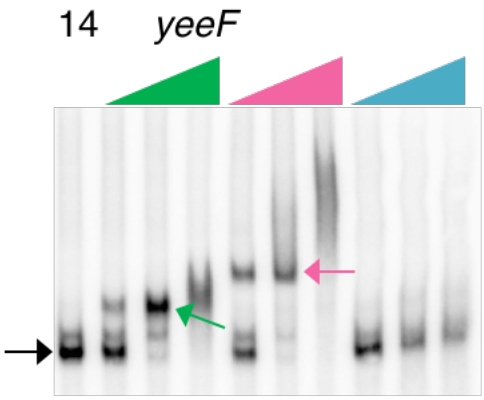
14 yeeF

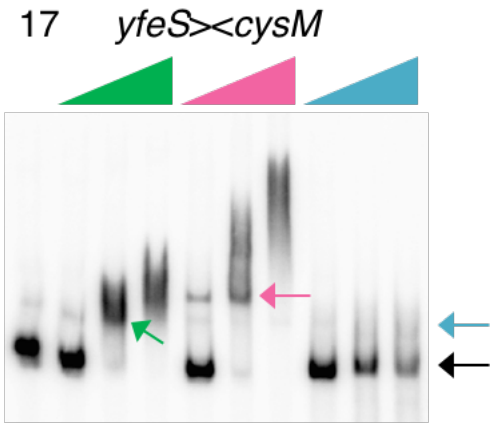
17 yfeS><cysM

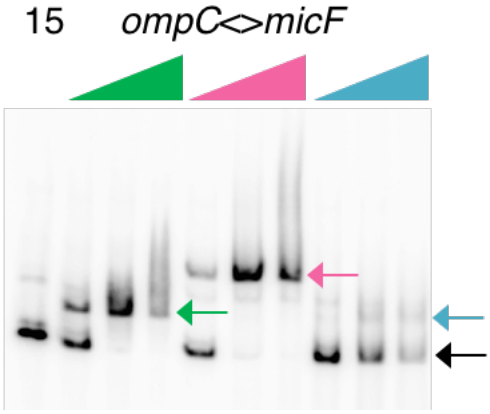
15 ompC<>micF

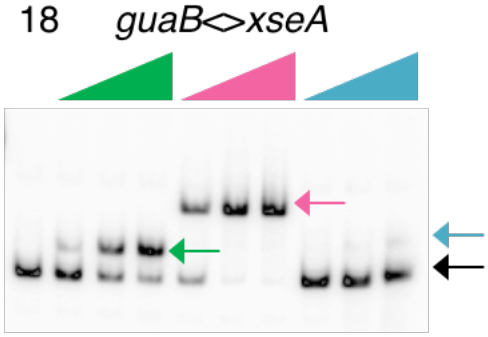
18 guaB<>xseA

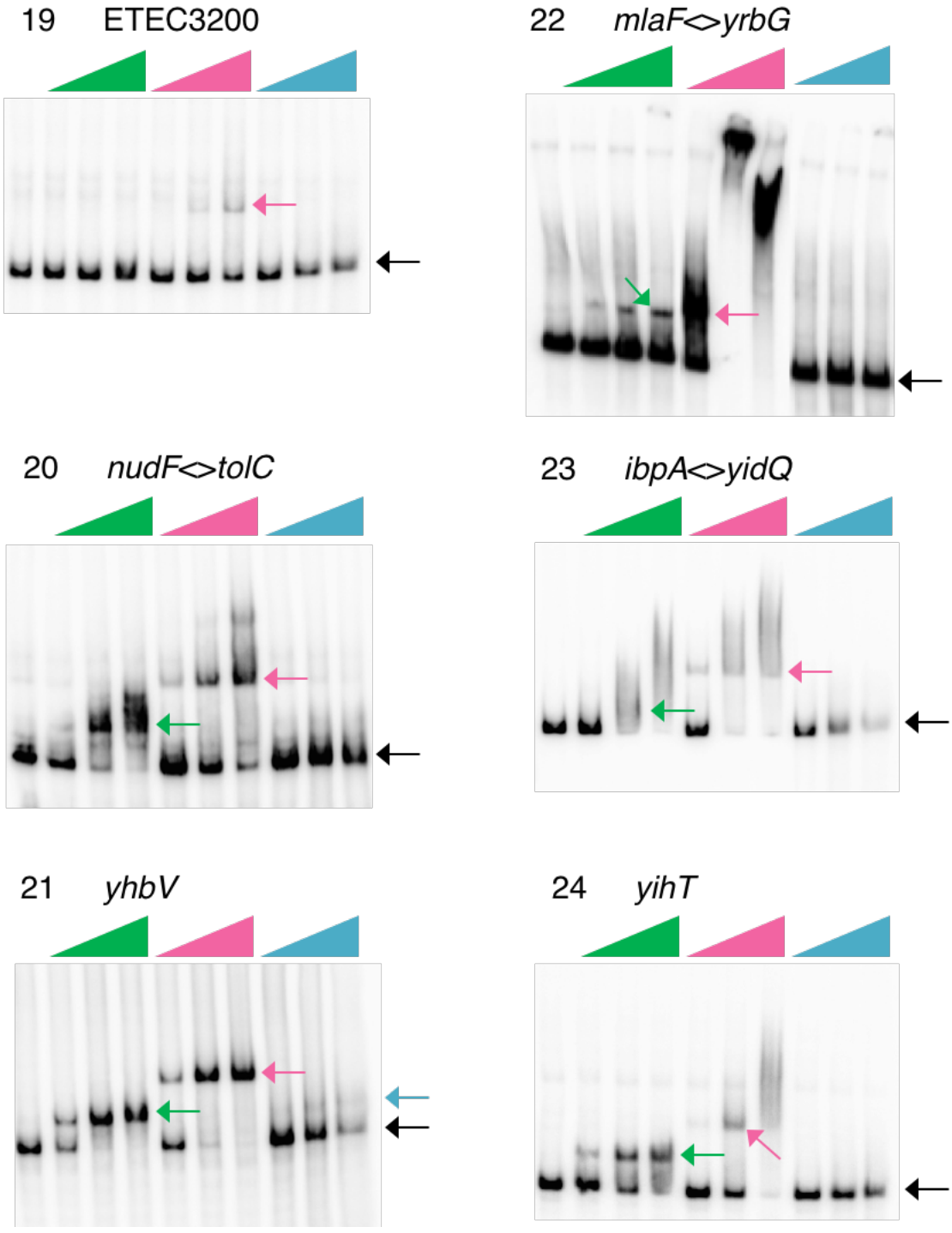
19 ETEC3200
22 mlaF<>yrbG
20 nudF<>tolC
23 ibpA<>yidQ
21 yhbV
24 yihT

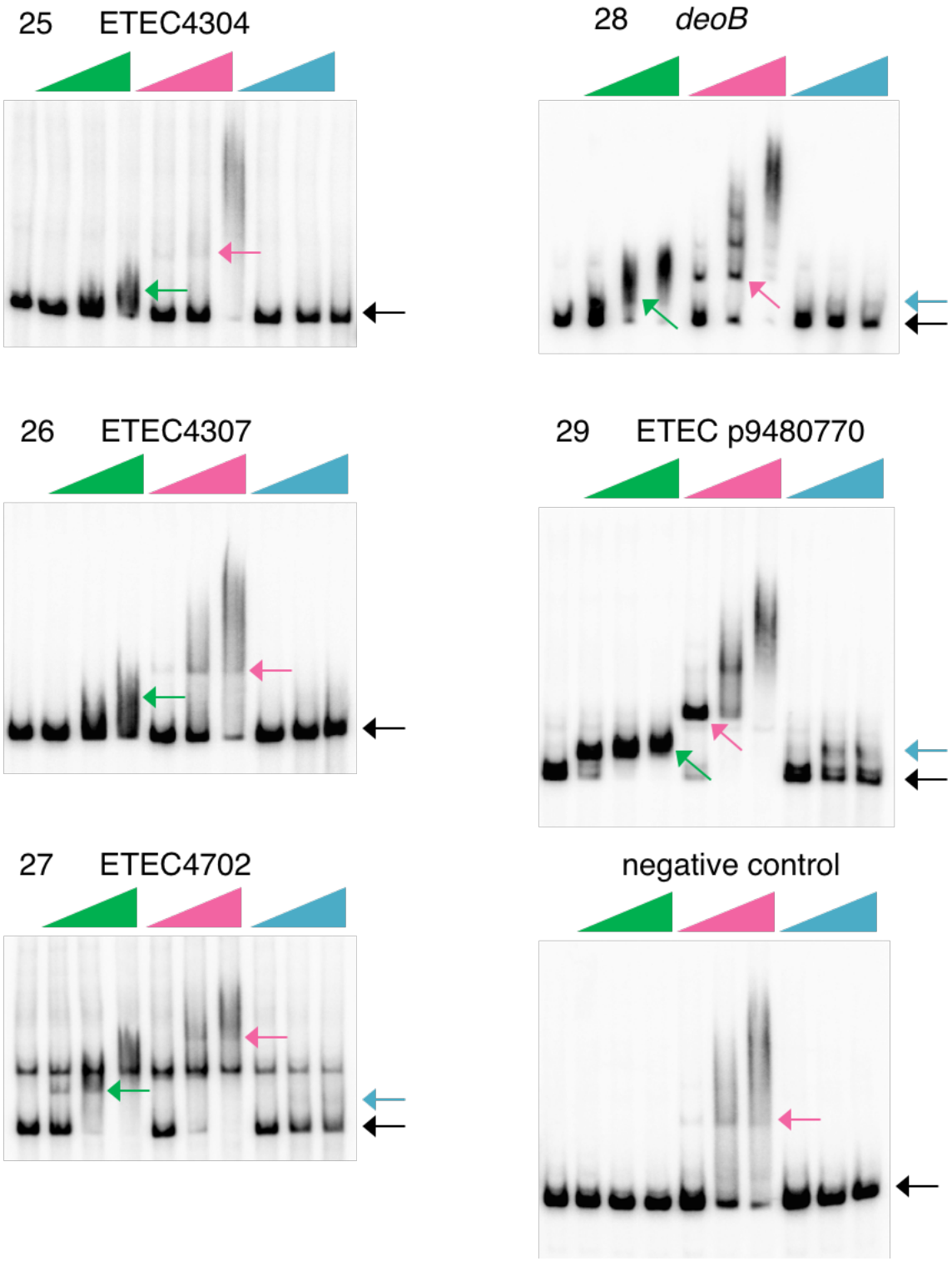
25 ETEC4304
28 deoB
26 ETEC4307
29 ETEC p9480770
27 ETEC4702
negative control

Appendix 2 Binding of MarA, Rob and SoxS to SoxS ChIP-exo targets

Images show EMSAs to assess the binding of MarA, Rob and SoxS to 16 SoxS ChIP-exo targets, from Seo *et al.* (2015), Sharma *et al.* (2017). Increasing MarA, Rob and SoxS concentrations (0.4 – 2 μM for MarA and SoxS; 0.08 – 0.4 μM for Rob) are shown by green, pink and blue triangles, respectively. Arrows indicate free DNA (black), MarA:DNA complexes (green), Rob:DNA complexes (pink) and SoxS:DNA complexes (blue).

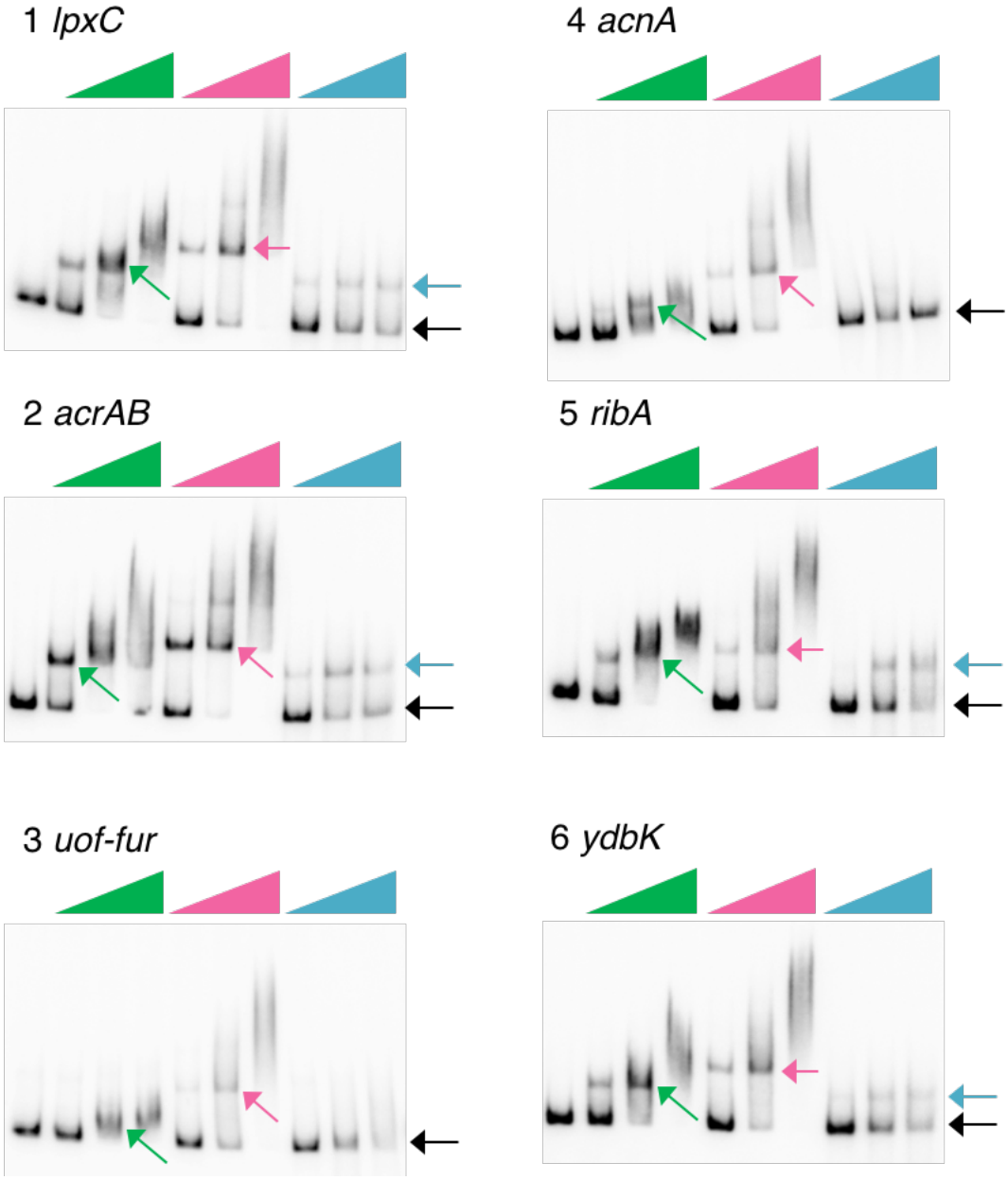

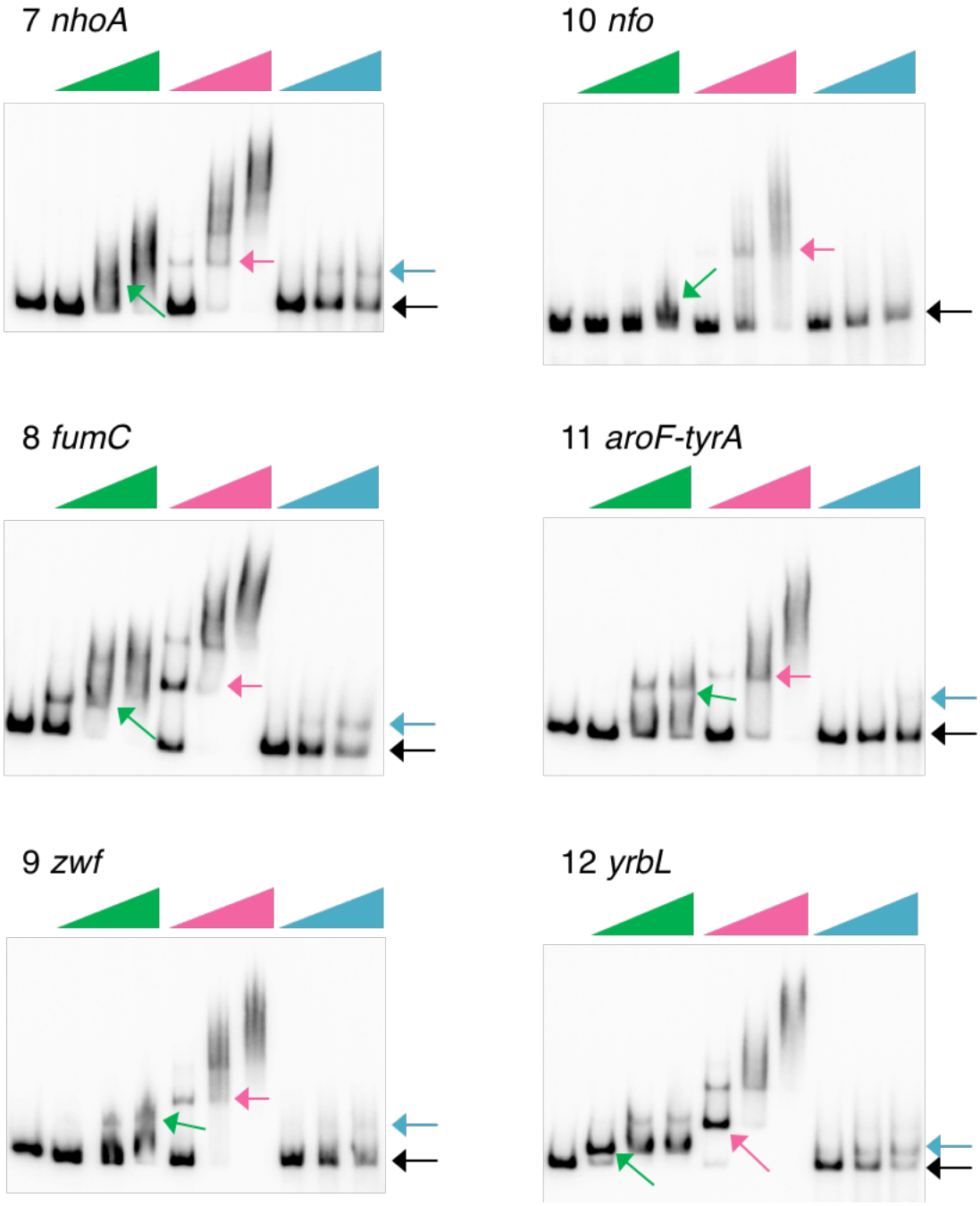
7 nhoA
10 nfo
8 fumC
11 aroF-tyrA
9 zwf
12 yrbL

13 *nepI*

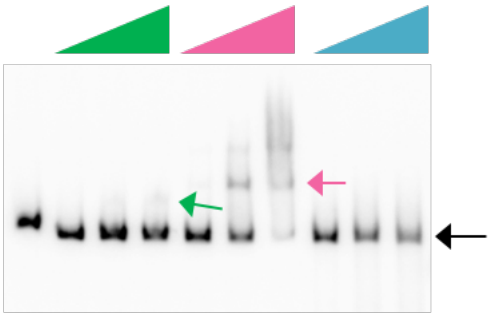

15 *fpr*

14 *sodA*

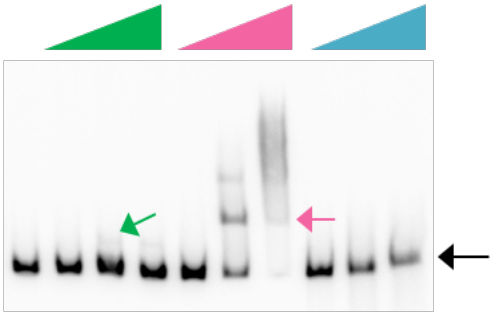

16 *soxS*

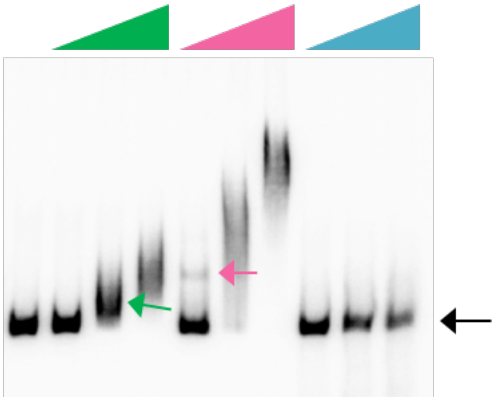

References

Alekshun, M. N. and S. B. Levy (1997). "Regulation of chromosomally mediated multiple antibiotic resistance: the mar regulon." Antimicrob Agents Chemother **41**(10): 2067-2075.

Alekshun, M. N. and S. B. Levy (1999). "Alteration of the Repressor Activity of MarR, the Negative Regulator of the Escherichia coli marRAB Locus, by Multiple Chemicals In Vitro." Journal of Bacteriology **181**(15): 4669-4672.

Alekshun, M. N. and S. B. Levy (1999). "The mar regulon: multiple resistance to antibiotics and other toxic chemicals." Trends in Microbiology **7**(10): 410-413.

Andrews, J. M. (2001). "Determination of minimum inhibitory concentrations." J Antimicrob Chemother **48 Suppl 1**: 5-16.

Aono, R. (1998). "Improvement of organic solvent tolerance level of Escherichia coli by overexpression of stress-responsive genes." Extremophiles **2**(3): 239-248.

Ariza, R. R., S. P. Cohen, N. Bachhawat, S. B. Levy and B. Demple (1994). "Repressor mutations in the marRAB operon that activate oxidative stress genes and multiple antibiotic resistance in Escherichia coli." Journal of Bacteriology **176**(1): 143-148.

Ariza, R. R., Z. Li, N. Ringstad and B. Demple (1995). "Activation of multiple antibiotic resistance and binding of stress-inducible promoters by Escherichia coli Rob protein." J Bacteriol **177**(7): 1655-1661.

Bar-Nahum, G., V. Epshtein, A. E. Ruckenstein, R. Rafikov, A. Mustaev and E. Nudler (2005). "A ratchet mechanism of transcription elongation and its control." Cell **120**(2): 183-193.

Barbosa, T. M. and S. B. Levy (2000). "Differential expression of over 60 chromosomal genes in Escherichia coli by constitutive expression of MarA." J Bacteriol **182**(12): 3467-3474.

Barne, K. A., J. A. Bown, S. J. Busby and S. D. Minchin (1997). "Region 2.5 of the Escherichia coli RNA polymerase sigma70 subunit is responsible for the recognition of the 'extended-10' motif at promoters." Embo j **16**(13): 4034-4040.

Barnhart, M. M. and M. R. Chapman (2006). "Curli biogenesis and function." Annu Rev Microbiol **60**: 131-147.

Battesti, A., N. Majdalani and S. Gottesman (2011). "The RpoS-Mediated General Stress Response in Escherichia coli." Annual Review of Microbiology **65**(1): 189-213.

Baxter, K., J. Lee, L. Minakhin, K. Severinov and D. M. Hinton (2006). "Mutational analysis of sigma70 region 4 needed for appropriation by the bacteriophage T4 transcription factors AsiA and MotA." J Mol Biol **363**(5): 931-944.

Benoff, B., H. Yang, C. L. Lawson, G. Parkinson, J. Liu, E. Blatter, Y. W. Ebright, H. M. Berman and R. H. Ebright (2002). "Structural Basis of Transcription Activation: The CAP-αCTD-DNA Complex." Science **297**(5586): 1562-1566.

Bio-Rad Quick Start™ Bradford Protein Assay.

Blair, J. M. A., M. A. Webber, A. J. Baylay, D. O. Ogbolu and L. J. V. Piddock (2015). "Molecular mechanisms of antibiotic resistance." Nat Rev Micro **13**(1): 42-51.

Blatter, E. E., W. Ross, H. Tang, R. L. Gourse and R. H. Ebright (1994). "Domain organization of RNA polymerase alpha subunit: C-terminal 85 amino acids constitute a domain capable of dimerization and DNA binding." Cell **78**(5): 889-896.

Briongos-Figuero, L. S., T. Gomez-Traveso, P. Bachiller-Luque, M. Dominguez-Gil Gonzalez, A. Gomez-Nieto, T. Palacios-Martin, M. Gonzalez-Sagrado, A. Duenas-Laita and J. L. Perez-Castrillon (2012). "Epidemiology, risk factors and comorbidity for urinary tract infections caused by extended-spectrum beta-lactamase (ESBL)-producing enterobacteria." Int J Clin Pract **66**(9): 891-896.

Brown, N. L., J. V. Stoyanov, S. P. Kidd and J. L. Hobman (2003). "The MerR family of transcriptional regulators." FEMS Microbiol Rev **27**(2-3): 145-163.

Browning, D. F. and S. J. Busby (2016). "Local and global regulation of transcription initiation in bacteria." Nat Rev Microbiol **14**(10): 638-650.

Browning, D. F., D. C. Grainger and S. J. Busby (2010). "Effects of nucleoid-associated proteins on bacterial chromosome structure and gene expression." Curr Opin Microbiol **13**(6): 773-780.

Burova, E., S. C. Hung, V. Sagitov, B. L. Stitt and M. E. Gottesman (1995). "Escherichia coli NusG protein stimulates transcription elongation rates in vivo and in vitro." J Bacteriol **177**(5): 1388-1392.

Busby, S. and R. H. Ebright (1994). "Promoter structure, promoter recognition, and transcription activation in prokaryotes." Cell **79**(5): 743-746.

Campagne, S., M. E. Marsh, G. Capitani, J. A. Vorholt and F. H. T. Allain (2014). "Structural basis for −10 promoter element melting by environmentally induced sigma factors." Nature Structural &Amp; Molecular Biology **21**: 269.

Campbell, E. A., O. Muzzin, M. Chlenov, J. L. Sun, C. A. Olson, O. Weinman, M. L. Trester-Zedlitz and S. A. Darst (2002). "Structure of the bacterial RNA polymerase promoter specificity sigma subunit." Mol Cell **9**(3): 527-539.

Campbell, E. A., L. F. Westblade and S. A. Darst (2008). "Regulation of bacterial RNA polymerase sigma factor activity: a structural perspective." Curr Opin Microbiol **11**(2): 121-127.

Casaz, P., L. K. Garrity-Ryan, D. McKenney, C. Jackson, S. B. Levy, S. K. Tanaka and M. N. Alekshun (2006). "MarA, SoxS and Rob function as virulence factors in an Escherichia coli murine model of ascending pyelonephritis." Microbiology **152**(Pt 12): 3643-3650.

Cavanagh, A. T. and K. M. Wassarman (2014). "6S RNA, a global regulator of transcription in Escherichia coli, Bacillus subtilis, and beyond." Annu Rev Microbiol **68**: 45-60.

Cayley, S., B. A. Lewis, H. J. Guttman and M. T. Record, Jr. (1991). "Characterization of the cytoplasm of Escherichia coli K-12 as a function of external osmolarity. Implications for protein-DNA interactions in vivo." J Mol Biol **222**(2): 281-300.

Chakraborty, A., D. Wang, Y. W. Ebright, Y. Korlann, E. Kortkhonjia, T. Kim, S. Chowdhury, S. Wigneshweraraj, H. Irschik, R. Jansen, B. T. Nixon, J. Knight, S. Weiss and R. H. Ebright (2012). "Opening and closing of the bacterial RNA polymerase clamp." Science **337**(6094): 591-595.

Cheng, X., Emily J. Guinn, E. Buechel, R. Wong, R. Sengupta, Irina A. Shkel and M. T. Record (2016). "Basis of Protein Stabilization by K Glutamate: Unfavorable Interactions with Carbon, Oxygen Groups." Biophysical Journal **111**(9): 1854-1865.

Chubiz, L. M., G. D. Glekas and C. V. Rao (2012). "Transcriptional Cross Talk within the mar-sox-rob Regulon in Escherichia coli Is Limited to the rob and marRAB Operons." Journal of Bacteriology **194**(18): 4867-4875.

Chuc, N. T. and G. Tomson (1999). ""Doi moi" and private pharmacies: a case study on dispensing and financial issues in Hanoi, Vietnam." Eur J Clin Pharmacol **55**(4): 325-332.

Ciampi, M. S. (2006). "Rho-dependent terminators and transcription termination." Microbiology **152**(Pt 9): 2515-2528.

Cohen, S. P., H. Hachler and S. B. Levy (1993). "Genetic and functional analysis of the multiple antibiotic resistance (mar) locus in Escherichia coli." J Bacteriol **175**(5): 1484-1492.

Cohen, S. P., L. M. McMurry, D. C. Hooper, J. S. Wolfson and S. B. Levy (1989). "Cross-resistance to fluoroquinolones in multiple-antibiotic-resistant (Mar) Escherichia coli selected by tetracycline or chloramphenicol: decreased drug accumulation associated with membrane changes in addition to OmpF reduction." Antimicrobial Agents and Chemotherapy **33**(8): 1318-1325.

Cohen, S. P., L. M. McMurry and S. B. Levy (1988). "marA locus causes decreased expression of OmpF porin in multiple-antibiotic-resistant (Mar) mutants of Escherichia coli." Journal of Bacteriology **170**(12): 5416-5422.

Colland, F., G. Orsini, E. N. Brody, H. Buc and A. Kolb (1998). "The bacteriophage T4 AsiA protein: a molecular switch for sigma 70-dependent promoters." Mol Microbiol **27**(4): 819-829.

Costerton, J. W., P. S. Stewart and E. P. Greenberg (1999). "Bacterial Biofilms: A Common Cause of Persistent Infections." Science **284**(5418): 1318-1322.

Crossman, L. C., R. R. Chaudhuri, S. A. Beatson, T. J. Wells, M. Desvaux, A. F. Cunningham, N. K. Petty, V. Mahon, C. Brinkley, J. L. Hobman, S. J. Savarino, S. M. Turner, M. J. Pallen, C. W. Penn, J. Parkhill, A. K. Turner, T. J. Johnson, N. R. Thomson, S. G. J. Smith and I. R. Henderson (2010). "A Commensal Gone Bad: Complete Genome Sequence of the Prototypical Enterotoxigenic Escherichia coli Strain H10407." Journal of Bacteriology **192**(21): 5822-5831.

Danese, P. N., L. A. Pratt and R. Kolter (2000). "Exopolysaccharide Production Is Required for Development of Escherichia coli K-12 Biofilm Architecture." Journal of Bacteriology **182**(12): 3593-3596.

Dangi, B., A. M. Gronenborn, J. L. Rosner and R. G. Martin (2004). "Versatility of the carboxy-terminal domain of the alpha subunit of RNA polymerase in transcriptional activation: use of the DNA contact site as a protein contact site for MarA." Mol Microbiol **54**(1): 45-59.

Dangi, B., P. Pelupessey, R. G. Martin, J. L. Rosner, J. M. Louis and A. M. Gronenborn (2001). "Structure and dynamics of MarA-DNA complexes: an NMR investigation." J Mol Biol **314**(1): 113-127.

Darst, S. A., N. Opalka, P. Chacon, A. Polyakov, C. Richter, G. Zhang and W. Wriggers (2002). "Conformational flexibility of bacterial RNA polymerase." Proc Natl Acad Sci U S A **99**(7): 4296-4301.

Das, T., P. K. Sharma, H. J. Busscher, H. C. van der Mei and B. P. Krom (2010). "Role of extracellular DNA in initial bacterial adhesion and surface aggregation." Appl Environ Microbiol **76**(10): 3405-3408.

Davis, C. A., M. W. Capp, M. T. Record, Jr. and R. M. Saecker (2005). "The effects of upstream DNA on open complex formation by Escherichia coli RNA polymerase." Proc Natl Acad Sci U S A **102**(2): 285-290.

deHaseth, P. L., M. L. Zupancic and M. T. Record, Jr. (1998). "RNA polymerase-promoter interactions: the comings and goings of RNA polymerase." J Bacteriol **180**(12): 3019-3025.

Dillon, S. C. and C. J. Dorman (2010). "Bacterial nucleoid-associated proteins, nucleoid structure and gene expression." Nat Rev Microbiol **8**(3): 185-195.

Donhofer, A., S. Franckenberg, S. Wickles, O. Berninghausen, R. Beckmann and D. N. Wilson (2012). "Structural basis for TetM-mediated tetracycline resistance." Proc Natl Acad Sci U S A **109**(42): 16900-16905.

Doniselli, N., P. Rodriguez-Aliaga, D. Amidani, J. A. Bardales, C. Bustamante, D. G. Guerra and C. Rivetti (2015). "New insights into the regulatory mechanisms of ppGpp and DksA on Escherichia coli RNA polymerase-promoter complex." Nucleic Acids Res **43**(10): 5249-5262.

Duval, V., K. Foster, J. Brewster and S. B. Levy (2017). "A Novel Regulatory Cascade Involving BluR, YcgZ, and Lon Controls the Expression of Escherichia coli OmpF Porin." Frontiers in microbiology **8**: 1148-1148.

Duval, V. and I. M. Lister (2013). "MarA, SoxS and Rob of Escherichia coli – Global regulators of multidrug resistance, virulence and stress response." International journal of biotechnology for wellness industries **2**(3): 101-124.

Estrem, S. T., T. Gaal, W. Ross and R. L. Gourse (1998). "Identification of an UP element consensus sequence for bacterial promoters." Proceedings of the National Academy of Sciences of the United States of America **95**(17): 9761-9766.

Estrem, S. T., W. Ross, T. Gaal, Z. W. Chen, W. Niu, R. H. Ebright and R. L. Gourse (1999). "Bacterial promoter architecture: subsite structure of UP elements and interactions with the carboxy-terminal domain of the RNA polymerase alpha subunit." Genes Dev **13**(16): 2134-2147.

Feklístov, A., B. D. Sharon, S. A. Darst and C. A. Gross (2014). "Bacterial Sigma Factors: A Historical, Structural, and Genomic Perspective." Annual Review of Microbiology **68**(1): 357-376.

Gallant, C. V., C. Daniels, J. M. Leung, A. S. Ghosh, K. D. Young, L. P. Kotra and L. L. Burrows (2005). "Common β-lactamases inhibit bacterial biofilm formation." Molecular microbiology **58**(4): 1012-1024.

Gallegos, M. T., R. Schleif, A. Bairoch, K. Hofmann and J. L. Ramos (1997). "Arac/XylS family of transcriptional regulators." Microbiol Mol Biol Rev **61**(4): 393-410.

Gama-Castro, S., V. Jiménez-Jacinto, M. Peralta-Gil, A. Santos-Zavaleta, M. I. Peñaloza-Spinola, B. Contreras-Moreira, J. Segura-Salazar, L. Muñiz-Rascado, I. Martínez-Flores, H. Salgado, C. Bonavides-Martínez, C. Abreu-Goodger, C. Rodríguez-Penagos, J. Miranda-Ríos, E. Morett, E. Merino, A. M. Huerta, L. Treviño-Quintanilla and J. Collado-Vides (2008). "RegulonDB (version 6.0): gene regulation model of Escherichia coli K-12 beyond transcription, active (experimental) annotated promoters and Textpresso navigation." Nucleic Acids Res **36**(Database issue): D120-124.

Ganji, M., M. Docter, S. F. J. Le Grice and E. A. Abbondanzieri (2016). "DNA binding proteins explore multiple local configurations during docking via rapid rebinding." Nucleic Acids Research **44**(17): 8376-8384.

Gao, R. and A. M. Stock (2015). "Temporal Hierarchy of Gene Expression Mediated by Transcription Factor Binding Affinity and Activation Dynamics." mBio **6**(3).

Gaston, K., A. Bell, A. Kolb, H. Buc and S. Busby (1990). "Stringent spacing requirements for transcription activation by CRP." Cell **62**(4): 733-743.

Geertz, M., A. Travers, S. Mehandziska, P. Sobetzko, S. Chandra-Janga, N. Shimamoto and G. Muskhelishvili (2011). "Structural coupling between RNA polymerase composition and DNA supercoiling in coordinating transcription: a global role for the omega subunit?" MBio **2**(4).

Gentry, D. R. and R. R. Burgess (1989). "rpoZ, encoding the omega subunit of Escherichia coli RNA polymerase, is in the same operon as spoT." J Bacteriol **171**(3): 1271-1277.

George, A. M. (1996). "Multidrug resistance in enteric and other Gram-negative bacteria." FEMS Microbiology Letters **139**(1): 1-10.

George, A. M. and S. B. Levy (1983). "Amplifiable resistance to tetracycline, chloramphenicol, and other antibiotics in Escherichia coli: involvement of a non-plasmid-determined efflux of tetracycline." Journal of Bacteriology **155**(2): 531-540.

Ghosh, P., A. Ishihama and D. Chatterji (2001). "Escherichia coli RNA polymerase subunit omega and its N-terminal domain bind full-length beta' to facilitate incorporation into the alpha2beta subassembly." Eur J Biochem **268**(17): 4621-4627.

Gillette, W. K., R. G. Martin and J. L. Rosner (2000). "Probing the Escherichia coli transcriptional activator MarA using alanine-scanning mutagenesis: residues important for DNA binding and activation1." Journal of Molecular Biology **299**(5): 1245-1255.

Giro, M., N. Carrillo and A. R. Krapp (2006). "Glucose-6-phosphate dehydrogenase and ferredoxin-NADP(H) reductase contribute to damage repair during the soxRS response of Escherichia coli." Microbiology **152**(Pt 4): 1119-1128.

Gonzales-Siles, L. and Å. Sjöling (2016). "The different ecological niches of enterotoxigenic Escherichia coli." Environmental Microbiology **18**(3): 741-751.

Goossens, H., M. Ferech, R. Vander Stichele and M. Elseviers (2005). "Outpatient antibiotic use in Europe and association with resistance: a cross-national database study." The Lancet **365**(9459): 579-587.

Grainger, D. C., M. D. Goldberg, D. J. Lee and S. J. Busby (2008). "Selective repression by Fis and H-NS at the Escherichia coli dps promoter." Mol Microbiol **68**(6): 1366-1377.

Greenberg, J. T., P. Monach, J. H. Chou, P. D. Josephy and B. Demple (1990). "Positive control of a global antioxidant defense regulon activated by superoxide-generating agents in Escherichia coli." Proc Natl Acad Sci U S A **87**(16): 6181-6185.

Griffith, K. L., M. M. Fitzpatrick, E. F. Keen, 3rd and R. E. Wolf, Jr. (2009). "Two functions of the C-terminal domain of Escherichia coli Rob: mediating "sequestration-dispersal" as a novel off-on switch for regulating Rob's activity as a transcription activator and preventing degradation of Rob by Lon protease." J Mol Biol **388**(3): 415-430.

Griffith, K. L., I. M. Shah, T. E. Myers, M. C. O'Neill and R. E. Wolf Jr (2002). "Evidence for “Pre-recruitment” as a New Mechanism of Transcription Activation in Escherichia coli: The Large Excess of SoxS Binding Sites per Cell Relative to the Number of SoxS Molecules per Cell." Biochemical and Biophysical Research Communications **291**(4): 979-986.

Griffith, K. L., I. M. Shah and R. E. Wolf, Jr. (2004). "Proteolytic degradation of Escherichia coli transcription activators SoxS and MarA as the mechanism for reversing

the induction of the superoxide (SoxRS) and multiple antibiotic resistance (Mar) regulons." Mol Microbiol **51**(6): 1801-1816.

Gruber, T. M. and C. A. Gross (2003). "Multiple Sigma Subunits and the Partitioning of Bacterial Transcription Space." Annual Review of Microbiology **57**(1): 441-466.

Gunnelius, L., K. Hakkila, J. Kurkela, H. Wada, E. Tyystjärvi and T. Tyystjärvi (2014). "The omega subunit of the RNA polymerase core directs transcription efficiency in cyanobacteria." Nucleic Acids Res **42**(7): 4606-4614.

Gupta, S. K., J. Keck, P. K. Ram, J. A. Crump, M. A. Miller and E. D. Mintz (2008). "Part III. Analysis of data gaps pertaining to enterotoxigenic Escherichia coli infections in low and medium human development index countries, 1984-2005." Epidemiol Infect **136**(6): 721-738.

Guy, R., L. Geoghegan, M. Heginbothom, R. Howe, B. Muller-Pebody, J. S. Reilly, J. Wilson, C. Wiuff, T. Wyatt and A. P. Johnson (2016). "Non-susceptibility of Escherichia coli, Klebsiella spp., Pseudomonas spp., Streptococcus pneumoniae and Staphylococcus aureus in the UK: temporal trends in England, Northern Ireland, Scotland and Wales." Journal of Antimicrobial Chemotherapy **71**(6): 1564-1569.

Hachler, H., S. P. Cohen and S. B. Levy (1991). "marA, a regulated locus which controls expression of chromosomal multiple antibiotic resistance in Escherichia coli." J Bacteriol **173**(17): 5532-5538.

Hampton, T. (2013). "Report reveals scope of US antibiotic resistance threat." Jama **310**(16): 1661-1663.

Harder, K. J., H. Nikaido and M. Matsuhashi (1981). "Mutants of Escherichia coli That Are Resistant to Certain Beta-Lactam Compounds Lack the ompF Porin." Antimicrobial Agents and Chemotherapy **20**(4): 549.

Harvey, R. B., R. C. Anderson, K. J. Genovese, T. R. Callaway and D. J. Nisbet (2005). "Use of competitive exclusion to control enterotoxigenic strains of Escherichia coli in weaned pigs123." Journal of Animal Science **83**(13_suppl).

Helmann, J. D. (2002). "The extracytoplasmic function (ECF) sigma factors." Adv Microb Physiol **46**: 47-110.

Henderson, K. L., L. C. Felth, C. M. Molzahn, I. Shkel, S. Wang, M. Chhabra, E. F. Ruff, L. Bieter, J. E. Kraft and M. T. Record (2017). "Mechanism of transcription initiation and promoter escape by E. coli RNA polymerase." Proceedings of the National Academy of Sciences **114**(15): E3032.

Hidalgo, E., V. Leautaud and B. Demple (1998). "The redox-regulated SoxR protein acts from a single DNA site as a repressor and an allosteric activator." Embo j **17**(9): 2629-2636.

Hobbs, E. C., X. Yin, B. J. Paul, J. L. Astarita and G. Storz (2012). "Conserved small protein associates with the multidrug efflux pump AcrB and differentially affects antibiotic resistance." Proc Natl Acad Sci U S A **109**(41): 16696-16701.

Hoiby, N., T. Bjarnsholt, M. Givskov, S. Molin and O. Ciofu (2010). "Antibiotic resistance of bacterial biofilms." Int J Antimicrob Agents **35**(4): 322-332.

Hook-Barnard, I. G. and D. M. Hinton (2009). "The promoter spacer influences transcription initiation via σ⁷⁰ region 1.1 of Escherichia coli RNA polymerase." Proceedings of the National Academy of Sciences **106**(3): 737.

Huseby, D. L., F. Pietsch, G. Brandis, L. Garoff, A. Tegehall and D. Hughes (2017). "Mutation Supply and Relative Fitness Shape the Genotypes of Ciprofloxacin-Resistant Escherichia coli." Molecular biology and evolution **34**(5): 1029-1039.

Igarashi, K., N. Fujita and A. Ishihama (1991). "Identification of a subunit assembly domain in the alpha subunit of Escherichia coli RNA polymerase." J Mol Biol **218**(1): 1-6.

Igarashi, K., A. Hanamura, K. Makino, H. Aiba, H. Aiba, T. Mizuno, A. Nakata and A. Ishihama (1991). "Functional map of the alpha subunit of Escherichia coli RNA polymerase: two modes of transcription activation by positive factors." Proc Natl Acad Sci U S A **88**(20): 8958-8962.

Jair, K. W., W. P. Fawcett, N. Fujita, A. Ishihama and R. E. Wolf, Jr. (1996). "Ambidextrous transcriptional activation by SoxS: requirement for the C-terminal domain of the RNA polymerase alpha subunit in a subset of Escherichia coli superoxide-inducible genes." Mol Microbiol **19**(2): 307-317.

Jair, K. W., R. G. Martin, J. L. Rosner, N. Fujita, A. Ishihama and R. E. Wolf (1995). "Purification and regulatory properties of MarA protein, a transcriptional activator of Escherichia coli multiple antibiotic and superoxide resistance promoters." Journal of Bacteriology **177**(24): 7100-7104.

Jair, K. W., X. Yu, K. Skarstad, B. Thöny, N. Fujita, A. Ishihama and R. E. Wolf (1996). "Transcriptional activation of promoters of the superoxide and multiple antibiotic resistance regulons by Rob, a binding protein of the Escherichia coli origin of chromosomal replication." Journal of Bacteriology **178**(9): 2507-2513.

Jeon, Y. H., T. Yamazaki, T. Otomo, A. Ishihama and Y. Kyogoku (1997). "Flexible linker in the RNA polymerase alpha subunit facilitates the independent motion of the C-terminal activator contact domain." J Mol Biol **267**(4): 953-962.

Kaldalu, N., U. Toots, V. de Lorenzo and M. Ustav (2000). "Functional domains of the TOL plasmid transcription factor XylS." Journal of bacteriology **182**(4): 1118-1126.

Kansal, R., D. A. Rasko, J. W. Sahl, G. P. Munson, K. Roy, Q. Luo, A. Sheikh, K. J. Kuhne and J. M. Fleckenstein (2013). "Transcriptional Modulation of Enterotoxigenic

Escherichia coli Virulence Genes in Response to Epithelial Cell Interactions." Infection and Immunity **81**(1): 259-270.

Kapanidis, A. N., E. Margeat, S. O. Ho, E. Kortkhonjia, S. Weiss and R. H. Ebright (2006). "Initial transcription by RNA polymerase proceeds through a DNA-scrunching mechanism." Science **314**(5802): 1144-1147.

Kern, W. V., M. Oethinger, A. S. Jellen-Ritter and S. B. Levy (2000). "Non-target gene mutations in the development of fluoroquinolone resistance in Escherichia coli." Antimicrob Agents Chemother **44**(4): 814-820.

Keseler, I. M., A. Mackie, M. Peralta-Gil, A. Santos-Zavaleta, S. Gama-Castro, C. Bonavides-Martinez, C. Fulcher, A. M. Huerta, A. Kothari, M. Krummenacker, M. Latendresse, L. Muniz-Rascado, Q. Ong, S. Paley, I. Schroder, A. G. Shearer, P. Subhraveti, M. Travers, D. Weerasinghe, V. Weiss, J. Collado-Vides, R. P. Gunsalus, I. Paulsen and P. D. Karp (2013). "EcoCyc: fusing model organism databases with systems biology." Nucleic Acids Res **41**(Database issue): D605-612.

Kolb, A. K., D.; Kusano, S.; Ishihama, A. (1995). "Selectivity of the Escherichia coli RNA polymerase E sigma 38 for overlapping promoters and ability to support CRP activation." Nucleic Acids Res **23**(5): 819-826.

Koo, B.-M., V. A. Rhodius, G. Nonaka, P. L. deHaseth and C. A. Gross (2009). "Reduced capacity of alternative σs to melt promoters ensures stringent promoter recognition." Genes & Development **23**(20): 2426-2436.

Korner, H., H. J. Sofia and W. G. Zumft (2003). "Phylogeny of the bacterial superfamily of Crp-Fnr transcription regulators: exploiting the metabolic spectrum by controlling alternative gene programs." FEMS Microbiol Rev **27**(5): 559-592.

Kwon, H. J., M. H. Bennik, B. Demple and T. Ellenberger (2000). "Crystal structure of the Escherichia coli Rob transcription factor in complex with DNA." Nat Struct Biol **7**(5): 424-430.

Landick, R. (2001). "RNA polymerase clamps down." Cell **105**(5): 567-570.

Lane, W. J. and S. A. Darst (2006). "The structural basis for promoter -35 element recognition by the group IV sigma factors." PLoS Biol **4**(9): e269.

Lange, R. and R. Hengge-Aronis (1991). "Identification of a central regulator of stationary-phase gene expression in Escherichia coli." Mol Microbiol **5**(1): 49-59.

Lange, R. and R. Hengge-Aronis (1994). "The cellular concentration of the sigma S subunit of RNA polymerase in Escherichia coli is controlled at the levels of transcription, translation, and protein stability." Genes Dev **8**(13): 1600-1612.

Laptenko, O., J. Lee, I. Lomakin and S. Borukhov (2003). "Transcript cleavage factors GreA and GreB act as transient catalytic components of RNA polymerase." Embo j **22**(23): 6322-6334.

Lee, D. J., L. E. Bingle, K. Heurlier, M. J. Pallen, C. W. Penn, S. J. Busby and J. L. Hobman (2009). "Gene doctoring: a method for recombineering in laboratory and pathogenic Escherichia colistrains." BMC Microbiology **9**(1): 1-14.

Lee, D. J., S. D. Minchin and S. J. Busby (2012). "Activating transcription in bacteria." Annu Rev Microbiol **66**: 125-152.

Lee, J., R. Page, R. García-Contreras, J.-M. Palermino, X.-S. Zhang, O. Doshi, T. K. Wood and W. Peti (2007). "Structure and Function of the Escherichia coli Protein YmgB: A Protein Critical for Biofilm Formation and Acid-resistance." Journal of Molecular Biology **373**(1): 11-26.

Lewis, M. (1996). "Response: DNA Looping and Lac Repressor--CAP Interaction." Science **274**(5294): 1931-1932.

Li, Z. and B. Demple (1994). "SoxS, an activator of superoxide stress genes in Escherichia coli. Purification and interaction with DNA." J Biol Chem **269**(28): 18371-18377.

Liochev, S. I. and I. Fridovich (1992). "Fumarase C, the stable fumarase of Escherichia coli, is controlled by the soxRS regulon." Proc Natl Acad Sci U S A **89**(13): 5892-5896.

Lopez, P. J., J. Guillerez, R. Sousa and M. Dreyfus (1998). "On the mechanism of inhibition of phage T7 RNA polymerase by lac repressor." J Mol Biol **276**(5): 861-875.

Luijsterburg, M. S., M. C. Noom, G. J. Wuite and R. T. Dame (2006). "The architectural role of nucleoid-associated proteins in the organization of bacterial chromatin: a molecular perspective." J Struct Biol **156**(2): 262-272.

Ma, D., M. Alberti, C. Lynch, H. Nikaido and J. E. Hearst (1996). "The local repressor AcrR plays a modulating role in the regulation of acrAB genes of Escherichia coli by global stress signals." Molecular Microbiology **19**(1): 101-112.

Madan Babu, M. and S. A. Teichmann (2003). "Evolution of transcription factors and the gene regulatory network in Escherichia coli." Nucleic Acids Research **31**(4): 1234-1244.

Maddocks, S. E. and P. C. F. Oyston (2008). "Structure and function of the LysR-type transcriptional regulator (LTTR) family proteins." Microbiology **154**(12): 3609-3623.

Majdalani, N. and S. Gottesman (2007). "Genetic dissection of signaling through the Rcs phosphorelay." Methods Enzymol **423**: 349-362.

Mandel, M. J. and T. J. Silhavy (2005). "Starvation for Different Nutrients in Escherichia coli Results in Differential Modulation of RpoS Levels and Stability." Journal of Bacteriology **187**(2): 434.

Maneewannakul, K. and S. B. Levy (1996). "Identification for mar mutants among quinolone-resistant clinical isolates of Escherichia coli." Antimicrob Agents Chemother **40**(7): 1695-1698.

Manganelli, R., R. Provvedi, S. Rodrigue, J. Beaucher, L. Gaudreau and I. Smith (2004). "Sigma factors and global gene regulation in Mycobacterium tuberculosis." Journal of bacteriology **186**(4): 895-902.

Mangel, W. F. and M. J. Chamberlin (1974). "Studies of ribonucleic acid chain initiation by Escherichia coli ribonucleic acid polymerase bound to T7 deoxyribonucleic acid. I. An assay for the rate and extent of ribonucleic acid chain initiation." J Biol Chem **249**(10): 2995-3001.

Marcusson, L. L., N. Frimodt-Moller and D. Hughes (2009). "Interplay in the selection of fluoroquinolone resistance and bacterial fitness." PLoS Pathog **5**(8): e1000541.

Martin, R. G., W. K. Gillette, N. I. Martin and J. L. Rosner (2002). "Complex formation between activator and RNA polymerase as the basis for transcriptional activation by MarA and SoxS in Escherichia coli." Mol Microbiol **43**(2): 355-370.

Martin, R. G., W. K. Gillette, S. Rhee and J. L. Rosner (1999). "Structural requirements for marbox function in transcriptional activation of mar/sox/rob regulon promoters in Escherichia coli: sequence, orientation and spatial relationship to the core promoter." Mol Microbiol **34**(3): 431-441.

Martin, R. G., W. K. Gillette and J. L. Rosner (2000). "Promoter discrimination by the related transcriptional activators MarA and SoxS: differential regulation by differential binding." Mol Microbiol **35**(3): 623-634.

Martin, R. G., K. W. Jair, R. E. Wolf Jr and J. L. Rosner (1996). "Autoactivation of the marRAB multiple antibiotic resistance operon by the marA transcriptional activator in Escherichia coli." Journal of Bacteriology **178**(8): 2216-2223.

Martin, R. G., P. S. Nyantakyi and J. L. Rosner (1995). "Regulation of the multiple antibiotic resistance (mar) regulon by marORA sequences in Escherichia coli." J Bacteriol **177**(14): 4176-4178.

Martin, R. G. and J. L. Rosner (1997). "Fis, an accessorial factor for transcriptional activation of the mar (multiple antibiotic resistance) promoter of Escherichia coli in the presence of the activator MarA, SoxS, or Rob." Journal of Bacteriology **179**(23): 7410-7419.

Martin, R. G. and J. L. Rosner (1997). "Fis, an accessorial factor for transcriptional activation of the mar (multiple antibiotic resistance) promoter of Escherichia coli in the presence of the activator MarA, SoxS, or Rob." J Bacteriol **179**(23): 7410-7419.

Martin, R. G. and J. L. Rosner (2002). "Genomics of the marA/soxS/rob regulon of Escherichia coli: identification of directly activated promoters by application of molecular genetics and informatics to microarray data." Mol Microbiol **44**(6): 1611-1624.

Martin, R. G. and J. L. Rosner (2011). "Promoter Discrimination at Class I MarA Regulon Promoters Mediated by Glutamic Acid 89 of the MarA Transcriptional Activator of Escherichia coli." Journal of Bacteriology **193**(2): 506-515.

Martínez-Antonio, A. and J. Collado-Vides (2003). "Identifying global regulators in transcriptional regulatory networks in bacteria." Current Opinion in Microbiology **6**(5): 482-489.

Martinez-Antonio, A., S. C. Janga, H. Salgado and J. Collado-Vides (2006). "Internal-sensing machinery directs the activity of the regulatory network in Escherichia coli." Trends Microbiol **14**(1): 22-27.

Martínez-Hackert, E. and A. M. Stock (1997). "Structural relationships in the OmpR family of winged-helix transcription factors11Edited by M. Gottesman." Journal of Molecular Biology **269**(3): 301-312.

May, T., A. Ito and S. Okabe (2009). "Induction of multidrug resistance mechanism in Escherichia coli biofilms by interplay between tetracycline and ampicillin resistance genes." Antimicrobial agents and chemotherapy **53**(11): 4628-4639.

Mazzariol, A., Y. Tokue, T. M. Kanegawa, G. Cornaglia and H. Nikaido (2000). "High-level fluoroquinolone-resistant clinical isolates of Escherichia coli overproduce multidrug efflux protein AcrA." Antimicrobial agents and chemotherapy **44**(12): 3441-3443.

McDermott, P. F., L. M. McMurry, I. Podglajen, J. L. Dzink-Fox, T. Schneiders, M. P. Draper and S. B. Levy (2008). "The marC Gene of Escherichia coli Is Not Involved in Multiple Antibiotic Resistance." Antimicrobial Agents and Chemotherapy **52**(1): 382-383.

McMurry, L. and S. Levy (2010). Evidence that Regulatory Protein MarA of Escherichia coli Represses rob by Steric Hindrance.

McMurry, L. M., M. Oethinger and S. B. Levy (1998). "Overexpression of marA, soxS, or acrAB produces resistance to triclosan in laboratory and clinical strains of Escherichia coli." FEMS Microbiology Letters **166**(2): 305-309.

Mechold, U., K. Potrykus, H. Murphy, K. S. Murakami and M. Cashel (2013). "Differential regulation by ppGpp versus pppGpp in Escherichia coli." Nucleic Acids Res **41**(12): 6175-6189.

Mekler, V., E. Kortkhonjia, J. Mukhopadhyay, J. Knight, A. Revyakin, A. N. Kapanidis, W. Niu, Y. W. Ebright, R. Levy and R. H. Ebright (2002). "Structural organization of bacterial RNA polymerase holoenzyme and the RNA polymerase-promoter open complex." Cell **108**(5): 599-614.

Merrick, M. J. (1993). "In a class of its own--the RNA polymerase sigma factor sigma 54 (sigma N)." Mol Microbiol **10**(5): 903-909.

Michán, C., M. Manchado and C. Pueyo (2002). "SoxRS Down-Regulation of rob Transcription." Journal of Bacteriology **184**(17): 4733-4738.

Mika, F., S. Busse, A. Possling, J. Berkholz, N. Tschowri, N. Sommerfeldt, M. Pruteanu and R. Hengge (2012). "Targeting of csgD by the small regulatory RNA RprA links

stationary phase, biofilm formation and cell envelope stress in Escherichia coli." Molecular microbiology **84**(1): 51-65.

Minogue, T. D., H. A. Daligault, K. W. Davenport, K. A. Bishop-Lilly, S. M. Broomall, D. C. Bruce, P. S. Chain, O. Chertkov, S. R. Coyne, T. Freitas, K. G. Frey, H. S. Gibbons, J. Jaissle, C. L. Redden, C. N. Rosenzweig, Y. Xu and S. L. Johnson (2014). "Complete Genome Assembly of Escherichia coli ATCC 25922, a Serotype O6 Reference Strain." Genome Announcements **2**(5): e00969-00914.

Minton, A. P. (2001). "The Influence of Macromolecular Crowding and Macromolecular Confinement on Biochemical Reactions in Physiological Media." Journal of Biological Chemistry **276**(14): 10577-10580.

Misra, V. K., J. L. Hecht, K. A. Sharp, R. A. Friedman and B. Honig (1994). "Salt Effects on Protein-DNA Interactions: The λcI Repressor and EcoRI Endonuclease." Journal of Molecular Biology **238**(2): 264-280.

Monsalve, M., B. Calles, M. Mencia, F. Rojo and M. Salas (1998). "Binding of phage phi29 protein p4 to the early A2c promoter: recruitment of a repressor by the RNA polymerase." J Mol Biol **283**(3): 559-569.

Monsalve, M., M. Mencia, F. Rojo and M. Salas (1996). "Activation and repression of transcription at two different phage phi29 promoters are mediated by interaction of the same residues of regulatory protein p4 with RNA polymerase." Embo j **15**(2): 383-391.

Monsalve, M., M. Mencia, M. Salas and F. Rojo (1996). "Protein p4 represses phage phi 29 A2c promoter by interacting with the alpha subunit of Bacillus subtilis RNA polymerase." Proc Natl Acad Sci U S A **93**(17): 8913-8918.

Munita, J. M. and C. A. Arias (2016). "Mechanisms of Antibiotic Resistance." Microbiol Spectr **4**(2).

Murakami, K., M. Kimura, J. T. Owens, C. F. Meares and A. Ishihama (1997). "The two alpha subunits of Escherichia coli RNA polymerase are asymmetrically arranged and contact different halves of the DNA upstream element." Proc Natl Acad Sci U S A **94**(5): 1709-1714.

Murakami, K. S. (2013). "X-ray crystal structure of Escherichia coli RNA polymerase σ70 holoenzyme." J Biol Chem **288**(13): 9126-9134.

Murakami, K. S. and S. A. Darst (2003). "Bacterial RNA polymerases: the wholo story." Current Opinion in Structural Biology **13**(1): 31-39.

Murakami, K. S., S. Masuda and S. A. Darst (2002). "Structural basis of transcription initiation: RNA polymerase holoenzyme at 4 A resolution." Science **296**(5571): 1280-1284.

Murray, H. D., D. A. Schneider and R. L. Gourse (2003). "Control of rRNA expression by small molecules is dynamic and nonredundant." Mol Cell **12**(1): 125-134.

Nechaev, S. and E. P. Geiduschek (2006). "The role of an upstream promoter interaction in initiation of bacterial transcription." Embo j **25**(8): 1700-1709.

Nguyen, T. V., P. V. Le, C. H. Le and A. Weintraub (2005). "Antibiotic Resistance in Diarrheagenic Escherichia coli and Shigella Strains Isolated from Children in Hanoi, Vietnam." Antimicrobial Agents and Chemotherapy **49**(2): 816-819.

Nichols, R. J., S. Sen, Y. J. Choo, P. Beltrao, M. Zietek, R. Chaba, S. Lee, K. M. Kazmierczak, K. J. Lee, A. Wong, M. Shales, S. Lovett, M. E. Winkler, N. J. Krogan, A. Typas and C. A. Gross (2011). "Phenotypic landscape of a bacterial cell." Cell **144**(1): 143-156.

Nikaido, H. (1994). "Porins and specific diffusion channels in bacterial outer membranes." J Biol Chem **269**(6): 3905-3908.

Nikaido, H. and Y. Takatsuka (2009). "Mechanisms of RND Multidrug Efflux Pumps." Biochimica et biophysica acta **1794**(5): 769-781.

Nucci, N. V. and J. M. Vanderkooi (2008). "Effects of Salts of the Hofmeister Series on the Hydrogen Bond Network of Water." Journal of molecular liquids **143**(2-3): 160-170.

Nuzhdin, S. V., A. Rychkova and M. W. Hahn (2010). "The strength of transcription-factor binding modulates co-variation in transcriptional networks." Trends Genet **26**(2): 51-53.

O'Neill, J. (2014). Antimicrobial resistance: tackling a crisis for the health and wealth of nations. Rev Antimicrob Resist.

O'Toole, G. A. and R. Kolter (1998). "Flagellar and twitching motility are necessary for Pseudomonas aeruginosa biofilm development." Mol Microbiol **30**(2): 295-304.

Oethinger, M., I. Podglajen, W. V. Kern and S. B. Levy (1998). "Overexpression of the marA or soxS regulatory gene in clinical topoisomerase mutants of Escherichia coli." Antimicrob Agents Chemother **42**(8): 2089-2094.

Okusu, H., D. Ma and H. Nikaido (1996). "AcrAB efflux pump plays a major role in the antibiotic resistance phenotype of Escherichia coli multiple-antibiotic-resistance (Mar) mutants." Journal of Bacteriology **178**(1): 306-308.

Österberg, S., T. d. Peso-Santos and V. Shingler (2011). "Regulation of Alternative Sigma Factor Use." Annual Review of Microbiology **65**(1): 37-55.

Paget, M. S. B. and J. D. Helmann (2003). "The σ70family of sigma factors." Genome Biology **4**(1): 203.

Park, J. S., M. T. Marr and J. W. Roberts (2002). "E. coli Transcription repair coupling factor (Mfd protein) rescues arrested complexes by promoting forward translocation." Cell **109**(6): 757-767.

Patten, C. L., M. G. Kirchhof, M. R. Schertzberg, R. A. Morton and H. E. Schellhorn (2004). "Microarray analysis of RpoS-mediated gene expression in Escherichia coli K-12." Mol Genet Genomics **272**(5): 580-591.

Picozzi, S. C. M., S. Casellato, M. Rossini, G. Paola, M. Tejada, E. Costa and L. Carmignani (2014). "Extended-spectrum beta-lactamase-positive Escherichia coli causing complicated upper urinary tract infection: Urologist should act in time." Urology annals **6**(2): 107-112.

Potrykus, K. and M. Cashel (2008). "(p)ppGpp: still magical?" Annu Rev Microbiol **62**: 35-51.

Praski Alzrigat, L., D. L. Huseby, G. Brandis and D. Hughes (2017). "Fitness cost constrains the spectrum of marR mutations in ciprofloxacin-resistant Escherichia coli." Journal of Antimicrobial Chemotherapy **72**(11): 3016-3024.

Pratt, L. A. and T. J. Silhavy (1998). "Crl stimulates RpoS activity during stationary phase." Mol Microbiol **29**(5): 1225-1236.

Prigent-Combaret, C., O. Vidal, C. Dorel and P. Lejeune (1999). "Abiotic surface sensing and biofilm-dependent regulation of gene expression in Escherichia coli." J Bacteriol **181**(19): 5993-6002.

Rabin, N., Y. Zheng, C. Opoku-Temeng, Y. Du, E. Bonsu and H. O. Sintim (2015). "Biofilm formation mechanisms and targets for developing antibiofilm agents." Future Med Chem **7**(4): 493-512.

Randall, L. P. and M. J. Woodward (2002). "The multiple antibiotic resistance (mar) locus and its significance." Research in Veterinary Science **72**(2): 87-93.

Revyakin, A., C. Liu, R. H. Ebright and T. R. Strick (2006). "Abortive initiation and productive initiation by RNA polymerase involve DNA scrunching." Science **314**(5802): 1139-1143.

Rhee, S., R. G. Martin, J. L. Rosner and D. R. Davies (1998). "A novel DNA-binding motif in MarA: the first structure for an AraC family transcriptional activator." Proc Natl Acad Sci U S A **95**(18): 10413-10418.

Rhodius, V. A., T. H. Segall-Shapiro, B. D. Sharon, A. Ghodasara, E. Orlova, H. Tabakh, D. H. Burkhardt, K. Clancy, T. C. Peterson, C. A. Gross and C. A. Voigt (2013). "Design of orthogonal genetic switches based on a crosstalk map of σs, anti-σs, and promoters." Mol Syst Biol **9**: 702.

Richey, B., D. S. Cayley, M. C. Mossing, C. Kolka, C. F. Anderson, T. C. Farrar and M. T. Record (1987). "Variability of the intracellular ionic environment of Escherichia coli. Differences between in vitro and in vivo effects of ion concentrations on protein-DNA interactions and gene expression." Journal of Biological Chemistry **262**(15): 7157-7164.

Robison, K., A. M. McGuire and G. M. Church (1998). "A comprehensive library of DNA-binding site matrices for 55 proteins applied to the complete Escherichia coli K-12 genome." J Mol Biol **284**(2): 241-254.

Rosner, J. L., B. Dangi, A. M. Gronenborn and R. G. Martin (2002). "Posttranscriptional Activation of the Transcriptional Activator Rob by Dipyridyl in Escherichia coli." Journal of Bacteriology **184**(5): 1407-1416.

Rosner, J. L. and J. L. Slonczewski (1994). "Dual regulation of inaA by the multiple antibiotic resistance (mar) and superoxide (soxRS) stress response systems of Escherichia coli." Journal of Bacteriology **176**(20): 6262-6269.

Ross, W., K. K. Gosink, J. Salomon, K. Igarashi, C. Zou, A. Ishihama, K. Severinov and R. L. Gourse (1993). "A third recognition element in bacterial promoters: DNA binding by the alpha subunit of RNA polymerase." Science **262**(5138): 1407-1413.

Ross, W. and R. L. Gourse (2005). "Sequence-independent upstream DNA-alphaCTD interactions strongly stimulate Escherichia coli RNA polymerase-lacUV5 promoter association." Proc Natl Acad Sci U S A **102**(2): 291-296.

Ruiz, C., L. M. McMurry and S. B. Levy (2008). "Role of the multidrug resistance regulator MarA in global regulation of the hdeAB acid resistance operon in Escherichia coli." J Bacteriol **190**(4): 1290-1297.

Santangelo, T. J. and I. Artsimovitch (2011). "Termination and antitermination: RNA polymerase runs a stop sign." Nat Rev Microbiol **9**(5): 319-329.

Schmidt, M. C. and M. J. Chamberlin (1987). "nusA protein of Escherichia coli is an efficient transcription termination factor for certain terminator sites." J Mol Biol **195**(4): 809-818.

Schneider, D. A., T. Gaal and R. L. Gourse (2002). "NTP-sensing by rRNA promoters in Escherichia coli is direct." Proc Natl Acad Sci U S A **99**(13): 8602-8607.

Schneiders, T., T. M. Barbosa, L. M. McMurry and S. B. Levy (2004). "The Escherichia coli Transcriptional Regulator MarA Directly Represses Transcription of purA and hdeA." Journal of Biological Chemistry **279**(10): 9037-9042.

Schneiders, T. and S. B. Levy (2006). "MarA-mediated Transcriptional Repression of the rob Promoter." Journal of Biological Chemistry **281**(15): 10049-10055.

Schwarz, S., C. Kehrenberg, B. Doublet and A. Cloeckaert (2006). "Molecular basis of bacterial resistance to chloramphenicol and florfenicol." FEMS Microbiology Reviews **28**(5): 519-542.

Sengupta, R., A. Pantel, X. Cheng, I. Shkel, I. Peran, N. Stenzoski, D. P. Raleigh and M. T. Record, Jr. (2016). "Positioning the Intracellular Salt Potassium Glutamate in the Hofmeister Series by Chemical Unfolding Studies of NTL9." Biochemistry **55**(15): 2251-2259.

Seo, S. W., D. Kim, H. Latif, E. J. O'Brien, R. Szubin and B. O. Palsson (2014). "Deciphering Fur transcriptional regulatory network highlights its complex role beyond iron metabolism in Escherichia coli." Nature Communications **5**: 4910.

Seo, Sang W., D. Kim, R. Szubin and Bernhard O. Palsson (2015). "Genome-wide Reconstruction of OxyR and SoxRS Transcriptional Regulatory Networks under Oxidative Stress in Escherichia coli K-12 MG1655." Cell Reports **12**(8): 1289-1299.

Seoane, A. S. and S. B. Levy (1995). "Characterization of MarR, the repressor of the multiple antibiotic resistance (mar) operon in Escherichia coli." J Bacteriol **177**(12): 3414-3419.

Sharma, P., J. R. J. Haycocks, A. D. Middlemiss, R. A. Kettles, L. E. Sellars, V. Ricci, L. J. V. Piddock and D. C. Grainger (2017). "The multiple antibiotic resistance operon of enteric bacteria controls DNA repair and outer membrane integrity." Nature Communications **8**(1): 1444.

Singh, S. S., A. Typas, R. Hengge and D. C. Grainger (2011). "Escherichia coli σ^{70} senses sequence and conformation of the promoter spacer region." Nucleic Acids Res **39**(12): 5109-5118.

Soisson, S. M., B. MacDougall-Shackleton, R. Schleif and C. Wolberger (1997). "Structural basis for ligand-regulated oligomerization of AraC." Science **276**(5311): 421-425.

Spellberg, B. and Y. Doi (2015). "The Rise of Fluoroquinolone-Resistant Escherichia coli in the Community: Scarier Than We Thought." The Journal of Infectious Diseases **212**(12): 1853-1855.

Srikumar, R., C. J. Paul and K. Poole (2000). "Influence of Mutations in the mexR Repressor Gene on Expression of the MexA-MexB-OprM Multidrug Efflux System of Pseudomonas aeruginosa." Journal of Bacteriology **182**(5): 1410-1414.

Straney, D. C. and D. M. Crothers (1987). "A stressed intermediate in the formation of stably initiated RNA chains at the Escherichia coli lac UV5 promoter." J Mol Biol **193**(2): 267-278.

Swint-Kruse, L. and K. S. Matthews (2009). "Allostery in the LacI/GalR family: variations on a theme." Current opinion in microbiology **12**(2): 129-137.

Swint-Kruse, L. and K. S. Matthews (2009). "Allostery in the LacI/GalR family: variations on a theme." Curr Opin Microbiol **12**(2): 129-137.

Taliaferro, L. P., E. F. Keen, 3rd, N. Sanchez-Alberola and R. E. Wolf, Jr. (2012). "Transcription activation by Escherichia coli Rob at class II promoters: protein-protein interactions between Rob's N-terminal domain and the σ(70) subunit of RNA polymerase." J Mol Biol **419**(3-4): 139-157.

Tavio, M. M., V. D. Aquili, J. B. Poveda, N. T. Antunes, J. Sanchez-Cespedes and J. Vila (2010). "Quorum-sensing regulator sdiA and marA overexpression is involved in in vitro-

selected multidrug resistance of Escherichia coli." J Antimicrob Chemother **65**(6): 1178-1186.

Tsai, C.-S. and S. C. Winans (2010). "LuxR-type quorum-sensing regulators that are detached from common scents." Molecular microbiology **77**(5): 1072-1082.

Tschowri, N., S. Busse and R. Hengge (2009). "The BLUF-EAL protein YcgF acts as a direct anti-repressor in a blue-light response of Escherichia coli." Genes Dev **23**(4): 522-534.

Tsujikawa, L., O. V. Tsodikov and P. L. deHaseth (2002). "Interaction of RNA polymerase with forked DNA: evidence for two kinetically significant intermediates on the pathway to the final complex." Proc Natl Acad Sci U S A **99**(6): 3493-3498.

Typas, A. and R. Hengge (2006). "Role of the spacer between the -35 and -10 regions in sigmas promoter selectivity in Escherichia coli." Mol Microbiol **59**(3): 1037-1051.

Ukah, U. V., M. Glass, B. Avery, D. Daignault, M. R. Mulvey, R. J. Reid-Smith, E. J. Parmley, A. Portt, P. Boerlin and A. R. Manges (2018). "Risk factors for acquisition of multidrug-resistant Escherichia coli and development of community-acquired urinary tract infections." Epidemiology and Infection **146**(1): 46-57.

Valentin-Hansen, P., L. Sogaard-Andersen and H. Pedersen (1996). "A flexible partnership: the CytR anti-activator and the cAMP-CRP activator protein, comrades in transcription control." Mol Microbiol **20**(3): 461-466.

Vila, J. and S. M. Soto (2012). "Salicylate increases the expression of marA and reduces in vitro biofilm formation in uropathogenic Escherichia coli by decreasing type 1 fimbriae expression." Virulence **3**(3): 280-285.

Vinué, L., L. M. McMurry and S. B. Levy (2013). "The 216-bp marB gene of the marRAB operon in Escherichia coli encodes a periplasmic protein which reduces the transcription rate of marA." FEMS Microbiology Letters **345**(1): 49-55.

Visweswariah, S. S. and S. J. W. Busby (2015). "Evolution of bacterial transcription factors: how proteins take on new tasks, but do not always stop doing the old ones." Trends in Microbiology **23**(8): 463-467.

Walker, K. A. and R. Osuna (2002). "Factors affecting start site selection at the Escherichia coli fis promoter." Journal of bacteriology **184**(17): 4783-4791.

Wall, M. E., D. A. Markowitz, J. L. Rosner and R. G. Martin (2009). "Model of transcriptional activation by MarA in Escherichia coli." PLoS Comput Biol **5**(12): e1000614.

Wang, S., R. Cosstick, J. F. Gardner and R. I. Gumport (1995). "The specific binding of Escherichia coli integration host factor involves both major and minor grooves of DNA." Biochemistry **34**(40): 13082-13090.

Washburn, R. S. and M. E. Gottesman (2015). "Regulation of Transcription Elongation and Termination." Biomolecules **5**(2): 1063-1078.

Webber, M. A. and L. J. Piddock (2001). "Absence of mutations in marRAB or soxRS in acrB-overexpressing fluoroquinolone-resistant clinical and veterinary isolates of Escherichia coli." Antimicrob Agents Chemother **45**(5): 1550-1552.

Webber, M. A. and L. J. V. Piddock (2003). "The importance of efflux pumps in bacterial antibiotic resistance." Journal of Antimicrobial Chemotherapy **51**(1): 9-11.

Weber, H., T. Polen, J. Heuveling, V. F. Wendisch and R. Hengge (2005). "Genome-wide analysis of the general stress response network in Escherichia coli: sigmaS-dependent genes, promoters, and sigma factor selectivity." J Bacteriol **187**(5): 1591-1603.

White, D. G., J. D. Goldman, B. Demple and S. B. Levy (1997). "Role of the acrAB locus in organic solvent tolerance mediated by expression of marA, soxS, or robA in Escherichia coli." Journal of Bacteriology **179**(19): 6122-6126.

White-Ziegler, C. A., S. Um, N. M. Perez, A. L. Berns, A. J. Malhowski and S. Young (2008). "Low temperature (23 degrees C) increases expression of biofilm-, cold-shock- and RpoS-dependent genes in Escherichia coli K-12." Microbiology **154**(Pt 1): 148-166.

Wigneshweraraj, S., D. Bose, P. C. Burrows, N. Joly, J. Schumacher, M. Rappas, T. Pape, X. Zhang, P. Stockley, K. Severinov and M. Buck (2008). "Modus operandi of the bacterial RNA polymerase containing the σ54 promoter-specificity factor." Molecular Microbiology **68**(3): 538-546.

Wong, G. T., R. P. Bonocora, A. N. Schep, S. M. Beeler, A. J. Lee Fong, L. M. Shull, L. E. Batachari, M. Dillon, C. Evans, C. J. Becker, E. C. Bush, J. Hardin, J. T. Wade and D. M. Stoebel (2017). "Genome-Wide Transcriptional Response to Varying RpoS Levels in Escherichia coli K-12." Journal of Bacteriology **199**(7).

Wu, J. and B. Weiss (1991). "Two divergently transcribed genes, soxR and soxS, control a superoxide response regulon of Escherichia coli." J Bacteriol **173**(9): 2864-2871.

Wu, J. and B. Weiss (1992). "Two-stage induction of the soxRS (superoxide response) regulon of Escherichia coli." J Bacteriol **174**(12): 3915-3920.

Yang, Y., V. C. Darbari, N. Zhang, D. Lu, R. Glyde, Y. P. Wang, J. T. Winkelman, R. L. Gourse, K. S. Murakami, M. Buck and X. Zhang (2015). "TRANSCRIPTION. Structures of the RNA polymerase-sigma54 reveal new and conserved regulatory strategies." Science **349**(6250): 882-885.

Yarnell, W. S. and J. W. Roberts (1999). "Mechanism of intrinsic transcription termination and antitermination." Science **284**(5414): 611-615.

Yuzenkova, Y., V. R. Tadigotla, K. Severinov and N. Zenkin (2011). "A new basal promoter element recognized by RNA polymerase core enzyme." The EMBO journal **30**(18): 3766-3775.

Zafar, M. A., N. Sanchez-Alberola and R. E. Wolf, Jr. (2011). "Genetic evidence for a novel interaction between transcriptional activator SoxS and region 4 of the sigma(70) subunit of RNA polymerase at class II SoxS-dependent promoters in Escherichia coli." J Mol Biol **407**(3): 333-353.

Zeng, L. R. and J. P. Xie (2011). "Molecular basis underlying LuxR family transcription factors and function diversity and implications for novel antibiotic drug targets." J Cell Biochem **112**(11): 3079-3084.

Zhang, G., E. A. Campbell, L. Minakhin, C. Richter, K. Severinov and S. A. Darst (1999). "Crystal structure of Thermus aquaticus core RNA polymerase at 3.3 A resolution." Cell **98**(6): 811-824.

Zhang, H., L. Gao, J. Zhang, W. Li, M. Yang, H. Zhang, C. Gao and Z.-G. He (2014). "A Novel marRAB Operon Contributes to the Rifampicin Resistance in Mycobacterium smegmatis." PLoS ONE **9**(8): e106016.

Zhou, Y., A. Kolb, S. J. Busby and Y. P. Wang (2014). "Spacing requirements for Class I transcription activation in bacteria are set by promoter elements." Nucleic Acids Res **42**(14): 9209-9216.

Ziervogel, B. K. and B. Roux (2013). "The Binding of Antibiotics in OmpF Porin." Structure (London, England : 1993) **21**(1): 76-87.

Zuo, Y., Y. Wang and T. A. Steitz (2013). "The mechanism of E. coli RNA polymerase regulation by ppGpp is suggested by the structure of their complex." Mol Cell **50**(3): 430-436.